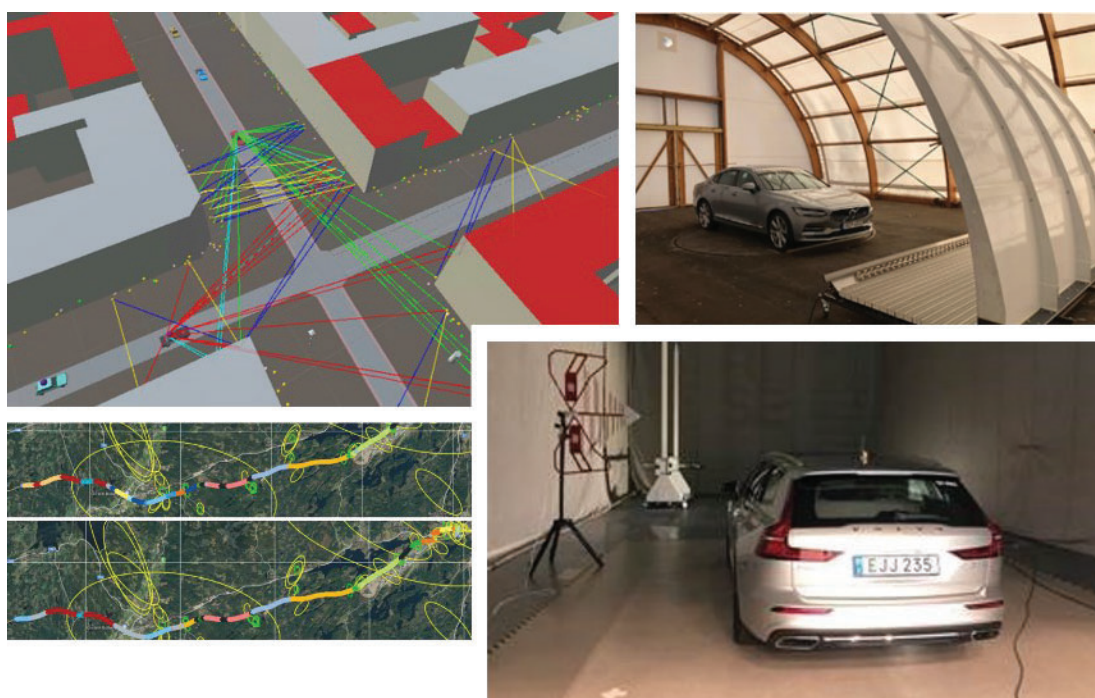# Simulation and Verification of Wireless Technologies (SIVERT)

Public Report

Author: Christian Patané Lötbäck, Volvo Car Corporation
Date: 2021-12-02
Project within FFI elektronik, mjukvara och kommunikation för fordonsindustrin

Table of Contents

FFI in short

FFI is a partnership between the Swedish government and automotive industry for joint funding of research, innovation and development concentrating on Climate & Environment and Safety. FFI has R&D activities worth approx. €100 million per year, of which half is governmental funding.

Currently there are five collaboration programs: Energy & Environment, Traffic safety and automated vehicles, Electronics, software and communications, Sustainable manufacturing and Efficient and connected transport systems. For more information: www.vinnova.se/ffi

1   Executive summary

SImulation and VErification of wiReless Technologies (SIVERT) commenced in April 2018 and was finalized in November 2021. The project was originally planned to be finalized in March 2021, but was extended mainly due to the pandemic and the resulting delay of the final demo. The project management has been handled by two persons from Volvo Cars, Martin Claesson and Christian Lötbäck. All project partners in the original application have been involved in the project until the end.

The project has addressed verification of vehicle connectivity modules including antennas in a comprehensive manner, from simulations in early phases of a vehicular project to final verification of implemented systems in complete vehicles. A simulation tool has been developed for vehicle-to-vehicle and vehicle-to-infrastructure communication, including channel model, communication stack, antenna patterns and mobility. Prototype test setups for complete vehicle multiple-input multiple-output (MIMO) over-the-air performance evaluation have been extensively investigated in terms of key performance indicators and uncertainty, by means of Round Robin measurement campaigns and other theoretical and practical studies. The prototype test setups have been used to measure the performance of next generation vehicular connectivity modules. Also, test scenarios for field tests have been delivered and examples of how this can be realized with a field logging tool have been provided.

Comparing the outcome from the project with the originally defined scope in the FFI application, most of the targets have been met. The only exception is the virtual drive test (VDT) prototype test setup, where only a feasibility study was managed within the scope of the project. One reason for this was the lack of test equipment for performing advanced scenarios. The findings have been widely shared in the industry by means of publications and dissemination and the simulation tool has been publicly shared. Also, areas for further development have been identified, which may be the basis for a follow-up project.

2   Background

The use of wireless communication in vehicles is growing rapidly and is a key technology to increase road safety and efficiency. It enables vehicles to share important information about, e.g., traffic congestions, dangerous road conditions and accidents. Sharing this information can be done through direct communication (vehicle-to-vehicle, vehicle-to-infrastructure) or via cloud-based cellular systems with a large number of users connected simultaneously. At the same time, the infotainment system in vehicles becomes more and more dependent on an internet connection to provide the driver with a premium experience and continuous over-the-air updates of the vehicle software require a reliable connection. All these functions rely on wireless systems that are becoming more complex and the number of communication technologies within a vehicle is increasing. Choice of technology, algorithms, antenna placements, etc. all impact the end performance in different ways. The automotive industry needs to secure the quality and usability of wireless technologies under different circumstances and cannot solely rely on suppliers.

Today there is room for improvement in testing wireless communication in vehicles. A big part of the verification is done using field testing late in projects. This results in two main concerns; problems found are difficult and costly to rectify (late discovery) and the testing environment is usually not repeatable, which can make it difficult to compare and evaluate performance for different solutions. Increasing the scope of simulations before design, together with increased verification in earlier stages of the vehicle projects, gives an opportunity to:

- Design wireless systems with better performance and reliability.
- Identify issues earlier in the vehicle projects.
- Compare performance of different solutions in a repeatable manner.
- Reduce the amount of field testing and expeditions.

Some directional channel models of interest for simulations are covered by previous efforts (FFI WCAE) and in the literature, but there are scenarios where detailed information is lacking, e.g., for the tunnel scenario. There is also an opportunity to enhance the system simulator developed in FFI WCAE, which currently outputs a channel matrix, to include antenna patterns and communication stacks. Such enhancements would enable simulation results in form of reliability of the complete wireless link, e.g. packet error rate for various available wireless communication technologies. This can be used in improving system design and the requirement specifications sent to suppliers. There is also potential for synergy effects by using similar channel models in component verification. Real time emulation through cabled bench tests can verify the intended behaviour of the components and provide useful system feedback before there is an actual vehicle to test.

Later in a vehicle development project, complete vehicle system performance measurements are necessary. There has been a great effort in standardizing these kinds of tests for mobile devices [2][3][4]. The idea is to find issues and determine performance to a larger extent before testing in real networks. Some of the work done can be transferred to automotive testing, but many details differ between small devices and a vehicle.

Since there is no standardized test method for vehicular over-the-air (OTA) communication performance that can be adopted by OEMs, there is a clear need to investigate available testing methods further. Organizations like 5GAA and IMT-2020 are also discussing this. The abilities and limitations of each method need to be determined with the goal to recommend one (or several) methods for vehicle testing. Previous efforts in FFI WCAE focused on OTA multiprobe ring measurements which proved to work well for SISO systems [1]. MIMO measurements are however more complex and have limitations for large test objects in the multiprobe ring. Initial testing was therefore also performed on the radiated two-stage method called wireless cable [5]. Deliveries from these investigations in WCAE will be used as valuable input to SIVERT. In addition, the Reverberation Chamber (RC) technology, that for many years have been used for mobile devices [6], and the recently introduced Random Line-of-Sight (RLOS) technology [7] will also be investigated and compared with.

The FFI SIVERT project is part of a bigger picture for securing wireless communication performance with end goal of increased road safety and efficiency.

3   Purpose, research questions and method

The project scope is outlined in [8] and aims to study how verification of wireless technologies in vehicles can be done in earlier phases of vehicle projects compared to the traditional approach, where field tests are utilized. Utilizing controlled lab environments will also facilitate the assessment of device performance by eliminating variables from a live network. By doing so the cost of verification can be decreased and better quality can be ensured. The work was divided into three main work packages, where simulations, component verification and system (complete vehicle) verification were studied. Details of these different work packages and the research questions addressed in each of them are given in Section 4.

4 Objectives

The project is covering a wide range of verification aspects and thus has been divided into three main work packages. For each of these work packages, clear objectives were defined. These are summarized in the following subsections.

4.1 Work Package 1: Channel models and system simulations

- WP1A: Channel models
  - **Objective:** To get directional channel models for the relevant systems operating at 2.4 GHz -6 GHz in urban, tunnel, highway and open-pit mine environments.
  - **Comments:** This WP started with a literature overview of available directional channel models for the considered systems and scenarios. Some scenarios were covered by previous efforts in WCAE and some scenarios are covered in the literature, Special emphasis was on channel models with geometrical descriptions, e.g. the newly developed COST IRACON channel for intersections and the Quadriga model, in order to support spatial consistency in simulations. A multilink channel sounding system was also developed for measurements in scenarios where important parameters are missing in the literature. The work on open-pit mine and tunnels was, however, put at lower priority during the project due to limitations during the pandemic.
- WP1B: Simulation framework
  - **Objective:** Simulate the link and network level performance, including antenna arrangements and lower communication protocol layers in different key environments.
  - **Comments:** This WP used the channel models form WP 1A and developed a cluster-based simulation framework for joint analysis of V2I and V2V communication, including the influence of antenna arrangements and the lower communication protocol layers. The scenarios include urban intersections with different geometries and highway scenarios.

4.2 Work Package 2: Component verification

- WP2A: Virtual drive test
  - **Objective:** Emulation of geometry-based channel models for component testing and achieve a repeatable virtual drive test setup in a lab environment emulating higher level network behaviour. The main focus was cellular 4G technology.
  - **Comments:** There are several steps towards this objective. The first step was to find a field logging tool, which could be used to record field data for later playback in the lab. Once that was evaluated and a tool was available, scenarios of interest for testing were defined. Finally, a suitable virtual drive test setup was investigated. During the project, the work package refined the goal somewhat. Testing with geometry-based channel models was carried out within WP3 and WP2 instead focused on real field data. Also, more focus was given to the evaluation and implementation of a field logging tool, which partly could be used for recording data for VDT, but also for efficient evaluation of telematics connectivity units in field and to support one of the test methods within WP3.

4.3 Work Package 3: System verification

- WP3A: Multiprobe ring
  - **Objective:** Evaluate the multiprobe ring method feasibility for measurement of MIMO systems.
  - **Comments:** In the project focus were put on LTE 2x2 MIMO systems. However, besides the signaling unit, the developed multiprobe ring setup is more or less agnostic to wireless technology. During the project, a channel emulator (CE) was successfully

integrated into the test setup enabling real-time emulation of realistic propagation conditions. After some tests and analysis, it was concluded that the multiprobe ring method cannot be implemented with phase-controlled waves for OTA tests of large objects such as cars or trucks. This means that there is no plane wave synthesis (quiet zone) generated at the UE (vehicle) side. Rather a statistical approach can be performed, where the superposition of all down-link (DL) signals has a constant statistical distribution (a stationary process) in the test zone. Like a 2D RC. The above is the major drawback of the method as it limits the capability to correctly create channel model correlation at the UE side. However, besides that, the method has proven to give, in its "statistical mode", repeatable and reliable results. In the project, we have performed several validations and tests regarding significant channel properties (correlation, RMS delay spread, etc.), calibration procedures, Round Robin tests and radio performance tests.

- WP3B: Wireless Cable
  - **Objective:** Evaluate the wireless cable method.
  - **Comments:** A CE was successfully integrated into the test setup enabling real-time emulation of realistic propagation conditions. The method has been implemented to work in two modes: its default wireless mode, and in a simplified conductive mode which can be used when the radio has accessible antenna ports. In the wireless mode methods to perform OTA test in; a shielded cavity, in a semi-anechoic chamber (semi-AC), as well as in a novel "roof-top box" has been implemented. Several validations and tests regarding significant channel properties (correlation, isolation criterion, reference signal received power (RSRP) distribution, etc.), calibration procedures, Round Robin tests, MSA analysis, on vehicle installation effects, radio performance tests, etc. have been successfully performed within the project. For future investigations, a novel method for finding the complex valued inversion matrix without any phase information from the device under test (DUT) has been theoretically described. The latter proposal will most likely work for higher-order MIMO systems.

- WP3C: Random Line-of-Sight (RLOS)
  - **Objective:** Verify the Random line-of-sight (Random-LOS) measurement system and compare measurement results with results from the other methods in the project.
  - **Comments:** There are several steps towards this objective. The Random-LOS measurement system consists of a reflector antenna and a dual-polarized linear array feed. First was the test zone of the system characterized, where measurement data was compared to simulation results. Thereafter, verification of both passive and active measurements using the system was performed. The passive measurement verification was performed by measuring the radiation patterns of a stand-alone antenna, as well as a complete vehicle including antenna. As a part of this, also repeatability measurements were performed on the radiation pattern measurements of the complete vehicle with an antenna. The active measurement verification was performed by measuring data throughput for a stand-alone antenna including an LTE modem and for a vehicle-mounted antenna including an LTE modem. Initially, the throughput measurements were planned to be performed with a CE, but due to the limited availability of a CE instrument, this was not possible in practice. The throughput measurements were therefore performed using only a communication tester.

- WP3D: Reverberation Chamber
  - **Objective:** Evaluate the RC method for vehicular testing.
  - **Comments:** A CE was successfully integrated into the test setup enabling real-time emulation of realistic propagation conditions. To enable tests of fully-sized vehicles such as cars and trucks a tent of highly conductive (metallic) textile was invested by RISE and turned into an RC by adding mode stirrers etc. The length, width and height of the tent

is 16-, 8- and 6-meters enabling OTA tests all the way down to approximately 100 MHz. The upper limit is set by the capabilities of the radio frequency (RF) components and instrumentation and in its present state, up to 18 GHz can be tested. Several validations regarding significant channel properties (correlation, key-hole effect, RMS delay spread, etc.), calibration procedures, Round Robin tests, MSA analysis, on vehicle installation effects, radio performance tests, etc., have been successfully performed within the project. The project has also, already, led to several business cases between RISE and Swedish automotive companies within vehicular OTA testing.

- WP3E: Evaluation & Prototype
  - **Objective:** Find the most suitable performance measurement method for full vehicle evaluation and implement a functional prototype measurement set-up.
  - **Comments:** Using the test setups defined in WP3A-D, a Round Robin measurement campaign was carried out. The goal of this measurement campaign was to understand if the test methods provided results representative to real-world operation. The same set of reference devices with known performance was measured with all test methods, as well as in real field operation. These results provided clear guidance on the methods' ability to differentiate between a good and a bad device. Also, a set of key performance indicators was defined and evaluated for each method. An extensive summary table has been provided.

5 Results and deliverables

5.1 Delivery to FFI goals

The table below summarizes the main targets as defined in [8] and their status after completion of the project.

Defined target [8]	Actual (at project conclusion)	Comment
A simulation framework with realistic temporal behavior when it comes to packet error rates and latencies. The framework will include relevant channel models, antennas and radio communication stack for realistic C-ITS simulations.	Fulfilled	A simulation framework with defined test scenarios for V2V and V2I have been delivered.
A prototype test setup for component testing using channel emulation and virtual drive test.	Partly fulfilled	Test setup for virtual drive test has not been achieved, however, feasibility analysis of such test setup provided.
Investigation of four complete vehicle wireless verification methods in lab. Alignment with component testing to complement and increase testing efficiency.	Fulfilled	
Round-robin testing of at least two vehicular devices in all four methods used for method comparison.	Fulfilled	Reference antennas from CTIA were used.
Selection of full vehicle measurement verification method based on investigation and real testing.	Fulfilled	A verification strategy has been defined internally based on these methods.
Prototype setup of selected method.	Fulfilled	Extensive investigations of key performance indicators, procedures and measurement uncertainties. Measurement system analysis according to Six Sigma for all selected methods.
Increased skill and knowledge in: wireless system simulations and communication stacks, V2V and V2I channel models, wireless vehicle component testing, wireless system performance testing of complete vehicle.	Fulfilled	Various papers and disseminations to spread the knowledge.

5.2 Example results

This section summarizes the most important results from each work package.

5.2.1 Work Package 1: Channel models and system simulations

5.2.1.1 Multilink channel sounder for vehicular applications

Simulation is a necessary tool to test and evaluate wireless communication systems. To gain trust in the simulated results of the wireless propagation channel, real measurements must be performed. These measurements can be used both as a source for developing new channel models to be used in a simulation framework. Or as validity check for the implemented ray tracing simulator.

Since wireless channels in vehicular environments are far from static, we need to measure all radio channels between several radios simultaneously to be able to evaluate the channels at a given time.
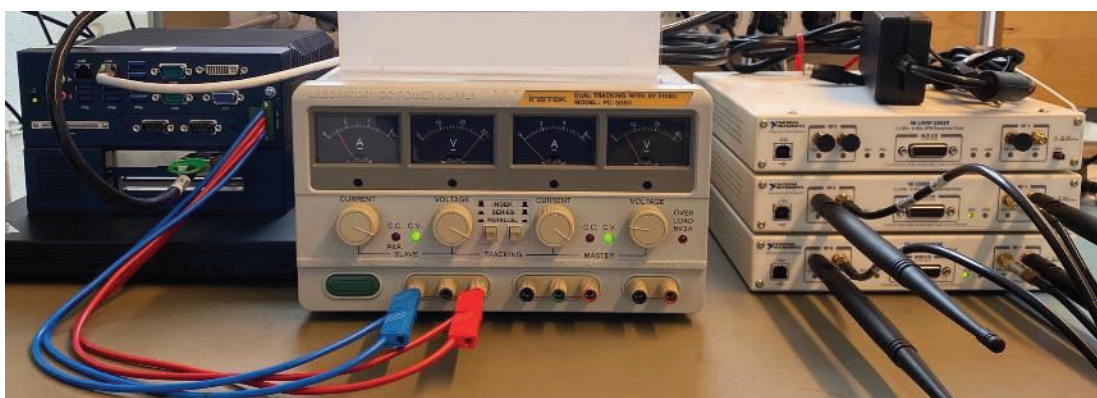
Figure 5.2.1-1. Laboratory setup of the system. To the left are two host computers, in the middle a power supply, and to the right three NI-USRP 2953r.

To this end, a new channel sounder has been developed. It is based on the National Instruments USRP-2953r software-defined radio (SDR). The radios have a maximum instantaneous bandwidth of 40 MHz and can be tuned from 1.2 GHz to 6 GHz. The frequency of interest for vehicular communication is 5.9 GHz, which is within the operational range. To be able to measure multiple links, at least three radios are needed. Since vehicles and road-side units are naturally distributed, the radios cannot be synced, and time aligned from a shared reference source over cables. Rather, each radio is connected to its own host computer and a stable rubidium clock. The clocks have in turn been connected to each other overnight to be synced and can thereafter be separated and be able to maintain coherent for long enough to perform measurements. Another source of reference that can be used – when under open sky – is the pulse-per-second (PPS) transmitted in the GPS signal.

The sounder has been implemented in LabVIEW Communications Design Suite 5.0, on a Windows 10 computer. The computer (called Host) is connected to the USRP (called Target) via a PCIe x4 gen1 interface. Depending on the host, the interface will allow transfer rates from 200 MB/s up to 800 MB/s. This is a relatively high throughput; hence processing must be performed on the FPGA to reduce the amount of data sent back to the host. Since the signal is repeated M times for averaging to gain a better signal to noise ratio, a natural step would be to perform the averaging on the FPGA which will reduce the amount of data – sent back to the host – with a factor of M.
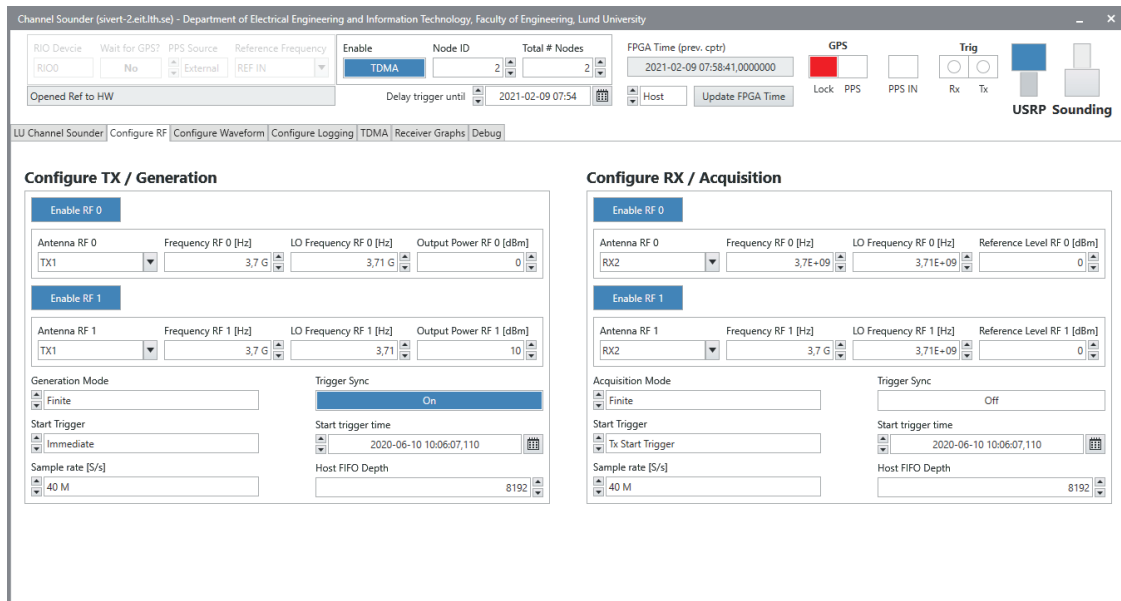
Figure 5.2.1-2. Graphical user interface for the sounder.

The sounder is of the correlative type, which means that the transmitted signal inhibits good autocorrelation properties. The pulse used is the Zadoff-Chu sequence. It has the good autocorrelation properties that we desire and has a fairly flat frequency response.

5.2.1.2 Investigation on available V2X simulation framework matching FFI SIVERT WP1 criteria

As an initial step we reviewed the V2X frameworks available for the vehicular research community. The focus of the evaluation was to asses capabilities of the frameworks against WP1 criteria. In particular, we were seeking the support of 3D environment, vehicle dynamics, V2X communications stack simulation capabilities, availability/coupling between mobility and communication parts of the simulation frameworks, antenna radiation patterns modeling capabilities, multi-path signal propagation modelling capabilities. With this objectives we evaluated several solutions reported in the literature, including "Architectures for distributed, interactive and integrated traffic simulations" [WP1-1], "Connection of the SUMO Microscopic Traffic Simulator and the Unity 3D Game Engine to Evaluate V2X Communication-Based Systems" [WP1-2], "3D driving simulator with VANET capabilities to assess cooperative systems: 3DSimVanet" [WP1-3], "Vehicular Networks Simulation With Realistic Physics" [WP1-4].

For the sake of brevity, we omit detailed review in this report and highlight only the conclusion drawn. Non of the reviewed alternatives could fulfill all SIVERT criteria. However, after careful evaluation, VENERIS simulation framework proposed in [WP1-4] supported the most capabilities matching our criteria.

5.2.1.3 Decision on V2X simulation framework architecture.

After the processing all the gathered information and PoCs we concluded the following way to proceed:

1. We reutilize and extend Uniy3D and any required Veneris modules implemented.
2. We implement GSCM approach directly in Unity3D. Due to full-scale ray-tracing could be not feasible due to lack of EMP data, the suitable alternative currently available is Geometry-based Stochastic Channel Modelling (GSCM). GSCM also requires some ray shooting, but in general to a much lesser extent. Saying that, we could use native to Unity3D engine ray-tracing approach to enable GSCM.
3. As a communication simulator we opt to NS-3. OMNEST license is sensibly pricing and NS-3 supports similar functionality free of charge. As we also discussed above, the Veneris to

Omnet++ API implementation is still at the very early stage and should be quite safe to change communication simulation engine now, without loosing the development speed.

4. Finally, to enable bi-directionally coupled V2X simulations our ambition is to implement API between Unity3D and NS-3. This will also require the solution synchronizing their operation, since Unity3D is operating on regular time steps updates, while NS-3 (as well as other communication simulators, e.g. Omnet++) are event-based.

5.2.1.4 SIVERT V2X framework architecture.

As a starting point, we focused on implementing Unity3D – NS-3 bi-directional API. In order to properly asses the C-ITS application, the vehicles and V2X communication input/output should be able to influence each other in real-time. Bi-directional coupling will enable actual C-ITS scenarios verification. Online interaction between Unity and NS-3 modules could bring realism to the next level. It should be, however, noted, that Unity3D is a time-step based platform (updates/calculates on fixed periodic time instances); NS3 is built upon event-driven paradigm and doesn't have regular updates. Also, depending on the expected functionality API could become a large project itself.
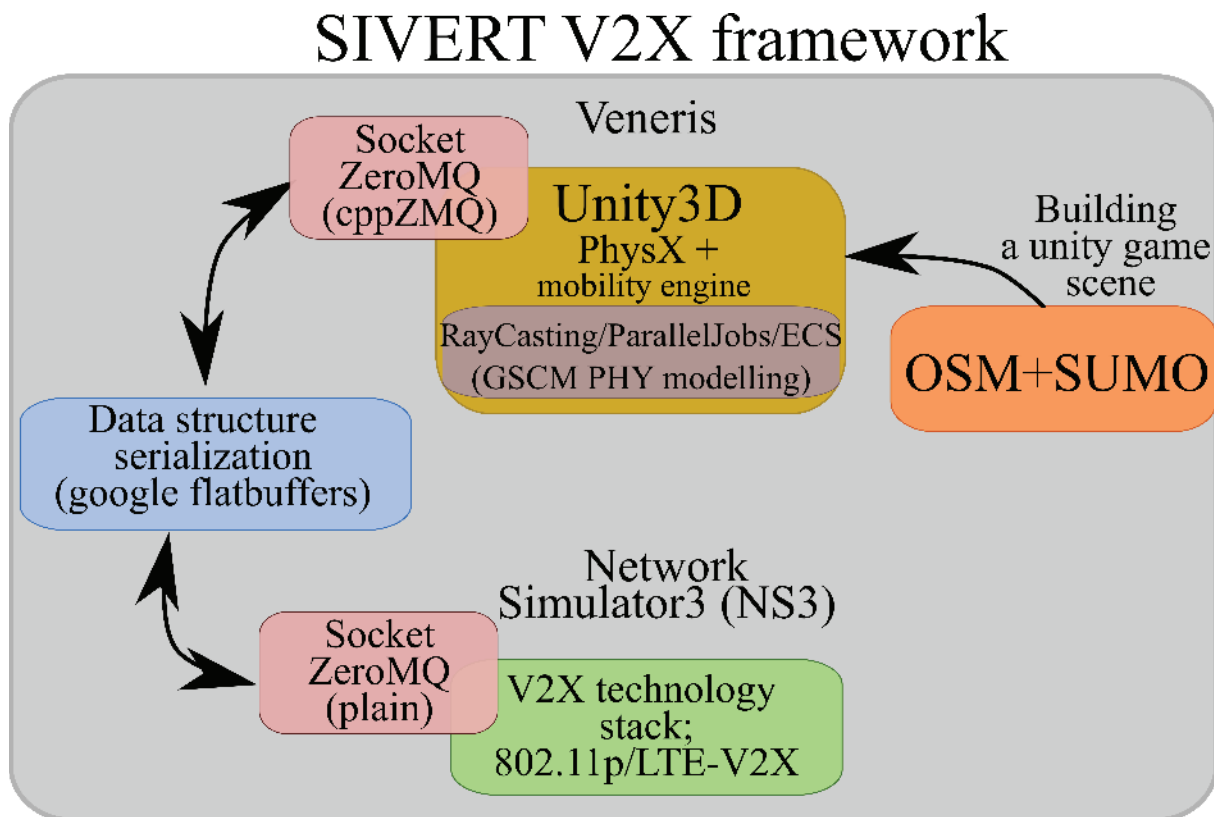
Figure 5.2.1-3. SIVERT simulation framework architecture.

As a result of investigation of available simulators and frameworks, their functionalities, licenses they are distributed under and architectures of other V2X frameworks, we come up with the architecture for SIVERT simulation framework shown on the Figure 5.2.1-3. The vehicle mobility and logic, road infrastructure and surroundings are modelled using Unity3D majorly by reutilizing and extending the Veneris simulation framework implementation. Geometry-based stochastic modelling for V2V and V2I scenarios will be also implemented and run in Unity3D. The V2X technology stack is simulated by means of Network Simulator 3 bi-directionally coupled with Unity3D via TCP/IP based API. For API, to serialize, define and efficiently support coordination between Unity3D and NS3, the data structures are implemented using google flatbuffer capabilities. ZeroMQ framework is utilized to establish TCP/IP and maintain socket on specified ports on loopback interface and define PUB/SUB/REQ/RESP patterns to support API operation.

5.2.1.5 Bi-directional SIVERT API between Unity3D and NS3

In order to enable bi-directionally coupled real-time V2X simulations, Unity3D and NS3 should be synchronized and exchange information necessary to support their synchronized operation. For this the decision is to establish and support TCP/IP socket on dedicated ports and exchange regular updated in format defined by API.

In order to achieve this ZeroMQ patterns to enable bi-directional exchange between Unity3D and NS3 parts of the simulation framework should be defined and implemented on both sides of API. API format should be defined to support the constant update of NS3 from Unity3D with scene's initial configuration (e.g. number of vehicles, channel model, time of vehicle initialization, etc.) and where necessary, dynamic updates on the current vehicle position, GSCM calculations, event-triggered messages where C-ITS logic requires, etc. At the same time by means of API Unity3D should be able to receive real-time updates about status of V2X messages exchange outcome modelled in NS3.

To facilitate the data exchange through API, we utilize google flatbuffers serialization framework. Implementation of the initial flatbuffers structures is done to support bi-directional exchange. Currently there two main flatbuffer data structures: a) schema to send updates from Unity3D to NS3 calculated by unity at each FixedUpdate() call when all the PhysX periodic updates are calculated (e.g. Vehicles' position update, GSCM spectrum gain calculated for each channel, data to support C-ITS scenarios on stack level, etc.); b) schema to send event of received V2X messages, it's parameters and content back from NS3 to Unity3D.

As example below is shown generated data structure to exchange data about the V2X beacon message content upon its reception by vehicle node in NS3.


```csharp
namespace SivertAPI.MsgReceived
{

using global::System;
using global::FlatBuffers;

public struct MsgRecAPI : IFlatbufferObject
{
  private Table __p;
  public ByteBuffer ByteBuffer { get { return __p.bb; } }
  public static MsgRecAPI GetRootAsMsgRecAPI(ByteBuffer _bb) { return GetRootAsMsgRecAPI(_bb, new MsgRecAPI()); }
  public static MsgRecAPI GetRootAsMsgRecAPI(ByteBuffer _bb, MsgRecAPI obj) { return (obj.__assign(_bb.GetInt(_bb.Position) +
  public void __init(int _i, ByteBuffer _bb) { __p.bb_pos = _i; __p.bb = _bb; }
  public MsgRecAPI __assign(int _i, ByteBuffer _bb) { __init(_i, _bb); return this; }

  public Vec3Rx? Pos { get { int o = __p.__offset(4); return o != 0 ? (Vec3Rx?)(new Vec3Rx()).__assign(o + __p.bb_pos, __pb
  public PacketInfo? PackContent { get { int o = __p.__offset(6); return o != 0 ? (PacketInfo?)(new PacketInfo()).__assign(o
  public string MsgContent { get { int o = __p.__offset(8); return o != 0 ? __p.__string(o + __p.bb_pos) : null; } }
#if ENABLE_SPAN_T
  public Span<byte> GetMsgContentBytes() { return __p.__vector_as_span(8); }
#else
  public ArraySegment<byte>? GetMsgContentBytes() { return __p.__vector_as_arraysegment(8); }
#endif
  public byte[] GetMsgContentArray() { return __p.__vector_as_array<byte>(8); }

  public static void StartMsgRecAPI(FlatBufferBuilder builder) { builder.StartObject(3); }
  public static void AddPos(FlatBufferBuilder builder, Offset<Vec3Rx> posOffset) { builder.AddStruct(0, posOffset.Value, 0);
  public static void AddPackContent(FlatBufferBuilder builder, Offset<PacketInfo> PackContentOffset) { builder.AddStruct(1, P
  public static void AddMsgContent(FlatBufferBuilder builder, StringOffset MsgContentOffset) { builder.AddOffset(2, MsgConten
  public static Offset<MsgRecAPI> EndMsgRecAPI(FlatBufferBuilder builder) {
    int o = builder.EndObject();
    return new Offset<MsgRecAPI>(o);
  }
  public static void FinishMsgRecAPIBuffer(FlatBufferBuilder builder, Offset<MsgRecAPI> offset) { builder.Finish(offset.Value
  public static void FinishSizePrefixedMsgRecAPIBuffer(FlatBufferBuilder builder, Offset<MsgRecAPI> offset) { builder.FinishS
};
```

Figure 5.2.1-4. flatbuffer generated structure on Unity3D (C#) side of API.

```
#ifndef FLATBUFFERS_GENERATED_MSGRECEIVEDSCHEMA_SIVERTAPI_MSGRECEIVED_H_
#define FLATBUFFERS_GENERATED_MSGRECEIVEDSCHEMA_SIVERTAPI_MSGRECEIVED_H_

#include "flatbuffers/flatbuffers.h"

namespace SivertAPI {
namespace MsgReceived {

struct Vec3Rx;

struct PacketInfo;

struct MsgRecAPI;

FLATBUFFERS_MANUALLY_ALIGNED_STRUCT(8) Vec3Rx FLATBUFFERS_FINAL_CLASS {
 private:
  double x_;
  double y_;
  double z_;

 public:
  Vec3Rx() {
    memset(static_cast<void *>(this), 0, sizeof(Vec3Rx));
  }
  Vec3Rx(double _x, double _y, double _z)
      : x_(flatbuffers::EndianScalar(_x)),
        y_(flatbuffers::EndianScalar(_y)),
        z_(flatbuffers::EndianScalar(_z)) {
  }
  double x() const {
    return flatbuffers::EndianScalar(x_);
  }
  double y() const {
    return flatbuffers::EndianScalar(y_);
  }
  double z() const {
    return flatbuffers::EndianScalar(z_);
  }
};
FLATBUFFERS_STRUCT_END(Vec3Rx, 24);

FLATBUFFERS_MANUALLY_ALIGNED_STRUCT(8) PacketInfo FLATBUFFERS_FINAL_CLASS {
 private:
  uint32_t senderID_;
  uint32_t receiverID_;
  int64_t timeReceived_;
  uint8_t sent_;
```

Figure 5.2.1-5. flatbuffer generated structure on NS3 (C++) side of API.

After data structures are defined they could be subsequently easy wrapped and unwrapped to/from byte buffer and exchanged over our TCP/IP ZeroMQ enabled API connection.

Pictures below provide a glance on the part of API that sends info about BSM received by vehicle node.

```
void ReceivedPacket(Ptr<const Packet> packet, Ptr<Node> rxNode, Ptr<Node> txNode) {
    /*
     * Callback invoked when the BSM is received by the VehicleNode.
     * The actual callback signature is defined in the bsm-application.cc/h
     * as BSMreceived TraceSource in factory.
     */

    // Get pointer to node's mobility model
    Ptr<MobilityModel> mob = rxNode->GetObject<MobilityModel>();
    double x = mob->GetPosition().x;
    double y = mob->GetPosition().y;
    double z = mob->GetPosition().z;

    // Get packet content
    uint8_t *buffer = new uint8_t[packet->GetSize ()];
    packet->CopyData(buffer,packet->GetSize());
    std::string packContent = std::string((char*)buffer);
    int br = packContent.compare("Brake");
    std::string ContentToSend;
    // Make a flatbuffer API structure
    flatbuffers::FlatBufferBuilder builder(1024);
    if (br == 0){
        ContentToSend = packContent;
    }
    else{
        ContentToSend = packContent;
    }

    auto msgCont = builder.CreateString(ContentToSend);

    auto PacInfoToSend = PacketInfo(txNode->GetId(), rxNode->GetId(), Simulator::Now().GetNanoSeconds(), false);
    auto RxPosition = Vec3Rx(x,z,y);
    auto bufferToAPI = CreateMsgRecAPI(builder, &RxPosition, &PacInfoToSend, msgCont);
    builder.Finish(bufferToAPI);
    std::string topic = "fromNS";
    s_sendmore (*APIconnect_pub, topic);
    zmq::message_t msgToUnity(builder.GetSize());
    memcpy((void *)msgToUnity.data(), builder.GetBufferPointer(), builder.GetSize());
    APIconnect_pub->send(msgToUnity,0);
```

Figure 5.2.1-6. Part API. Wrapping data structure on the NS3 side and sending it to Unity3D.

Subsequently, on Unity3D side, the API implements the non-blocking reception of the messages from NS3.

```
ZError error;
ZMessage msg;
ZPollItem pollItem = ZPollItem.CreateReceiver();

while (client.PollIn(pollItem, out msg, out error, TimeSpan.Zero))
{
    try
    {
        var content = msg.Unwrap().ReadString();
        byte[] bytesMSG;
        bytesMSG = msg.Unwrap().Read();
        // Read flatbuffer
        try
        {
            ByteBuffer buf = new ByteBuffer(bytesMSG);
            var MsgFromNS3 = MsgRecAPI.GetRootAsMsgRecAPI(buf);
            // var pos = MsgFromNS3.Pos.Value;
            var RxInfo = MsgFromNS3.PackContent.Value;
            var RxID = MsgFromNS3.PackContent.Value.ReceiverID;
            var TxID = MsgFromNS3.PackContent.Value.SenderID;
            var Sent = MsgFromNS3.PackContent.Value.Sent;
            var NS3time = MsgFromNS3.PackContent.Value.TimeReceived; // NS3 time in nanoseconds
            string BeaconContent = MsgFromNS3.MsgContent;

            LogMessageToSqlDB((int)TxID, Stack_v2x_Tech.ToString(), Time.time, (int) TxID, (int) RxID, BeaconContent,
```

Figure 5.2.1-7. Part API. Receiving and Unwrapping data structure on the Unity3D side.

API enables bi-directionally coupled simulation run. With blocking time-synchronized Unity3D-->NS3 connection and non-blocking NS3-->Unity3D connection using PUB/SUB patterns.

Subsequently, during simulation run the API is called on every Unity3D PhysX position update to send corresponding flatbuffer structures to NS3 to update position of vehicle communication nodes, GSCM values, event-triggered messages and from NS3 to Unity3D about V2X beacon reception, etc.

Any required information can be efficiently exchanged in real-time through API to build the basis of our Real-time bi-directionally coupled realistic V2X simulator. Below is example of messages received via API from NS3 to Unity3D - API is called for every received BSM for every vehicle.
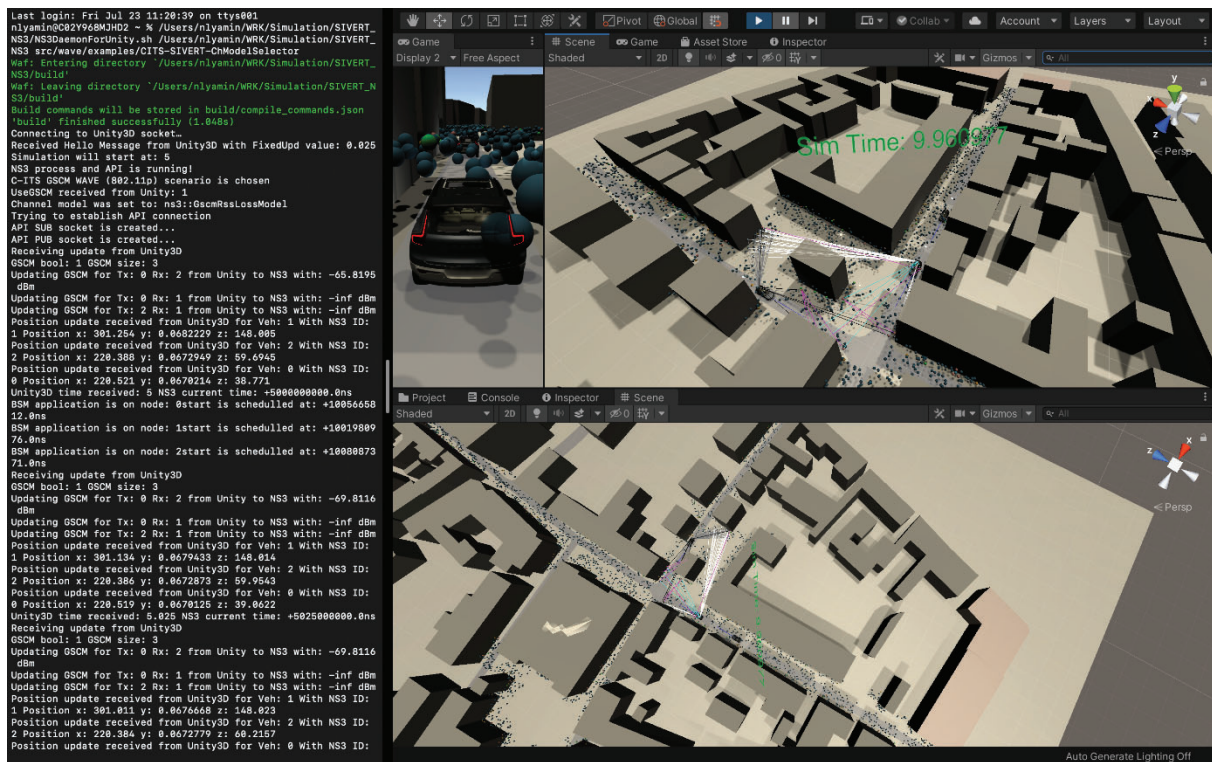

Figure 5.2.1-8: API message is generated and published at the time of BSM reception and received by Unity3D API side on every PhysX update calculation (the PhysX update step could be configured according the precision needs and computational resources available - in this example its value is 0.025s – 25ms).

API is defined currently to accommodate the project target C-ITS scenarios. Subsequently, to accommodate new features API could be easily extended by growing flatbuffer schemas, ZeroMQ patterns using the designed approach to facilitate required data exchange.

5.2.1.6   C-ITS Logic in Simulation Framework

The game logic implemented in Veneris is defined using FluentBehaviourTree paradigm. The paradigm doesn't presume any dedicated GUI builder, constructor etc. It's fully code-based approach. Before start interacting with game logic implementation, one need to get familiar with main concepts of FluentBehaviourTree, i.e. logic trees, nodes (action, sequence, condition, parallel, etc.), tree splicing (nesting), ticks, etc. One could refer to the tutorial from the FluentBehaviourTree's developer. In a nutshell tree progresses on each Update() of the game engine, making a tick. On each step tree nodes can return Success, Failure or Running (each node has to have BehaviourTreeStatus as an output type). Depending on the return of the node the tree progresses accordingly.

The main mobility tree logic is implemented and spliced in MOBILIDMPathTracker class (derived from AIBehaviour). The main tree is activated through AIlogic class for code structure and the rest of the classes with implementation are objects created in AIlogic. The main method to create the mobility logic is GetTree from there the sub-trees are sliced and implemented in other methods throughout the class.

If one needs to alter the default behavior, the obvious way is to splice a sub-tree into GetTree method implementation. In order to facilitate C-ITS scenario logic it has to be integrated into Vehicle AI behavior, i.e. defined in a behavior tree. As part of the SIVERT project we extended the tree with additional

behaviors to accommodate emergency brake and blind intersection crossing scenarios. Further C-ITS scenarios could be implemented into framework using similar approach.

As of PoC example we implement the DoCitsScenario() sub-tree. In this we implement EEBL (Emergency Electronic Brake Light) C-ITS scenario, see Figure 5.2.1-8. Considering the nature of EEBL, we nest its logic in DrivingActions as a condition together with Normal driving and Evasive Maneuver. Obviously, in order to integrate it into SIVERT framework on top of this the job on the API side should be done, i.e. flatbuffers should be extended to accommodate data structures, API class should be extended, NS3 application should be modified accordingly.

5.2.1.7 SIVERT simulation manager description

Simulation manager object implements attached scripts to control bi-directional API exchange, interact with GSCM channel module, select C-ITS logic (if any), communication stack to be used on NS3 side and in GSCM module and control the logging of the simulated scenario. Thus, simulation manager is a main control point to configure the simulation run parameters. It should be noted, however, that the scenario generation methods implemented in Veneris (generation of the scenario from sumo .rou, .net and .poly) are kept unchanged, meaning user should utilize them for initial scenario definition. Currently, SIVERT framework supports two V2X stacks: WAVE 802.11p and rel.14 LTE-V2X mode4. Two PoCs C-ITS logic scenarios are implemented: EEB and blind intersection crossing alert. User also can choose between GSCM model used as input to NS3 spectrum channel model (for both V2X stacks) or simpler path-loss model where we pass gain value for entire beacon transmission from GSCM. Also, it's possible to disable GSCM model and use standard spectrum and pat-loss models available in NS3.

5.2.1.8 V2X communication stacks: LTE-V2X and 802.11p

Currently two V2X stacks are available in SIVERT framework.

1. LTE-V2X Mode 4 module for NS3 implementation. The functionality and implementation of the module is described in "Performance Analysis of C-V2X Mode 4 Communication Introducing an Open-Source C-V2X Simulator" [WP1-5]. Module source code is available at https://github.com/FabianEckermann/ns-3_c-v2x. To enable bi-directionally coupled simulations in SIVERT framework module is subsequently extended to utilize the SIVERT API.

2. IEEE 802.11p (part of 802.11 family since IEEE 802.11.2012 standard) implementation of WAVE module, that is a part of NS3 official distributions. Similarly, module is subsequently extended to utilize the SIVERT API.

For both stacks API provides initial simulation parameters when starting simulation run in Awake() module (together with creating separate thread for NS3 process), i.e. number of vehicles, simulation start time (when all vehicles are added in Unity3D scene), type of channel model used. The passed parameters set could be always easily extended by including them into Initial connection extending the initNSserver configuration. When simulation is running, at each calculated update of PhysX vehicle parameters, GSCM channel and logic are updated, this updates are wrapped to API datastructures and are sent to NS3. NS3 in its turn uses API to exchange updates on the beacons received by vehicles.

5.2.1.9 SQLite based SIVERT data logger and python based plotters

To facilitate the logging capabilities of the framework, SQLite was integrated into SIVERT simulator to collect the simulation logs in structured form. Selected data from each simulation run of SIVERT is logged into SQLite database for further data post processing and analysis. The logging capabilities could be further extended to log the corresponded data of interest. To further present and analyse data the basic python based plotting helpers using sqlite, pandas and matplotlib libraries are implemented.

5.2.1.10 GSCM integration into NS3 Spectrum Channel Modelling approach

To benefit of the extensive NS3 capabilities regarding the wireless PHY channel modelling we re-utilise the spectrum channel modelling approach and spectrum error models from NS3. We extend NS3 with SIVERT-spectrum-propagation-loss and with SIVERT-model-spectrum-channel that implements the spectrum loss model and spectrum channel base classes. As input to the spectrum model we plug in the frequency-dependent spectrum gain implemented and calculated in GSCM in Unity3D and updated by API means for each Unity3D FixedUpdate(). Thus, we supply NS3 spectrum model with much more detailed and precise spectrum gain that is calculated using GSCM and takes closely into account multi-path environment, while benefiting from utilising already implemented interference and noise modules to calculate SINR and error models to calculate the packet reception. As it was mentioned before, user also always could switch to simpler path-loss model where only path loss from GSCM is passed or even turn off the GSCM and use implemented in NS3 path-loss and spectrum models.

5.2.1.11 Geometry based stochastic modelling in Unity3D

Unity 3D Game Engine (Unity) has been used as the core of SIVERT simulation framework. Unity3D provides scripting API via C#. Due to the fact that Unity is a game engine, it has a great variety of helpful built-in methods and classes to easily and efficiently manipulate with 3D objects in real-time:

- Objects control, which is used to control vehicles.

- Ray casting, which is used to trace rays in a Geometry-Based Stochastic Channel Modeling (GSCM).

- Job System and Entity Components System, which are used for parallelization of the radio-channel computation and for enhancing the performance of the whole framework.

5.2.1.11.1 Channel model study: The COST IRACON Geometry-Based Stochastic Channel Model for Vehicle-to-Vehicle Communication in Intersections

The approach presented in [WP1-6] aims to develop an approach for modeling realistic V2V channels based on channel sounder measurements. The authors conducted on-field measurements in four different types of intersections in Berlin, Germany. In the post-processing stage, authors extracted multi-path components (MPCs) and managed to describe the distribution of MPCs first, second, and third orders, as well as dense MPCs (DMCs). In simple words, DMCs can be explained by higher orders of reflections and other EM propagation effects, which are needed to complement the channel model to match with real measurements. Thus, the consideration of DMCs becomes crucial for realistic channel generation: they are highly correlated and give a proper channel profile.

The whole channel modeling approach is designed for 2D environments in Matlab, as shown below.
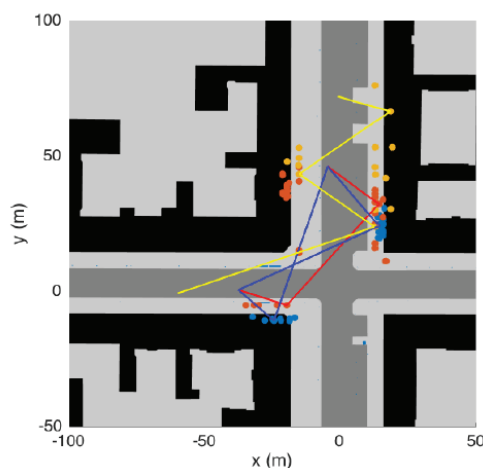
Figure 5.2.1-9. 2D locations MPCs along building facades. Depicted are first, second and third order interactions, shown as blue, red and yellow dots, respectively.

The code is available to the SIVERT team. With a small modification, the developed theory can be extended to 3D for the needs of the SIVERT framework, as shown below.

Scatterers in 2D   Scatterers in 3D
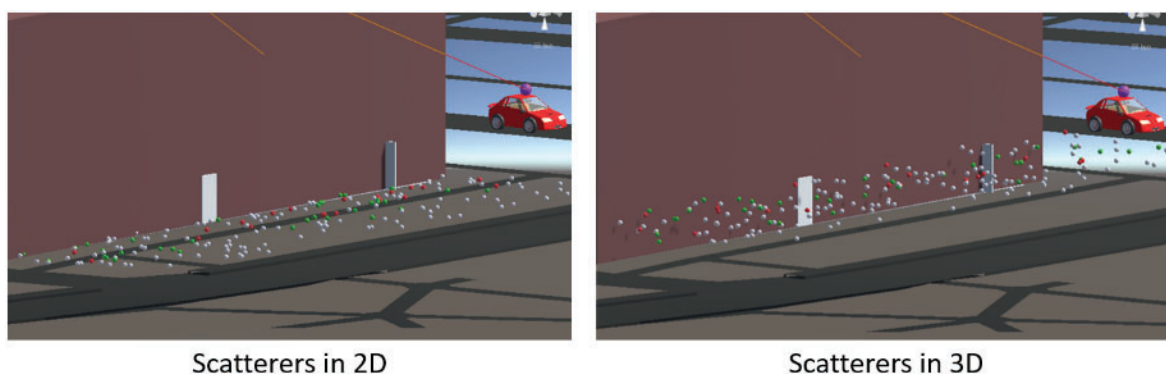
Figure 5.2.1-10. Elevation of the scatterers to a certain level (average antenna level) with a little variation in the heights.

5.2.1.11.2 Implementation of Geometry-based Stochastic Channel Modelling (GSCM) in Unity3D

The whole GSCM framework has been built up from scratch in Unity3D using a C# programming language. The aim of this framework is to enable real-time channel simulation for several V2V channel links.

The **first step** for GSCM is to have a defined 3D objects of the environment of the interest area. The framework utilizes Veneris (and, optionally, any other implementation of mesh object generation frameworks) scene generation. In particular, objects and their corresponding meshes are generated using the real-world data defined in openstreetmap.org. Again, it should be noted, that there are number of object generating tools are available in the open source, which could be used instead of Veneris to

generate the object and utilize for GSCM computations. The main input to the SIVERT GSCM implementation are meshes that correspond to the building on the scene.
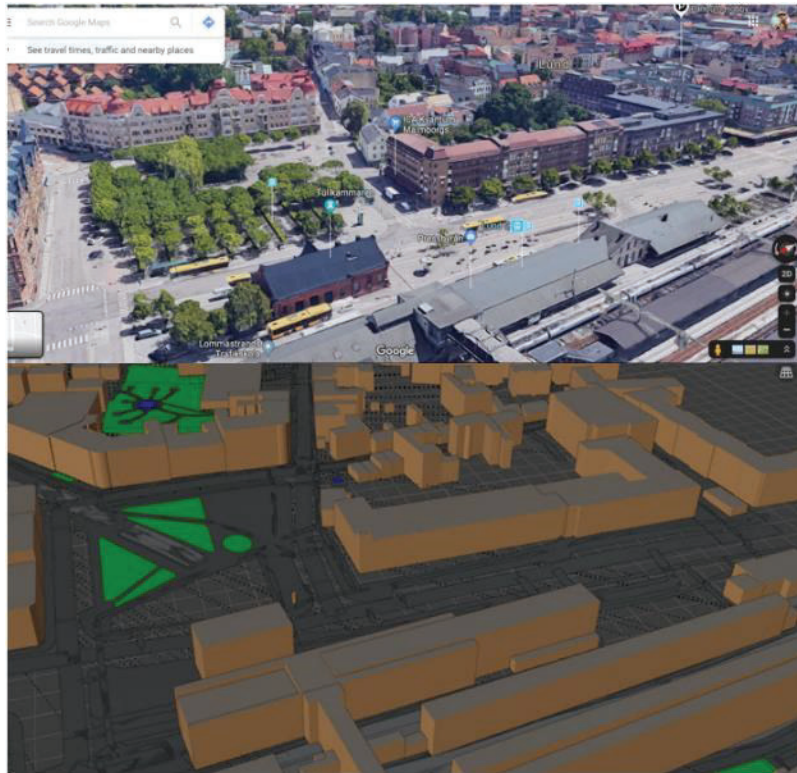
Figure 5.2.1-11. Lund C area: 3D photoshoot from google maps on the top and its generated version in Blender without vegetation and other small details.

The **second step** is to spawn the MPCs and DMCs around the buildings of interest.
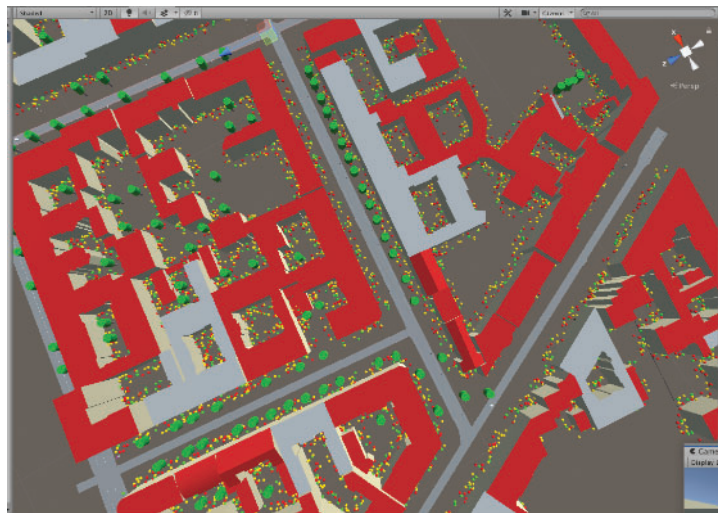
Figure 5.2.1-12. Scatterers spawning around buildings. Note, DMCs are not depicted in this picture.

The distribution of the MPCs is taken from the COST IRACON GSCM. For further details, refer to the paper. Note, the number of MPCs can be quite big, which leads to the complication of the real-time simulation.

The **third step** is to assign the Tx/Rx antenna object to the corresponded vehicles in the simulation. The position of the antennas will have influence on the multi-path estimation, due to the observed reflectors and scatterers. Obviously, when a vehicle is moving on the scene in the simulation run, the position of the transceivers are constantly changing, which means that the channel calculation is updated at each Unity3D update.
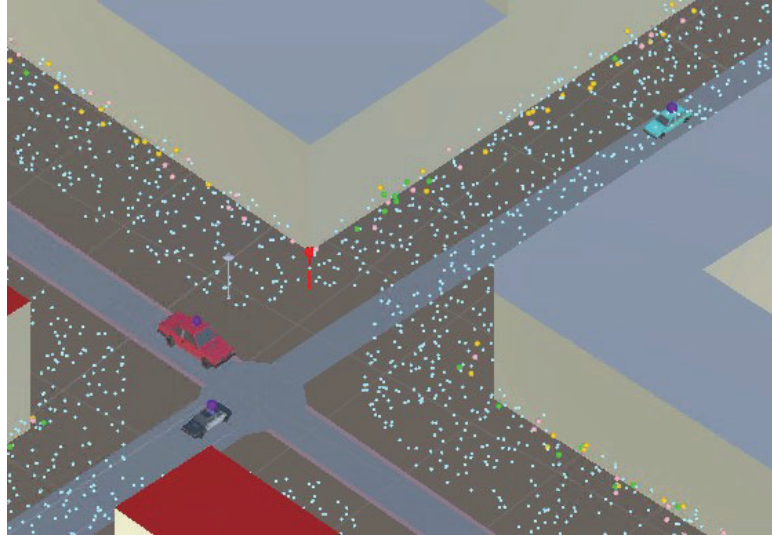
Figure 5.2.1-13. Three vehicles are moving in a scenario. Note, DMCs are depicted as cyan spheres.

The **fourth step** is to calculate channels for all links (all pairs of vehicles) based on the observed MPCs and DMCs and the Tx/Rx antenna positions in each update. This step becomes computationally extensive. To enable real-time channel calculation, extensive optimization work has been done.
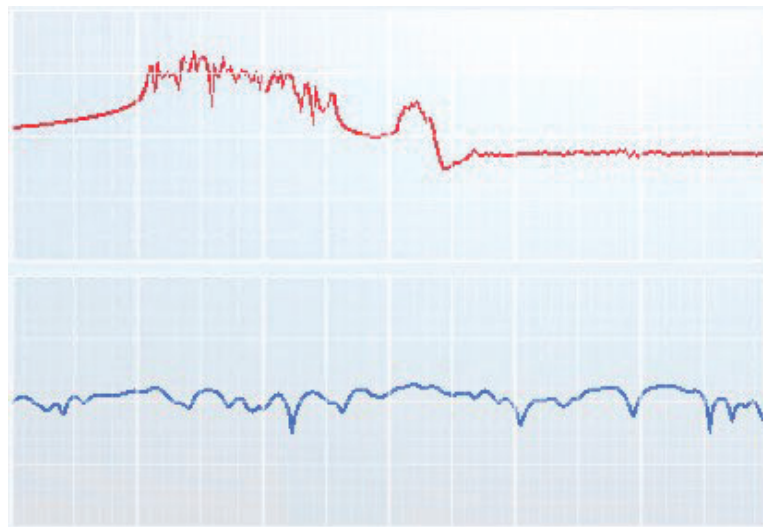
Figure 5.2.1-14. Channels in the time domain on the top and in the frequency domain on the bottom.

The **fifth step** is to take into account antenna radiation pattern. Depending on the direction of departure from a transmitting antenna and the direction of arrival to a receiving antenna, the attenuation and phase of a received signal change following the antennas' radiation patterns. When it comes to a 3D multi-path propagation environment, all paths depart and arrive with different elevation and azimuth angles. This effect has also a significant role in the whole communication performance. Thus, the antenna radiation pattern feature should be carefully accounted for. For an analytically described antenna radiation pattern, its implementation does not increase the computational complexity significantly. In channel

simulation scripting, an analytical formula can be written as a single code line, making the accounting of radiation patterns as effective as it can be.

3D Radiation pattern   Radiation pattern in the horizontal plane
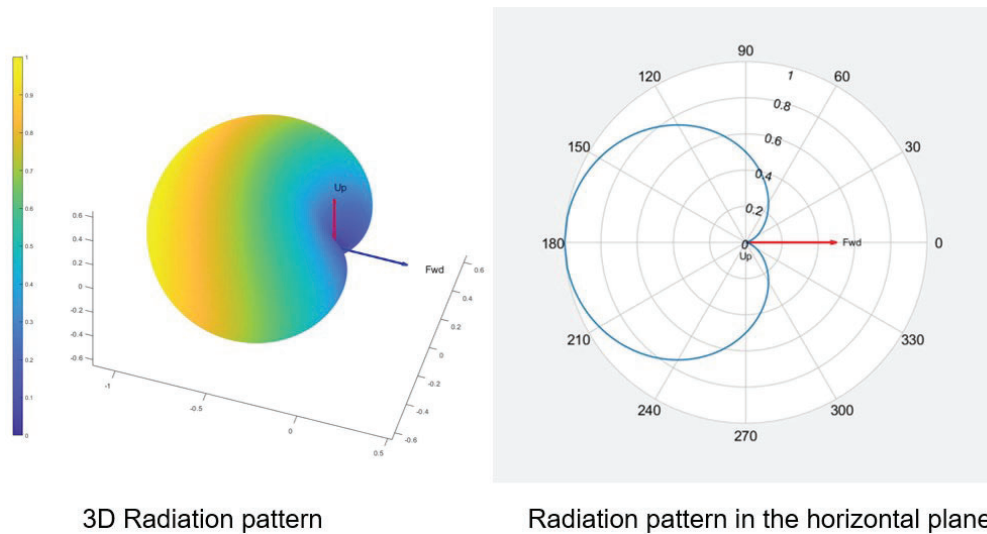
Figure 5.2.1-15. An example of analytical antenna radiation pattern.

However, implementing a realistic antenna radiation pattern may require additional focus on the computational performance of the Effective Aperture Distribution Function (EADF) since it is no longer a single code line, but an independent function with many parameters and operations such as an inverse Fourier transform and other forms of transformation.

5.2.1.11.3 EADF implementation antenna radiation pattern description

A standard theory of EADF has been used in the current SIVERT framework implementation. In the standard theory, it is assumed that an antenna measurement is done in 3D. In our case, when we have a real pattern, the measurements are done in 2D. Thus, we used a straightforward approach on extending antenna measurements from 2D to 3D: exact values on the horizontal plane and gradually decreasing to zero values with the increase of the elevation angle. Note, due to a rough granularity of the measurements' sampling, the reconstruction of the pattern may have some inconsistency, as illustrated in Figure 5.2.1-16. Our recommendation is to have a proper format of 3D antenna radiation pattern measurements with a high angular resolution, ideally, with angular step no more than 1 degree. If the measurements are formatted properly, the framework can use standard EADF algorithms, which are computationally efficient. Otherwise, an additional study on the extension of the EADF approach has to be done to overcome the inconsistency issues.

In the current implementation, we are using the straightforward approach. At first, the EADF and all pre-works are calculated in Matlab, and then the resulting EADF is imported as a CSV file into the SIVERT framework. Further weighting coefficients are calculated in the GSCM implementation in Unity parallel manner.
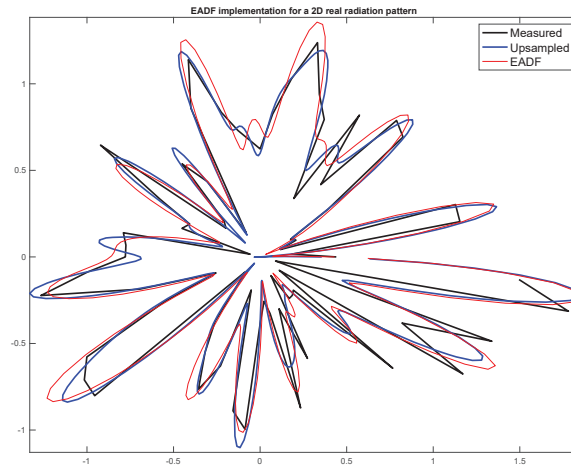
Figure 5.2.1-16. An example of reconstruction of a real antenna radiation pattern.

5.2.1.11.4 Performance optimization

As mentioned in the second step of GSCM implementation, the number of MPCs can be prohibitively enormous. Thus, the real-time computation of all channel links becomes nearly impossible. Due to this problem, a huge effort has been put into performance optimization.

Reduction of the number of unnecessary objects:
A straightforward approach is to remove all unnecessary interactive objects from the scene, such as unseen MPCs and buildings.
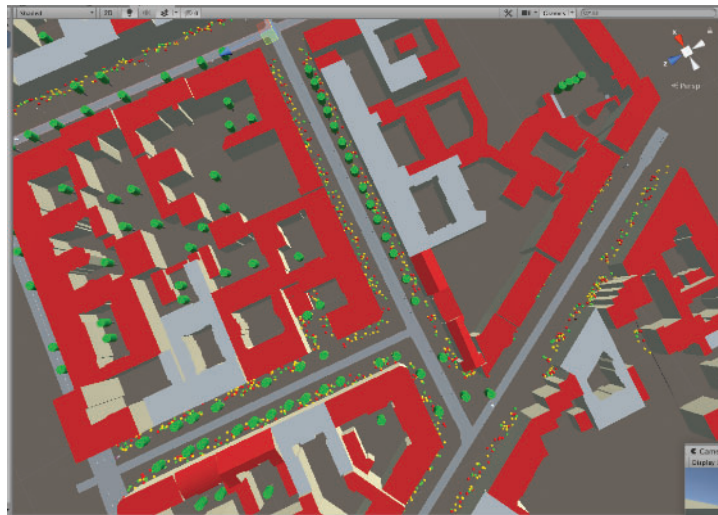
Figure 5.2.1-17. All unseen MPCs are removed from the scene. In comparison with Fig. 5.2.1-12, the number of MPCs is reduced from 18700 to 3360 elements. Unnecessary buildings are not removed yet.

To remove unseen MPCs, observation points have been regularly placed on the roads along which vehicles are moving. All MPCs are then checked on reachability. Once an MPC is reachable, it is kept in the scene; otherwise, it is removed. In the same way, unseen buildings are inactivated during the simulation.
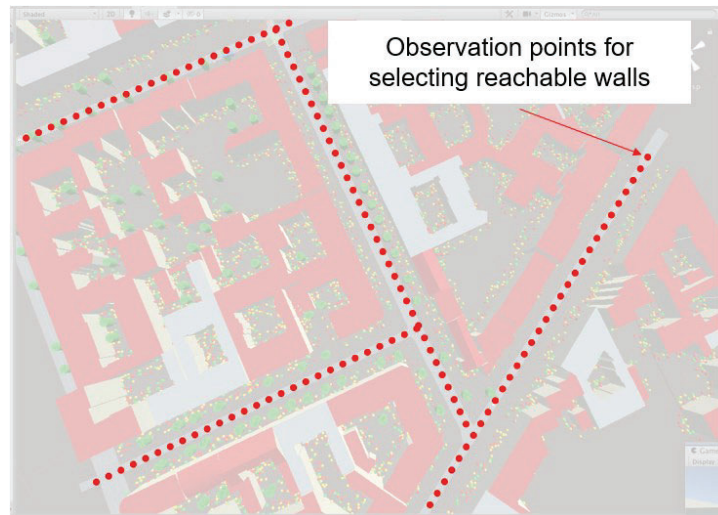
Figure 5.2.1-18. Placing observation points along roads.

Lookup tables:

Further complexity reduction can be achieved by introducing lookup tables for the second- and third-order of MPCs. Each MPC can see only a few other neighboring MPCs. Since the MPCs are static, their relations in terms of visibility are not changing. Hence, the list of seen MPCs, distances, and attenuations (in other words, channels between MPCs) can be pre-computed in the beginning of each iteration and saved as a lookup table to be used during Unity3D updates. For this purpose, each MPC gets its unique identity number (ID). Further call of an MPC is done by its ID. The acceleration of scripts' execution can be around 40 times.

	Seen MPCs' IDs					
MPC 1	2	8	10	31	62	
MPC 2	1	6	10	31	54	
MPC 3	4	7	13	99		
MPC 4	3	8	23	30	74	105
....						

Figure 5.2.1-19. Schematic visualization of a lookup table.

Parallelization of all FOR loops:

Another most powerful advantage of Unity3D is that it has a well-defined *C# Job System*, which allows writing simple and safe multithreaded code that interacts with the Unity Engine for enhanced game performance. This system significantly changes the way of scientific programming, allowing high-performance scientific applications. In the current GSCM implementation, the use of the Job System together with Entity Components System (also built-in scripting API) can increase the speed of the channel calculation script execution up to 100 times. Incorporating this new programming way took a huge team's effort, which leaves room for future channel simulation performance improvement. It is worth noting that the final integration of Job System into Unity3D was done in the mid-2020. Before this time, the Job System was under development (in other words, in the preliminary stage), and many bugs still were there, making its use challenging. However, Job System was incorporated into GSCM computation at the later stage of the project, considering the significant aforementioned performance boost and the plan to have a room for further framework development.
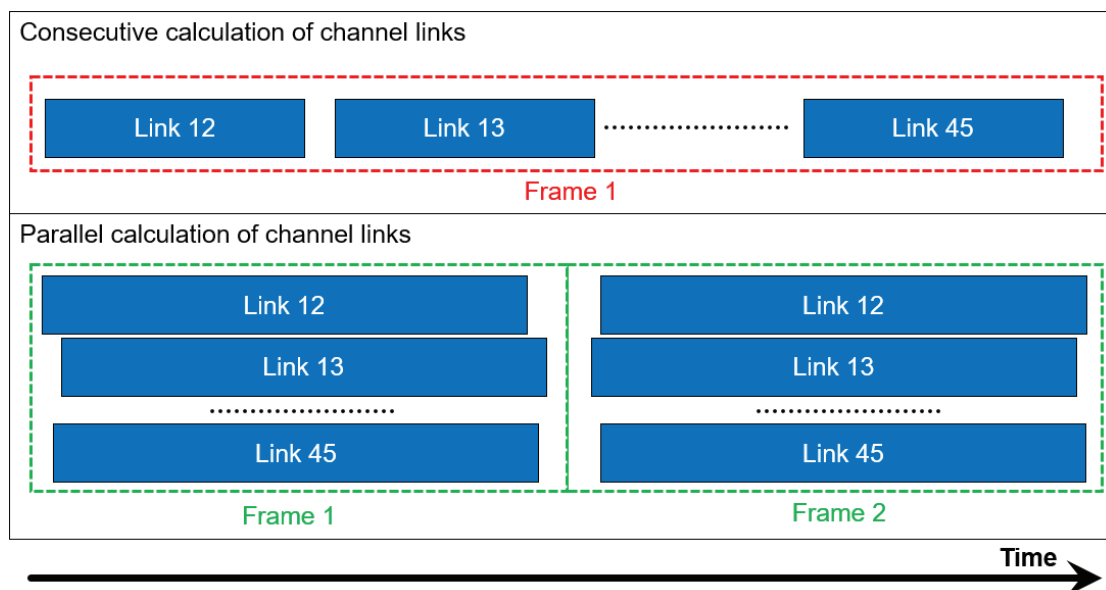
Figure 5.2.1-20. Comparison of channel links calculation in consecutive and parallel paradigms.

The main issue of the Unity3D Job System programming is that it needs exploitation of such called NativeContainers. Native containers are new container types that allow a job to access safely data shared with the main thread rather than working with a copy. In other words, the shared data use accelerates memory access and voids repetitive copying of data from different memory places. In the current GSCM implementation, the use of the Job System together with Entity Components System (also built-in scripting API) can increase the speed of the channel calculation script execution up to 100 times. The ECS allows keeping information of the interacting objects compactly (while without ECS, the bits of information of an object is spread over the whole allocated memory), accelerating memory access. Incorporating this new programming way took a huge team's effort, which leaves room for future channel simulation performance improvement.

Figure 5.2.1-21. Unity3D Profiler shows the channel modeling execution time. On the top, the performance of channel calculation for two vehicles without the Job System and ECS. On the bottom, the performance of three channel links calculation for three vehicles with the Job System and ECS.

5.2.1.11.5 Blind intersection warning C-ITS scenario modeling example

Here we present an example of the C-ITS scenario study, data collected and analytics results. We demonstrate the capabilities of the SIVERT framework by comparing 3 different reference antennas.

As an example we study the intersection scenario depicted on Figure 5.2.1-8. In this scenario the following convention (from Unity) is applied here-forth: vehicle that approaches intersection from the right - aka Vehicle 1, Vehicles approaching from the bottom are Vehicles 2 (closer to intersection) and Vehicle 0.

For demo purpose we create 3 simple reference antennas with simple patters: isotropic and two dipole with orthogonally oriented lobes, Figure 5.2.1-22. Dipole antenna with lobes oriented in parallel to the vehicle front direction. Dipole antenna with lobes oriented perpendicular to the vehicle front direction. Isotropic antenna with 0dB.

To produce the below figures C-ITS scenario with each antenna was run 50 times (150 runs in total). We evaluate the stretch of time between 5s when all the vehicles are inserted into the simulation at the beginning of the corresponding streets and start communication exchange till the time vehicles 1 and 2 meet at intersection, which is time interval between 5s and 11s. The statistics is aggregated from 50 runs for corresponding reference antennas. Each simulation run creates a sqlite database as output, data from which are processed and aggregated using helpers written in pyhton.

First, we evaluate the LoS channel when using 3 reference antennas between vehicles 2 and 0 that are moving in the street canyon, Figure 5.2.1-23. All RSS plots below will demonstrate the mean and standard deviation calculated from simulation runs using seaborn python package capabilities for statistical graphics.
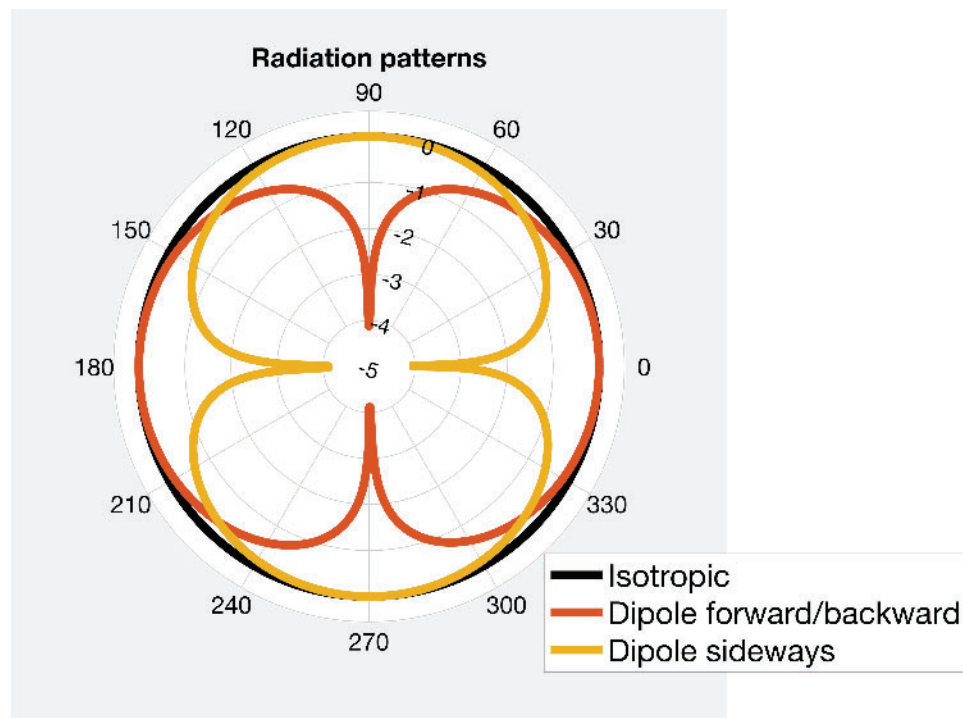
Figure 5.2.1-22. Three reference radiation patterns in 2D used for PoC comparison in Blind intersection crossing alert C-ITS scenario

Figure 5.2.1-23. LoS channel for 3 reference antennas.

Below, on Figure 5.2.1-24 we present the same statistics for NLoS channel between vehicle 2 and 1 driving on perpendicular roads of the intersection.
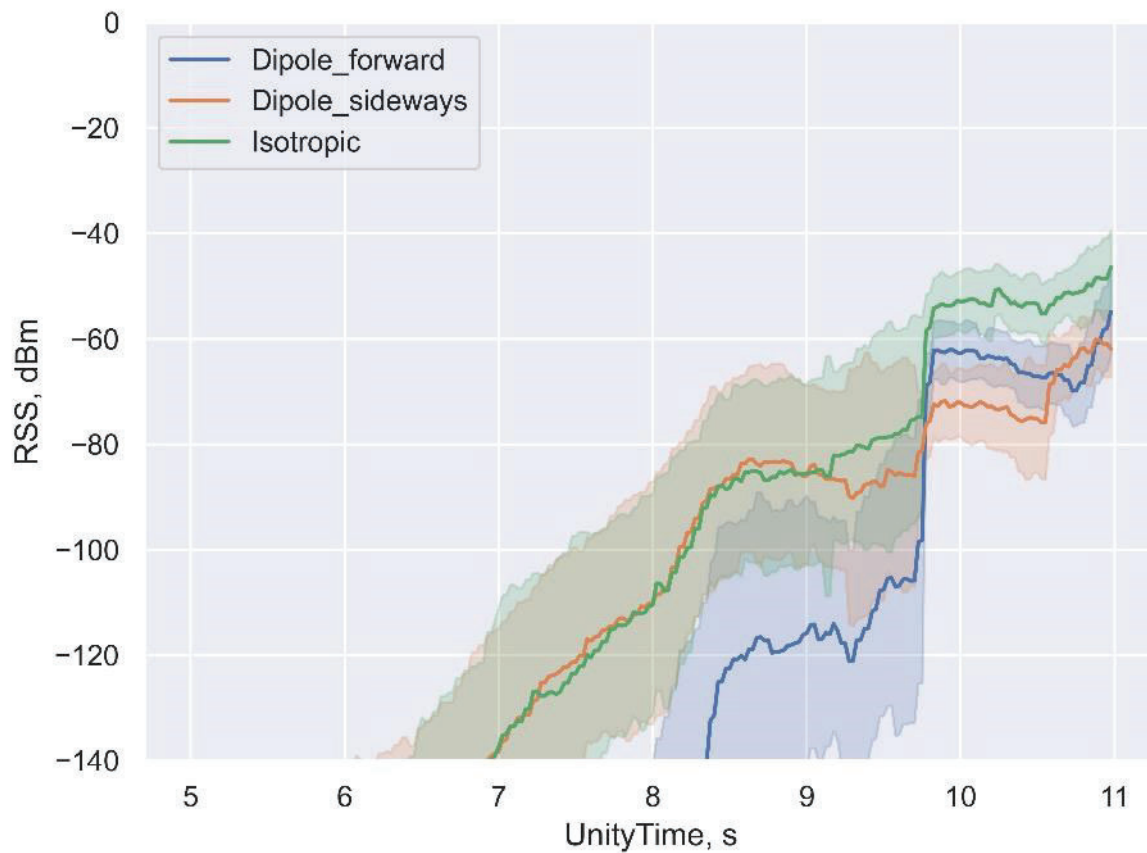
Figure 5.2.1-24. NLoS channel for 3 reference antennas.

Below, on Figure 5.2.1-25, we present the scatter plot for the raw data from all simulation runs that were used in producing statistics on Figure 5.2.1-24.
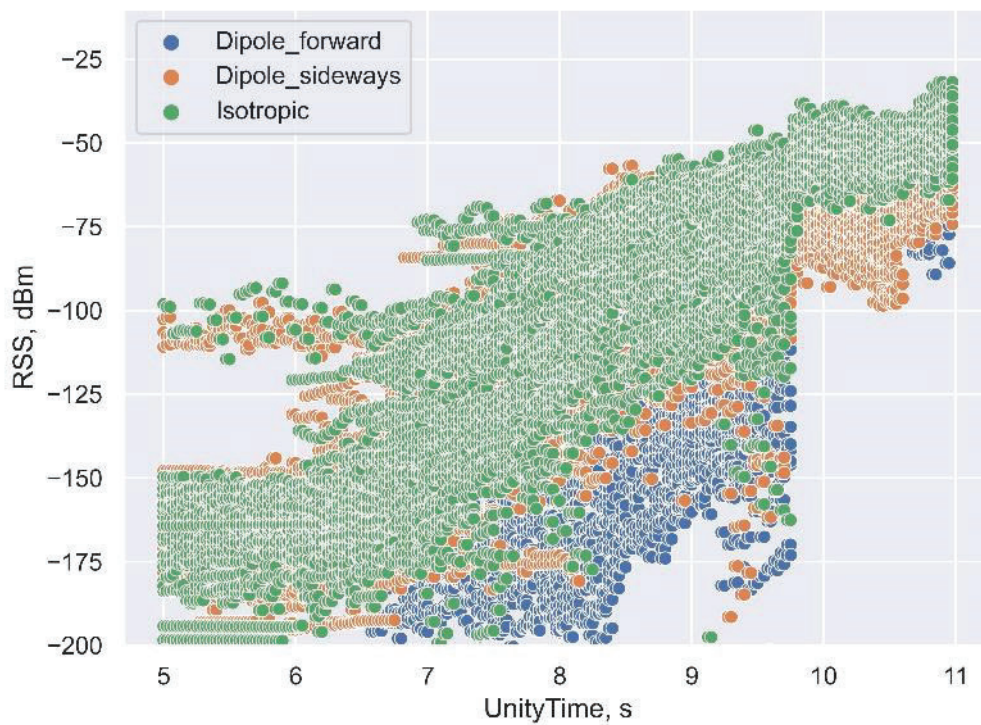
Figure 5.2.1-25. NLoS channel scatter raw plot for 3 reference antennas.

Note, that strong signal dips appearing in the 9-10s interval on Figure 5.2.1-24 are caused by the fact vehicle passing a small buiding that creates strong shadowing and mainly eliminates possibillities of 1st and 2nd order reflections eventhough the distance between vehicles decreeses. This demonstrates the signal propagation particularities in complex urban surroundings that would be nearly impossible to achieve with conventional path-loss models that are not utilising signal ray tracing capabilities.

As example of the application metric, we demonstrate the box plot of the manhattan distance between two vehicles for different simulation runs for each antenna of the first warning message received from vehicle 1 by vehicle 2 on Figure 5.2.1-26 below. In C-ITS simulation run vehicle 2 would start emergency braking upon reception of this message.
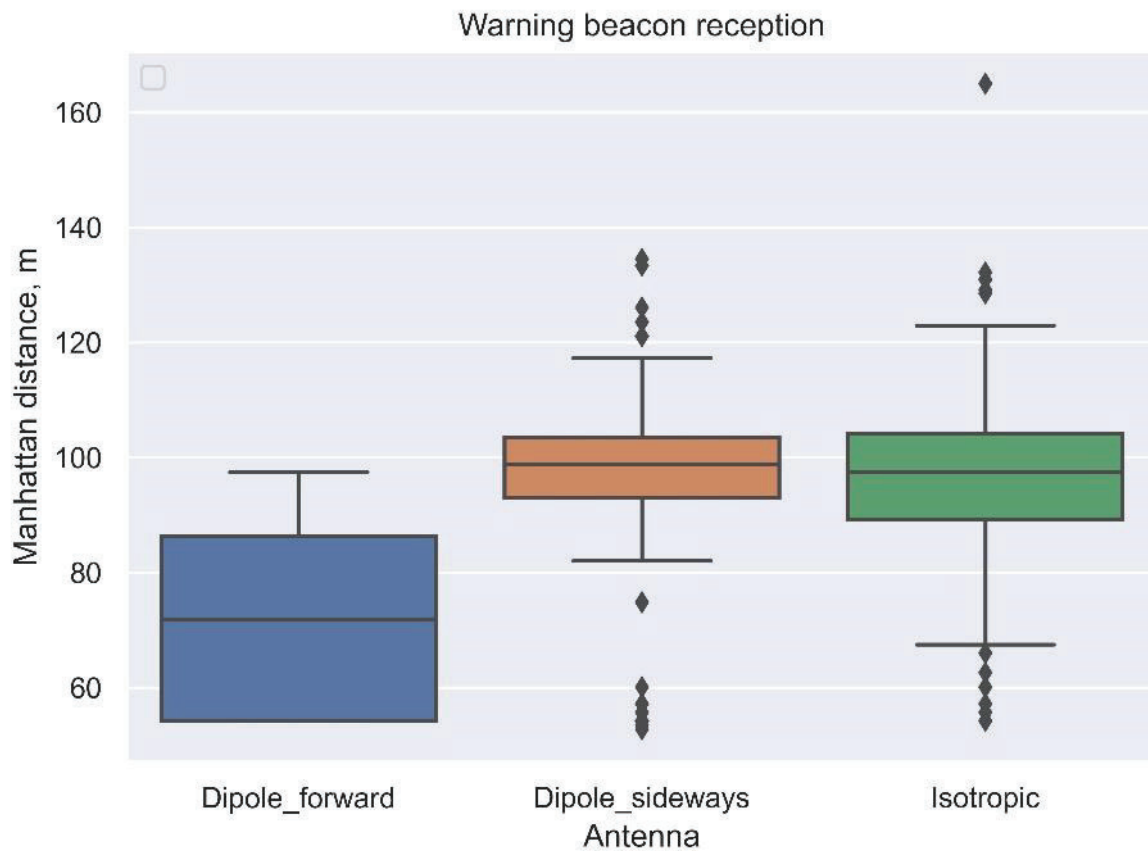
Figure 5.2.1-26. NLoS channel scatter raw plot for 3 reference antennas.

Two figures below show the beacon reception probability for varios sensitivity thresholds. Probability calculated is a probability that at certain Manhattan distance between vehicles 2 and 1 the RSS calculated by GSCM exceeds the threshold. We first present probability for Isotropic antenna with higher Manhattan distance bin resolution at Figure 5.2.1-27. Then we show comparison for all three reference antennas on the single plot with slightly lower resolution to be able to squize them on the same Figure 5.2.1-28.
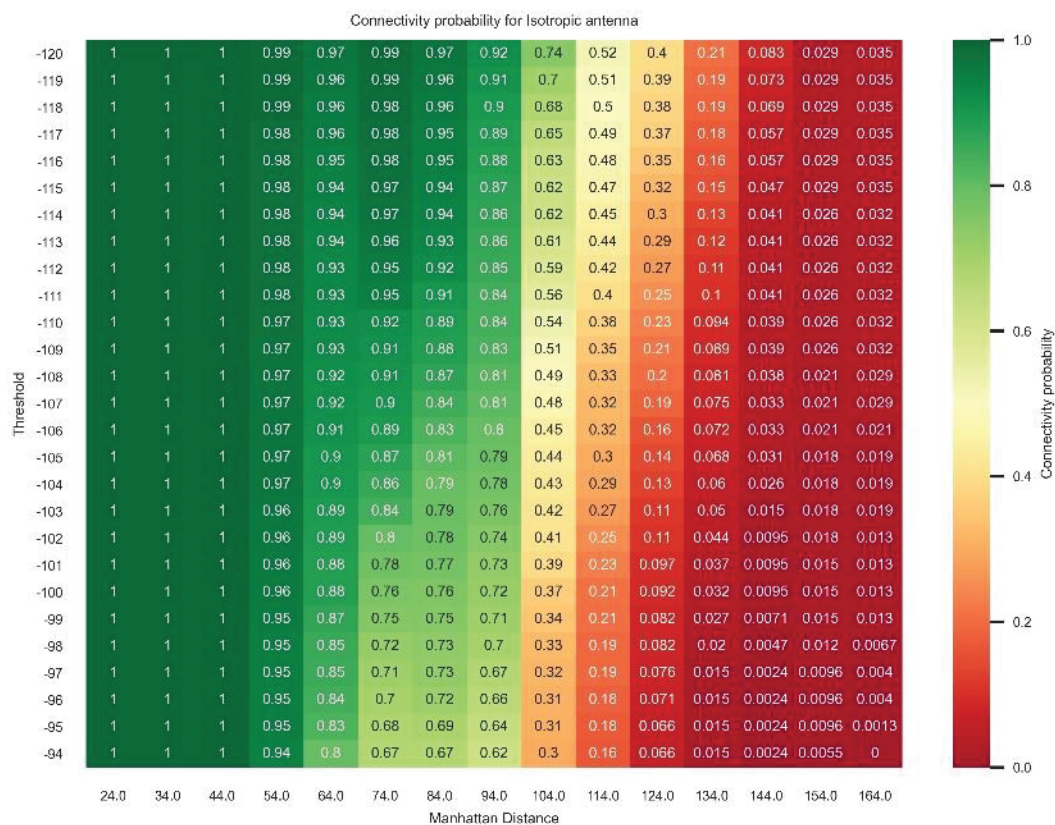
Figure 5.2.1-27. Connectivity probability heatmap Isotropic antenna in intersection for various sensitivity thresholds.
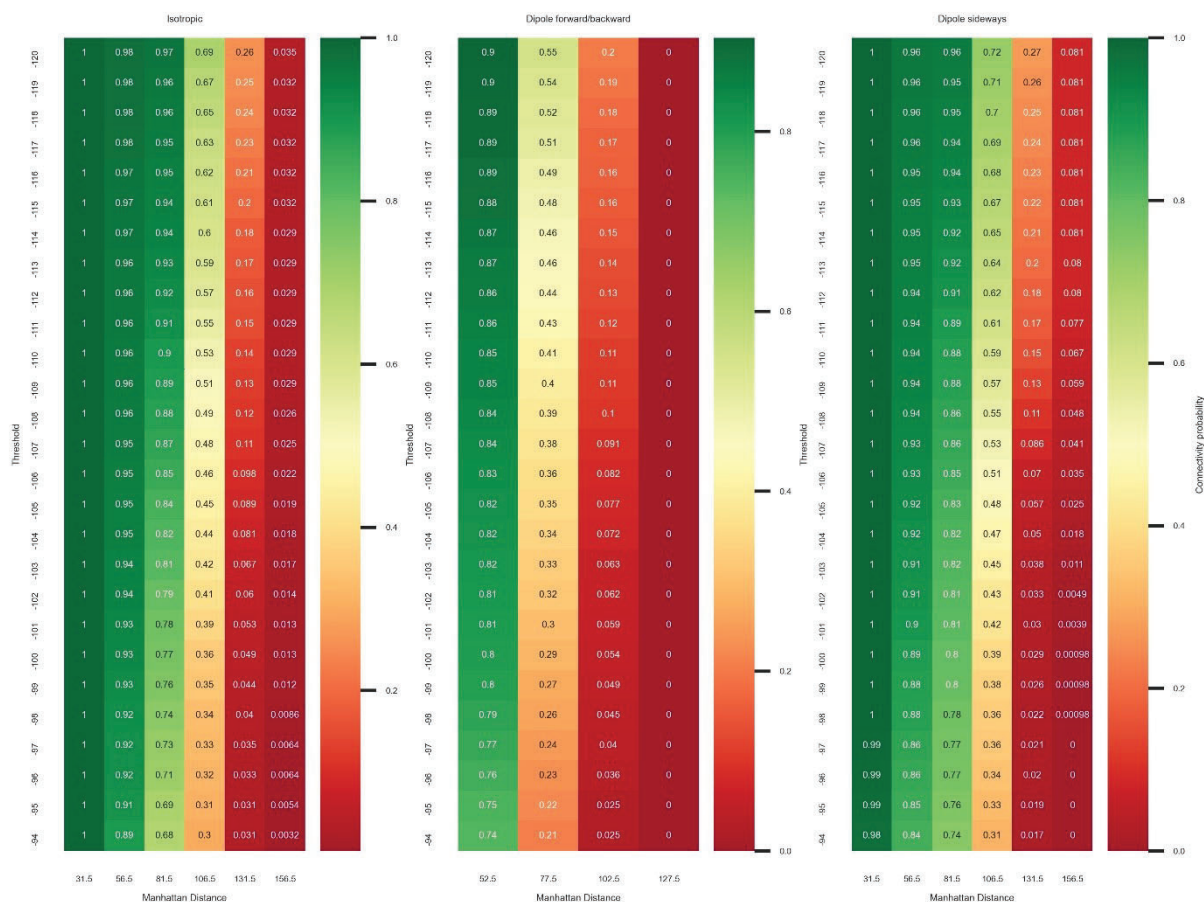
Figure 5.2.1-28. Connectivity probability heatmap antennas comparison in intersection for various sensitivity.

As a closing remark we present the frequency plot of the RSS distribution calculated for all simulation runs for various antennas for NLoS channel between vehicle 1 and 2 on Figure 5.2.1-29.
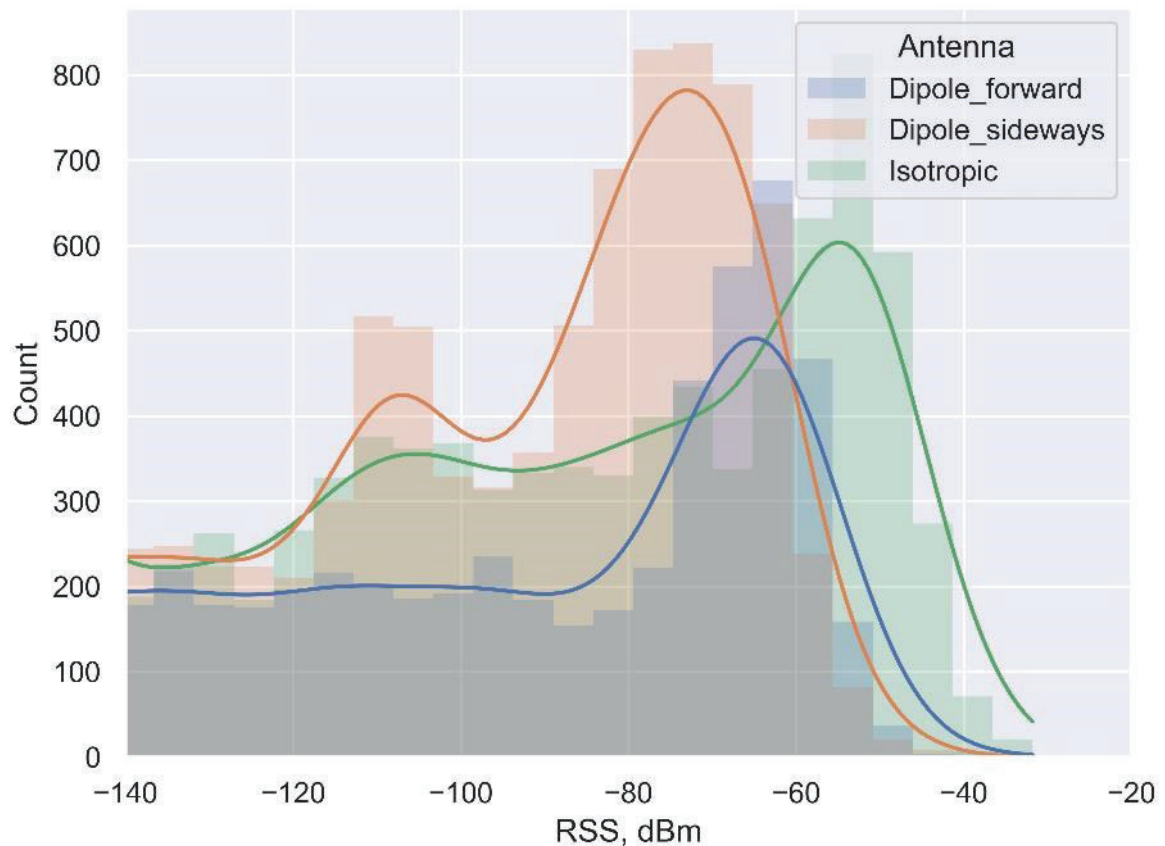
Figure 5.2.1-29. NLoS channel scatter raw.

We would like also to emphasize here that due to the architecture of the developed simulation framework which combines and extending NS3 and Veneris simulators it inherits the comprehensive logging capabilities and allows to add new KPI's of interest. Saying that, interested user depending of the objectives of the study, could collect and analyze very wide spectrum of the variables. NS3 provides rich logging capabilities in each module, which means that all the stack/communication related parameters, like information about transmitted, received beacons, Phy/Mac/Network/Facility layer parameters observed during simulation runs could be logged for both technologies utilized. Additionally, as mentioned in section 5.2.1.9 we implemented SQLite logging capabilities in Unity3D, to directly easier log and retrieve various KPI related both to communication (messages sent/received, GSCM values calculated, etc.) and vehicle (vehicle positions, speed, heading, acceleration, etc.) parameters to be able to process them for calculation of various KPI's distributions, e.g. time and probability distributions of different messages received, inter-vehicle distances, time to collision, connectivity probabilities, to name few, as was presented in the example above.

5.2.1.12 References

[WP1-1] J. Raghothama, M. Azhari, M. R. Carretero and S. Meijer, "Architectures for distributed, interactive and integrated traffic simulations," *2015 International Conference on Models and Technologies for Intelligent Transportation Systems (MT-ITS)*, Budapest, Hungary, 2015, pp. 387-394, doi: 10.1109/MTITS.2015.7223284.

[WP1-2] J. Raghothama, M. Azhari, M. R. Carretero and S. Meijer, "Architectures for distributed, interactive and integrated traffic simulations," *2015 International Conference on Models and Technologies for Intelligent Transportation Systems (MT-ITS)*, Budapest, Hungary, 2015, pp. 387-394, doi: 10.1109/MTITS.2015.7223284.

[WP1-3] Olaverri-Monreal, C.; Errea-Moreno, J.; Díaz-Álvarez, A.; Biurrun-Quel, C.; Serrano-Arriezu, L.; Kuba, M. Connection of the SUMO Microscopic Traffic Simulator and the Unity 3D Game Engine to Evaluate V2X Communication-Based Systems. *Sensors* 2018, *18*, 4399. https://doi.org/10.3390/s18124399

[WP1-4] E. Egea-Lopez, F. Losilla, J. Pascual-Garcia and J. M. Molina-Garcia-Pardo, "Vehicular Networks Simulation With Realistic Physics," in *IEEE Access*, vol. 7, pp. 44021-44036, 2019, doi: 10.1109/ACCESS.2019.2908651.

[WP1-5] "F. Eckermann, M. Kahlert and C. Wietfeld, "Performance Analysis of C-V2X Mode 4 Communication Introducing an Open-Source C-V2X Simulator," *2019 IEEE 90th Vehicular Technology Conference (VTC2019-Fall)*, Honolulu, HI, USA, 2019, pp. 1-5."

[WP1-6] C. Gustafson, K. Mahler, D. Bolin and F. Tufvesson, "The COST IRACON Geometry-Based Stochastic Channel Model for Vehicle-to-Vehicle Communication in Intersections," in *IEEE Transactions on Vehicular Technology*, vol. 69, no. 3, pp. 2365-2375, March 2020, doi: 10.1109/TVT.2020.2964277.

5.2.2 Work Package 2: Component verification

This work package has two main deliverables, setup and evaluation of a field logging tool and feasibility study of a virtual drive test setup. Results for each of these are described below.

5.2.2.1 Field logging tool

A field logging tool is used for recording data from a cellular chipset when operating in real cellular networks. This data can be used to evaluate the performance of the chipset and/or antenna connected to the chipset or saved for later playback in the lab so to enable repeatable testing without the need for an additional drive test (VDT, see below). This section focuses on the evaluation of different field logging tools commercially available, how to set these up to enable appropriate logging and how to appropriately analyze the large amount of data collected. Test scenarios are defined, and example results for the selected field logging tool provided. The results from drive tests using this tool have also been compared to lab testing, to validate the drive tests.

5.2.2.1.1 Test tool selection

There exist different field logging tools and their functionalities are quite similar. Some examples are ROMES4 from Rhode&Schwarz and Nemo from Keysight. In addition to this, each chipset manufacture also provides some logging capabilities via dedicated tools, such as QXDM for QUALCOMM and Shannon for Samsung. These have more of a diagnostic focus and are using different interfaces such as Android debug bridge (ADB), modem (AT Commands) and diagnostic interface.

Comparing the two commercially available tools mentioned above, major differences that have been found are based on limitations of using different functionalities, user friendliness of the tool and the way how different tools illustrate the results. Both tools have pros and cons. For example, ROMES4 offers the possibility of extracting parameters in real time through TCP/IP socket, while Nemo tool is more advanced in locking features. The choice of tool is therefore dependent on test scenarios of interest. The tools were evaluated on a wide range of parameters, such as forcing features, MIMO parameters, flexibility, L3 signaling, latency, hardware constraints, fees, GPS integration and export file formats etc. After evaluating these two different test tools, it was decided that the ROMES4 tool provides most benefits for this project.

5.2.2.1.2 Key performance indicators

The cellular modem reports numerous parameters as part of its diagnostics that can be used for evaluating the performance of the device. These parameters can be extracted using the ROMEs tool. However, since there is a large amount of data reported, smart decisions and configuration of the tool needs to be done, to extract the parameters that provide the most useful results. Such parameters will be referred to as Key Performance Indicators (KPIs). Figure 5.2.2-1 shows some of the parameters available. A complete list of KPI's can be found in the ROMES4 Manual.
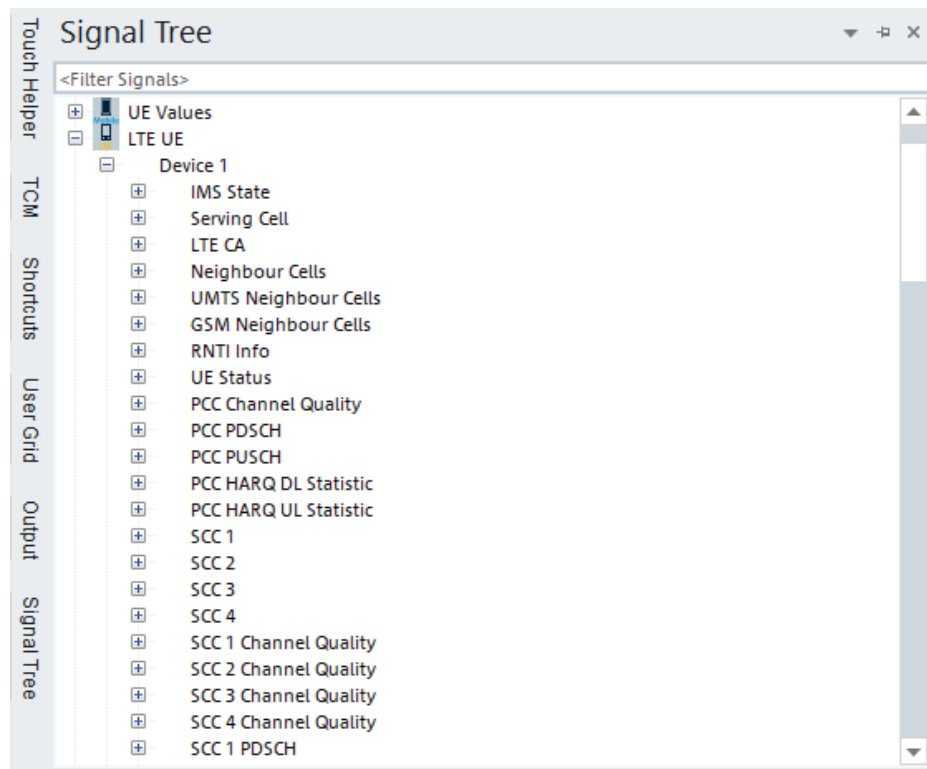
Figure 5.2.2-1. Snapshot Signal Tree in ROMEs Tool with all parameters section.

Many of the KPI's are important when analyzing the drive test, as all of them describe some specific performance for the DUT. In the analysis that has been performed on this document, the main assumption is that testing is done between two devices which at the same moment are connected into the same cell, share the same resource blocks, and have the same available power. In this way we can narrow down the focus and count everything else as part of the system, which seems to be quite fairly shared between two devices most of the time.

When performing field tests using two devices, one important error source is resource allocation for the two units. If the resource allocation is not the same for the two devices, the results are not comparable. Some of the parameters that can be extracted by ROMEs can be used to verify this.

For the performance evaluation, the following KPIs have been used in this study:

- o **Throughput**: This is the main KPI when benchmarking different units, it indicated how much data rate is possible to achieve with the device for the current network resources. This indicated how good the automotive unit is versus the reference device. Provides a clearer indication if one device is a bottleneck on the network if the performance of one unit has degraded a lot compared to the reference device.

- o **RSRP and RSRQ**: RSRP shows the signal power level for each antenna which indicated how good the antennas of the device are in correlation with the channel behaviors. While RSRQ indicates the quality of the channel which the device is being served. These two parameters give us a clear indication of expectation of the data rates from the device..

5.2.2.1.3 Drive test scenarios and performance evaluation

In order to perform a full analysis of the telematics unit, different test scenarios should be analyzed to make sure that the automotive telematic is performing well and the user experience is good. Therefore, to confirm and validate that the unit does not have any fault with the behavior and performance different stages should be taken into account. This helps to avoid errors and have over time info on how a specific unit has developed and encountered a problem or performance issue. The following stages have been considered for checking the status, behaviors and performance of the unit.

Stage 1 - Basic Test Case

This stage is to confirm that the device has the necessary capabilities and right configuration. Can mainly be used during the development phases of telematics. Example checklist is given below.

      i.   Check if Sim Card is ready

     ii.   Check that we have the right APN

    iii.   Check that the device has an IP

    iv.   Connection & Attach Procedure

     v.   Check all antennas are connected

This stage is a pre-requisite to pass in order to continue the test in other stages. It is normally performed in an office or lab environment.

Stage 2 - Behavior Test Case

These test cases are tested to make sure that the DUT can float and can make wise decisions during the selections of the band or cell. Meanwhile, certain algorithms or configuration of the Device should not affect the floating performance. Typical tests in this stage are handovers and cell re-selections, as well as roaming at border crossings. It is normally performed in an urban/suburban or tunnel scenario.

Example results from a handover test case can be found in Figure 5.2.2-2, where the logged physical cell ID is compared for an automotive telematics unit and a reference device.

Figure 5.2.2-2. Handover testing for an automotive telematics unit (upper part of figure) and a reference device (lower part of the figure). The different colors indicate connection to different cells. The parameters for each device were logged simultaneously using the same MNO. As can be seen, there are some differences in cell allocations.

Stage 3 - Performance Test Case

This stage confirms the capability of the unit in terms of performance if the necessary and possible data rate can be achieved. Performance tests should be carried out using both good and bad network coverage, to get a comprehensive understanding of the performance of the device under test. A specific area may also be chosen if a specific feature should be investigated, for example, cell edge performance. These tests are thus normally performed in a rural or suburban environment. KPIs are usually throughput or RSRP.

5.2.2.1.4   Proof of Concept

This subsection will provide results from the different drive test scenarios with a focus on rural and suburban areas, to prove that the test scenarios outlined in the former section provide correct performance evaluation. In order to do so, drive tests using reference antennas with known bad and good performance will be used. These antennas both consist of dual element (2x2 MIMO), which has been tuned to good and bad correlation and efficiency values [WP2-1]. The reference antennas will be connected to an automotive telematics unit.

Antenna performance comparison

These tests have been performed by comparing the performance of the bad and good reference antennas. The antennas are each connected to similar automotive telematics units, which both have the same chipsets and thus should have the same performance. The drive test has shown that the areas of interest are Rural and Suburban environments with low RSRP values, by excluding the Urban areas. The reasoning is that in Urban environment there are very high RSRP levels, where it is not possible to see differences in throughput between different antennas. Therefore, the drive test has been performed on route A (Rural) and route B (Suburban) as shown in Figure 5.2.2-3.
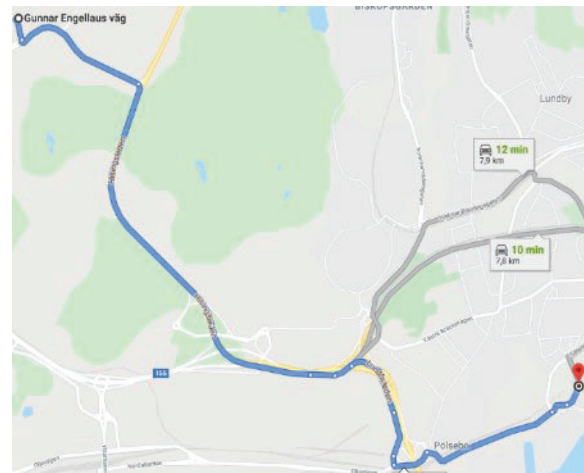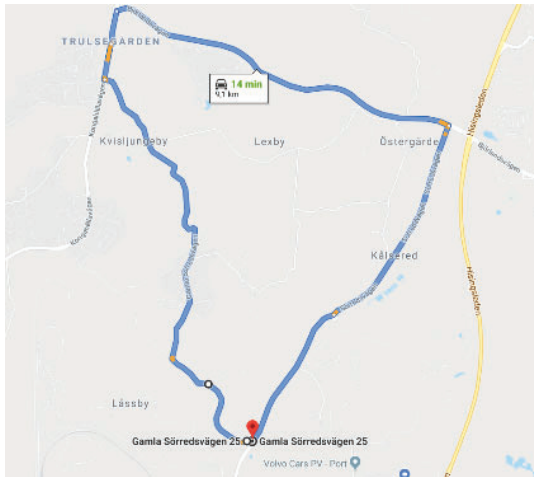
Figure 5.2.2-3. Route A in Torslanda (left) and route B, VCC to Eriksberg (right).

Measurements were performed on band 20 (commercially available for route A and B). In this setup, a relative comparison between the integrated antenna in a telematics connectivity unit and two reference antennas is performed (see Figure 5.2.2-4). Firstly, the Integrated antenna and good antenna are being tested simultaneously in a drive test and then in another drive test the Integrated Antenna and Bad antenna are tested. More details for the drive test can be found on i Table 5.2.2-1.
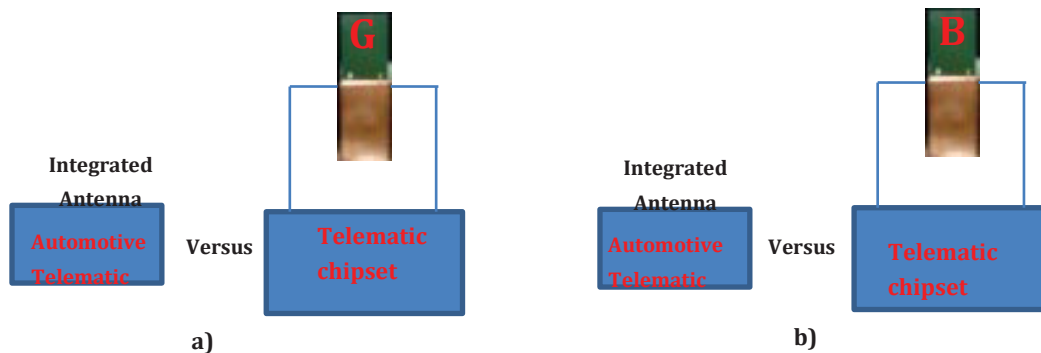
Figure 5.2.2-4. Schematics of the device setup. a) Good versus Integrated antenna, b) Bad versus Integrated antenna.

Table 5.2.2-1. Properties and details for the drive test in Band 20.

	Integrated Antenna	Reference Antennas (Good & Bad)
Antenna	Integrated	Band 13
Antenna Cable	NA	0.7m
Nr. of Antenna	2	2
Location	Sharkfin place	In the Roof front
Locked band	20	20
SIM	Telenor	Telenor
Computer	HP ZB 15 G3	
Vehicle	Volvo V60	
Speed & Traffic	20 to 50 km/h, Low	
Environment	Route A	
Duration	30 min	
Repetition	Two test runs done, due to relative comparison	
Antenna Placement		

Based on the analysis and investigation of the test data, we have concluded that the area of interest is low RSRP level when comparing different antenna that connects to the same chipset. This is concluded from the observations that the drive test in those scenarios obtain similar throughput at high RSRP level. Therefore, the data where RSRP is higher than -85 dBm has been excluded from analysis

The analysis of throughput and RSRP after the post-processing for the integrated antenna and the bad reference antenna is illustrated in Figure 5.2.2-5 and Figure 5.2.2-6. It shows that in average we get around 15% worse throughput and 11dB worse throughput when a bad reference antenna is used comparing to the integrated antenna. These results are in line with expectations and show how important it is to have a good antenna in low RSRP levels.

Similar results were obtained when the test was repeated.

Figure 5.2.2-5. In the left, CDF comparison of RSRP levels between Bad ref. and Integrated antenna it shows 11dB in favor of Integrated Antenna. In the right, 95% confidence interval of the RSRP difference for these two antennas.

Figure 5.2.2-6. Comparison of throughput and RSRP between the two units in low RSRP levels. The difference between the reference antenna and Bad antenna is 11 dB in average, while throughput is around 15%. The area on the right of the figure is excluded from analysis because the Modulation Code Schemes has not been shared in the same way between the two devices.

The analysis of throughput and RSRP after the post-processing for the integrated antenna and the good reference antenna is illustrated in Figure 5.2.2-7 and Figure 5.2.2-8. Analyses show that unit with good antenna receives around 6 % worse throughput comparing to unit with integrated reference antenna. For RSRP, the unit with good antenna receives 5.6dB worse performance in average.
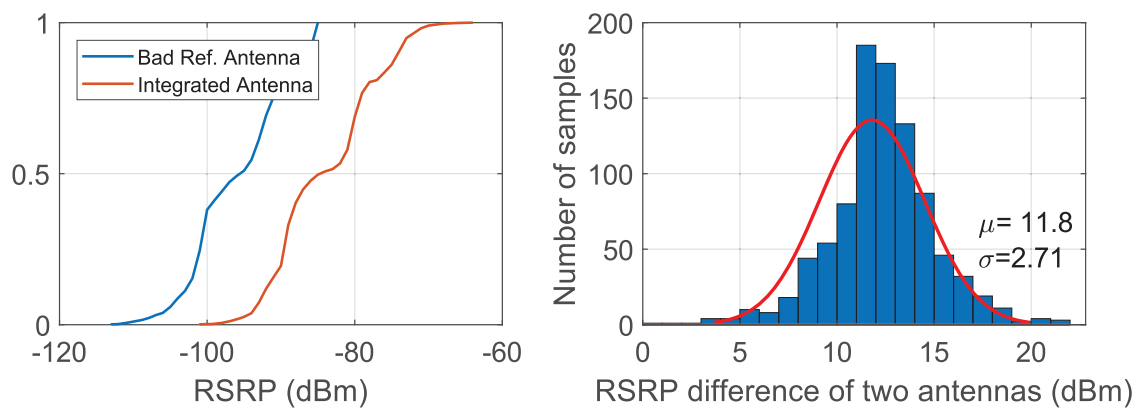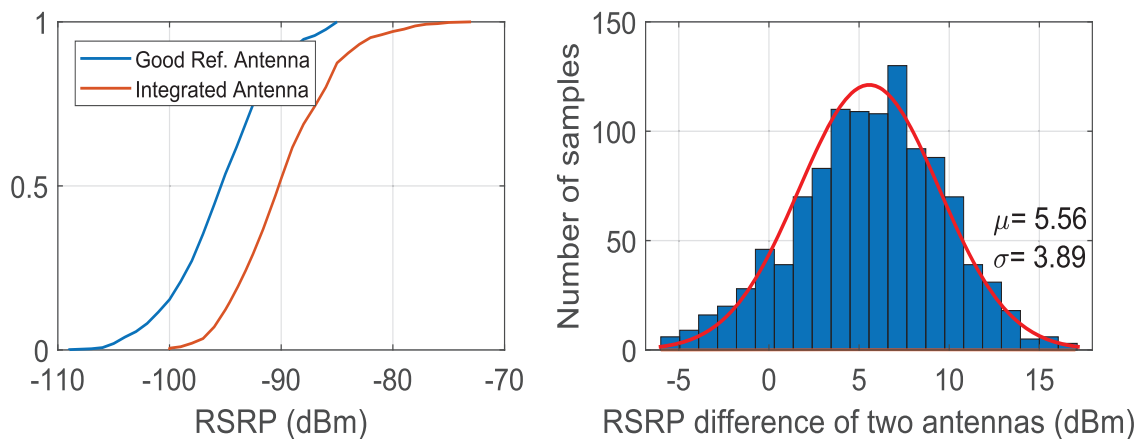
Figure 5.2.2-7. In the left, CDF comparison of RSRP levels between Good ref. and Integrated antenna it shows 5.6dB in favor of Integrated Antenna. In the right, 95% confidence interval of the RSRP difference for these two antennas.
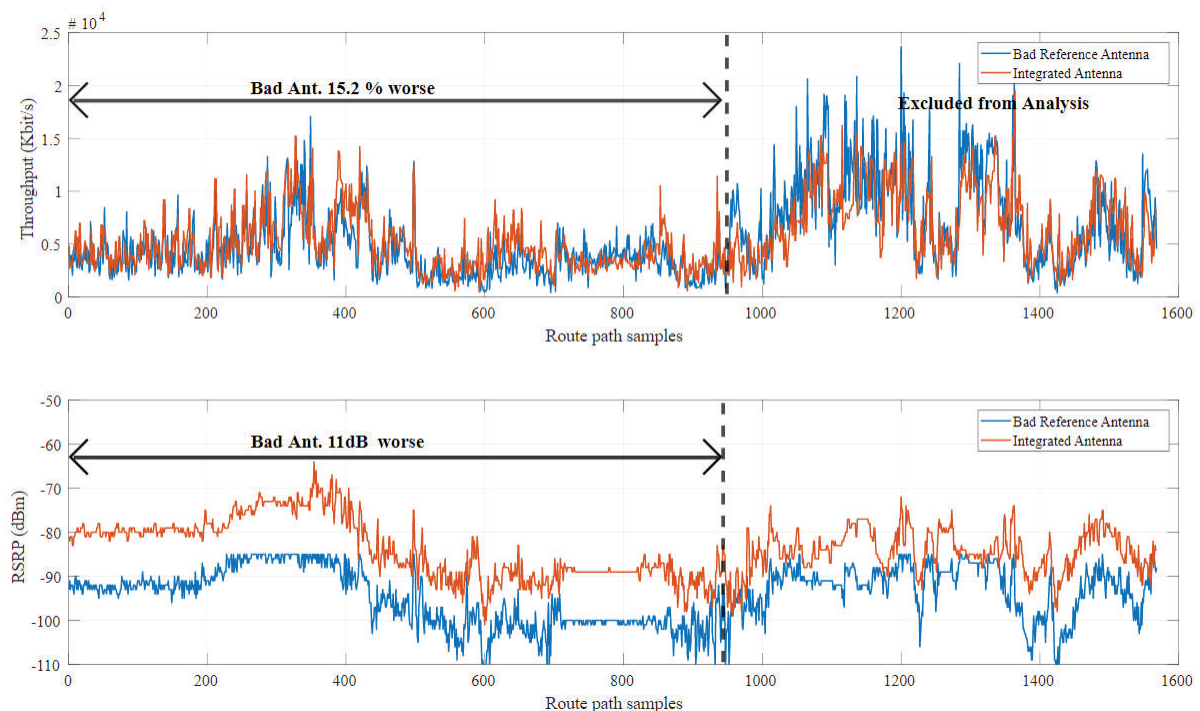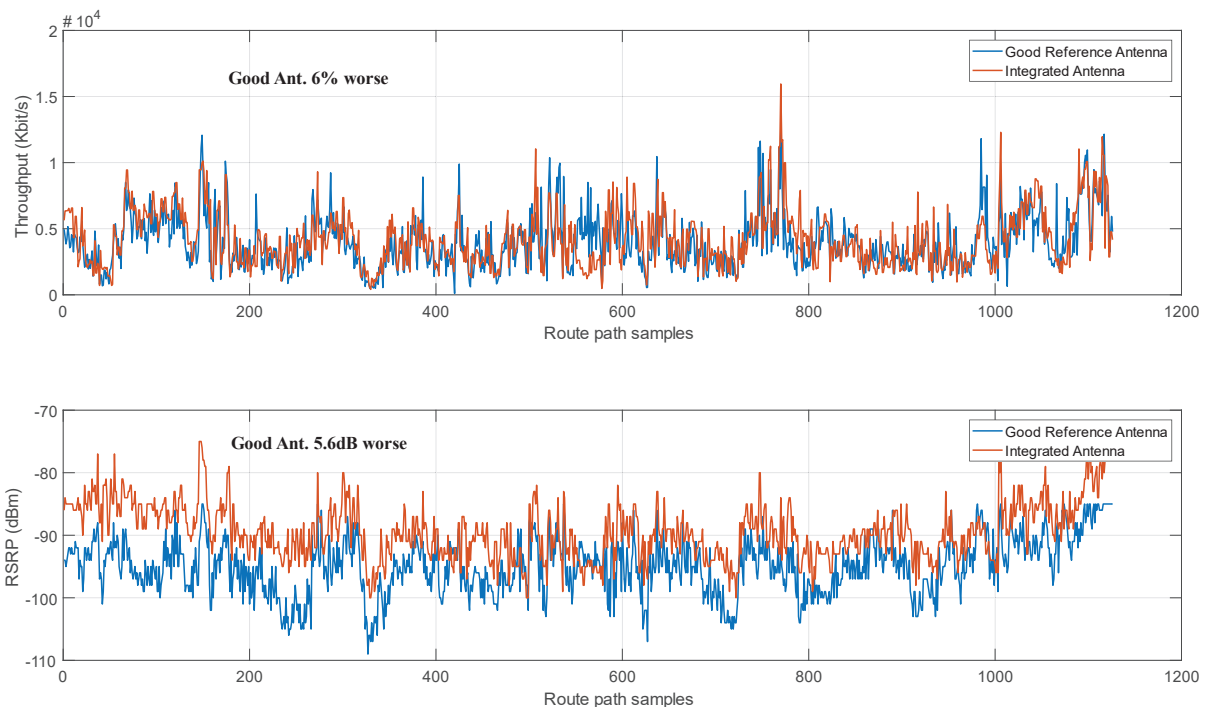

Figure 5.2.2-8. The figure shows the comparison of Throughput and RSRP between the two antennas in low RSRP levels. The comparison between the Integrated antenna and good reference antenna is 5.6 dB in average, while throughput is around 6%.

Chipset Performance Comparison

When comparing chipset performance, the throughput results can vary for different chipsets despite the same RSRP. This is due to that the transceivers may have different sensitivity levels. There may also be other effects at higher RSRP levels, based on different functionality of the different chipsets. For chipset comparison it may thus be of interest to compare the throughput for a wider range of RSRP levels compared to performing antenna performance analysis. Ideally, the same antenna should be used for this comparison as well, to make sure that the same RSRP values are received by the chipsets and thus the difference in the results only comes from the different chipset sensitivity levels.

In this study the focus will be on comparing the automotive telematics unit and SonyXZ3 (Qualipoc). The Qualipoc has a higher LTE category thus having a much better receiver than the automotive telematic. Comparison will be focused on band 20. The Qualipoc has two receiving antennas for band 20, as well as the automotive telematic unit.

Measurement of Band 20 has been performed in Route B which is from VCC to Eriksberg where most of the road has high RSRP values. During the drive test two devices Qualipoc and the automotive telematic have been compared. The Qualipoc has a much better LTE Category compared to the automotive telematic and the results are expected to be better at better network condition. The analysis of the data in Figure 5.2.2-9 has shown that the performance of throughput is quite similar in low & mid RSRP levels, while in high RSRP levels the Qualipoc has shown better performance by achieving extra peak performance, which is reasonable because of the LTE category. The test details are described in Table 5.2.2-2.

Table 5.2.2-2. Properties and details for the drive test in Band 20 for Automotive Telematic and QualiPoc.

	Automotive Telematic	Sony XZ3 (Qualipoc)
Antenna	Integrated PoC	Integrated
Nr. of Antenna	2	2
Location	Under windshield	Under windshield
Locked band	20	20
SIM	Telenor	Telenor
Computer	HP ZB 15 G3	
Vehicle	Volvo V60	
Speed & Traffic	20 to 70 km/h, Low	
Environment	Route B	
Antenna Placement		
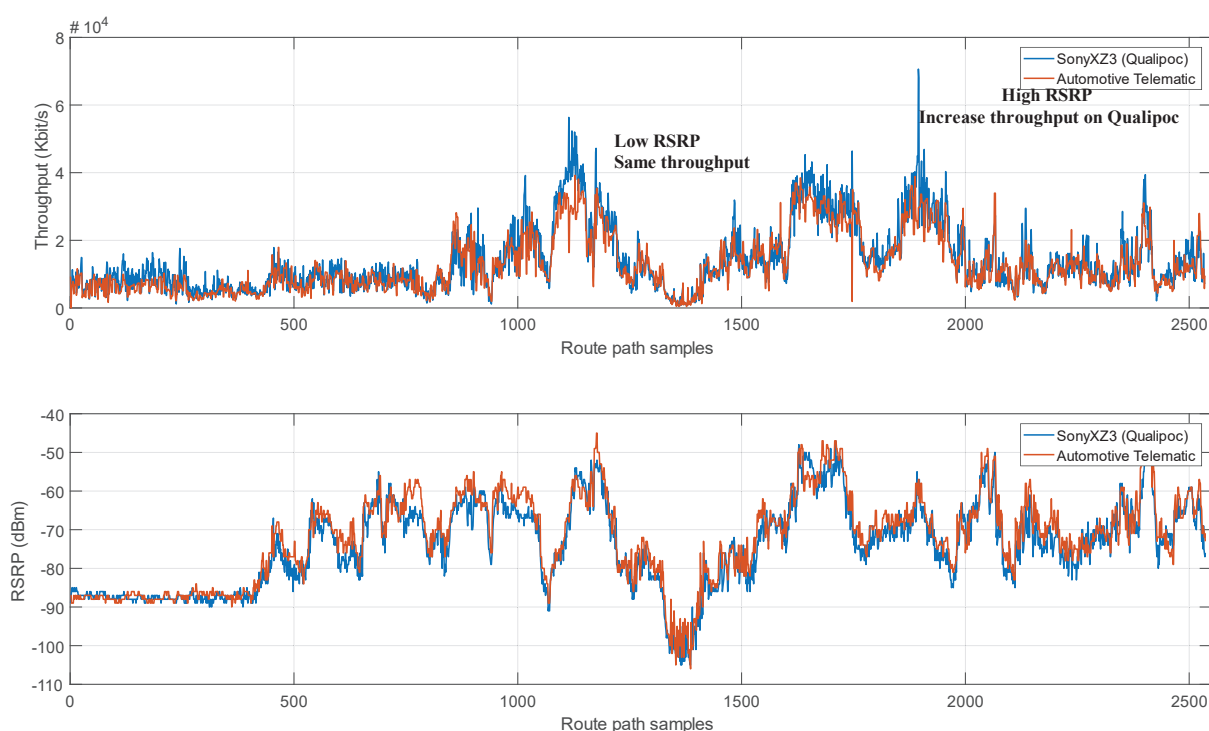
Figure 5.2.2-9. Comparison of Throughput and RSRP between Automotive Telematic and Qualipoc. The RSRP values between the two units are very similar. The difference in throughput is mostly observed high RSRP where Qualipoc has achieved some peak performance, while in mid and low RSRP levels the performance is almost the same.

5.2.2.1.5 Conclusions regarding field logging tool

It has been shown that ROMES4 is a powerful field logging tool, which may be used for logging various cellular data from the chipset in real field operation. KPIs have been discussed and test scenarios outlined. These test scenarios have further been shown to provide expected performance ranking, both for antenna and chipset comparison. The results show strong indications that the scenarios used are appropriate for evaluating the performance of automotive telematics units in real-world operation.

5.2.2.2 Virtual drive test (VDT)

This section will summarize the work regarding a virtual drive test solution, based on data recorded with the tool described in Section 5.2.2.1. The goal is to investigate a solution to reproduce the real-life scenario from field testing inside a controlled lab environment and provide a repeatable and automated verification platform for cellular based communication systems. Moreover, this solution should be integrated with application servers (such as FTP, iPerf, Spotify, or even Youtube) to verify the end-to-end performance. With this approach, it can also provide the possibility to check the relationship between the link performance (e.g., data throughput, packet error rate) under varying RF conditions and the application quality in terms of user experience (e.g., jerkiness, blurriness, tiling, jitter, latency, packet loss rate, etc.).

5.2.2.2.1 VDT process

VDT test procedure generally consists of three stages, including Record, Replay and Repeat.

Record

Record is the first stage and the start point of a complete VDT test process. At this stage, the field logging tool (and possibly an RF scanner) are used to collect data from the field testing. The field logging tool helps to extract data from the chipset of cellular modem, including network signaling (e.g., L3 messages), cell settings, RF link information (e.g., RSRP, RSRQ SINR, MIMO Rank Indicator) and so on. The RF scanner is used to collect and record the RF interference signal from other strong cells around the vehicle.

Replay

Replay is the second stage of VDT test process. At this stage, the big field test data is sliced into multiple small data sets based on different test scenarios such as network issues, handover time-out, bad coverage situations, high interference environment and so on. Then, inside an environment-controlled lab, the base station simulator and CE are used to replay/reproduce the live network cell setting and RF channel conditions of different test scenarios.

Almost all the commercial base station simulators can be used in VDT. However, there are only a couple of CEs supporting VDT concept, including Spirent Vertex and Keysight Propsim.

Repeat

The third stage of the VDT test process is repeat. It's to integrate the replay system into test system on software increment & SW continuous integration and repeat the specified test cases (or field test scenarios).

5.2.2.2.2 VDT test setup

Either the RF conducted approach or the over-the-air (OTA) approach (e.g., wireless cable or RC) should be chosen for the VDT replay test, which depends on the HW design of DUT. For sub-6 GHz cellular system, the RF conducted approach is most common. Meanwhile, for cellular systems working at higher frequencies, the OTA approach is preferable since the antenna component is highly integrated with the modem. The knowledge obtained in WP3 can be reused for the VDT replay with OTA approach.

A simple block diagram and picture of the test set-up is shown in Figure 5.2.2-10. The test setup consists of a base station simulator, CE and RF chamber/shield box. Depending on how many cells are needed to replay the specific logs, extra Base station or other equipment can be needed. It is crucial to sync CE and Base station simulator and be able to configure them simultaneously.
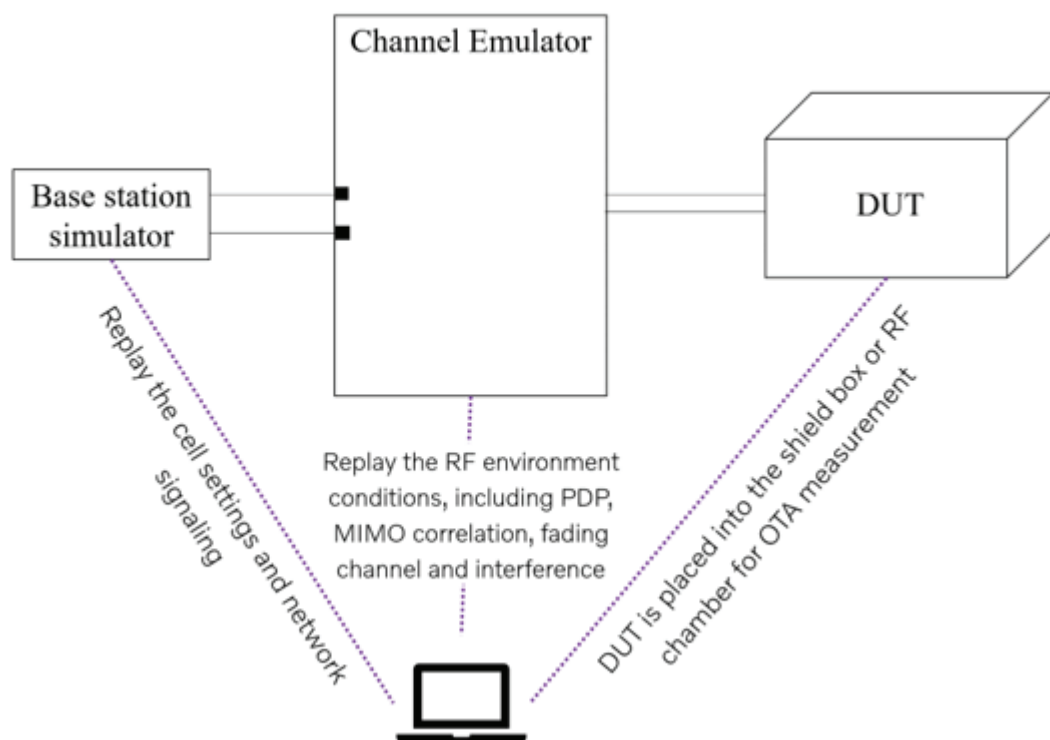
Figure 5.2.2-10. Block diagram of the VDT set-up (top) and picture of the test set-up of VDT inside lab with wireless cable OTA approach (bottom).

5.2.2.2.3   VDT test cases

There are 3 different test scenarios that can be handled by VDT solution, including Attach, Single cell performance, and Mobility performance.

The test scenario Attach is to verify the attach process when UE is registered to a cell/beam, and hand over to a new cell/beam. A typical KPI for this scenario is attach time distribution.

The test scenario Single cell performance is to verify the data throughput performance when the UE is connected to the replicated cell/beam with a certain network configuration under certain channel conditions. A typical KPI for this scenario is MAC layer or application layer data throughput.

The test scenario Mobility performance is to verify the data throughput performance when the UE is replicated to handover from one cell/beam to another cell/beam under different channel conditions. Typical KPIs for this scenario are hand-over success rate, attach time distribution and the data throughput.

For each test scenario, the test cases can be generated to cover the real-life situations, such as high interference environment, bad coverage area, the issues at the network side, handover between 3G cells and 4G cells and so on. However, due to the time and resource limitation, only some of these test cases are evaluated in the PoC of this project.

5.2.2.2.4 Commercially available VDT test setups

There are 3 different VDT solutions available in the market, including R&S CMW Cards, Spirent Vertex VDT, and Keysight Field2Lab. A short summary of each tool is provided below.

Vertex VDT
Vertex VDT is software that is developed by Spirent and works together with Vertex CE. The SW is used to replay only the varying physical channel conditions for RF link during the field test, such as PDP, MIMO correlation, RF power level, interference level and so on. It's a straightforward solution to verify RF link non-functional performance.

CMW Cards
CMW Cards is the software that is developed by R&S and works together with the base station simulator CMW500. This solution mainly replays Layer 3 messages together with limited information about varying physical channel conditions (only RSRP & RSRQ level and static standardized fading channel) from field test.

S8709A Virtual Drive Test Toolset
S8709A is the virtual drivel test solution developed by Keysight. As described in the previous two sections, Vertex and CMW Cards have different focuses on VDT. Keysight's S8709A toolset can be considered as the combination of the previous two solutions. This toolset works together with the base station simulator UXM and CE PROPSIM F64.

UXM is used to replay of varying RRC/NAS configs, varying cell/neighboring cell configs, resource allocation together with mobility information from the field logs, which is similar to R&S CMW Cards. PROPSIM F64 is to reproduce the varying fading channels, which is close to Spirent Vertex VDT.

In this project, Vertex VDT has been evaluated.

5.2.2.2.5 Proof of concept – Vertex VDT

Since Vertex VDT only replay the varying RF conditions, the single cell performance test is evaluated in the PoC of this solution. The single cell performance test is performed in an urban area.

The test route for which field data was recorded is shown in Figure 5.2.2-11. The simulated velocity of the vehicle is summarized in Figure 5.2.2-12.
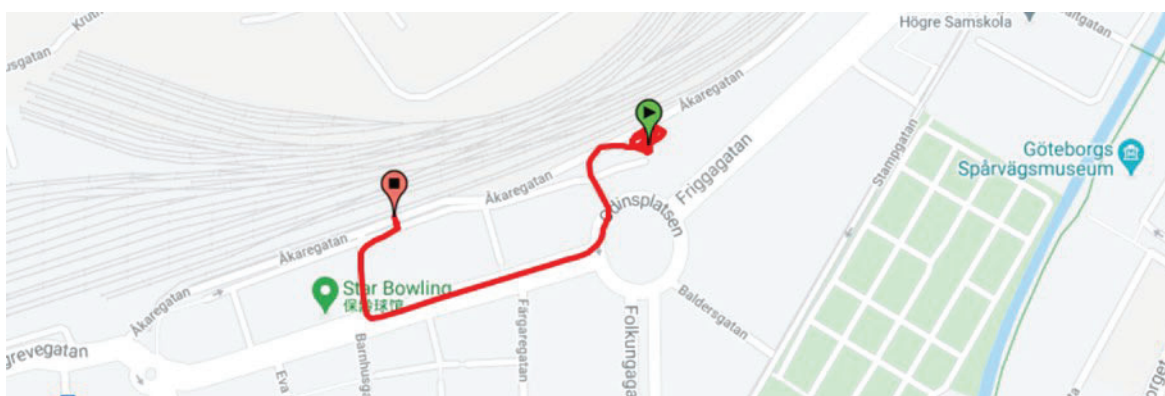
Figure 5.2.2-11. Test route for recording of field data.
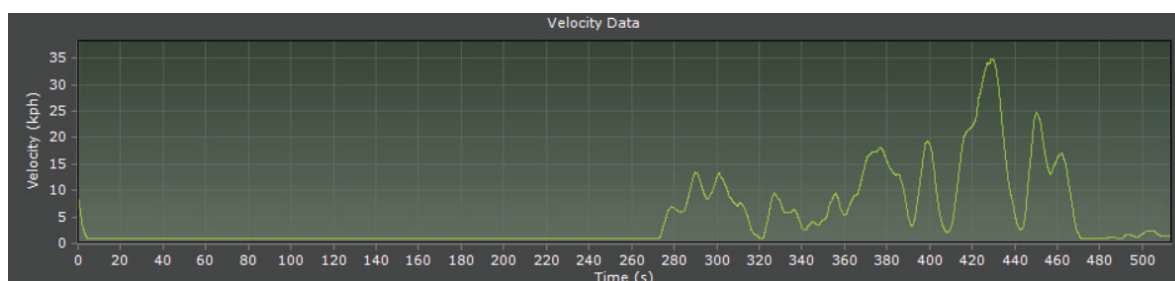
Figure 5.2.2-12. Velocity of the vehicle in the field test.

The replay test is performed in RF conducted approach. The RSRP values and RSSI values recorded during the drive test are replayed. The interference signal is added to match the RSSI level. Since the field logging tool couldn't capture PDP profile, the channel fading is chosen to use the standardized EVA model, which is dynamically changing according to vehicle velocity. Since there is no algorithm to map MIMO rank indicator to MIMO correlation values (or diversity levels at TX & RX side), the modelled setting is used, which randomly generates MIMO correlation between upper & lower specifications, where the lower limit is 1 and higher limit is 8. The simulated cell after processing by the VDT SW is according to Figure 5.2.2-13.
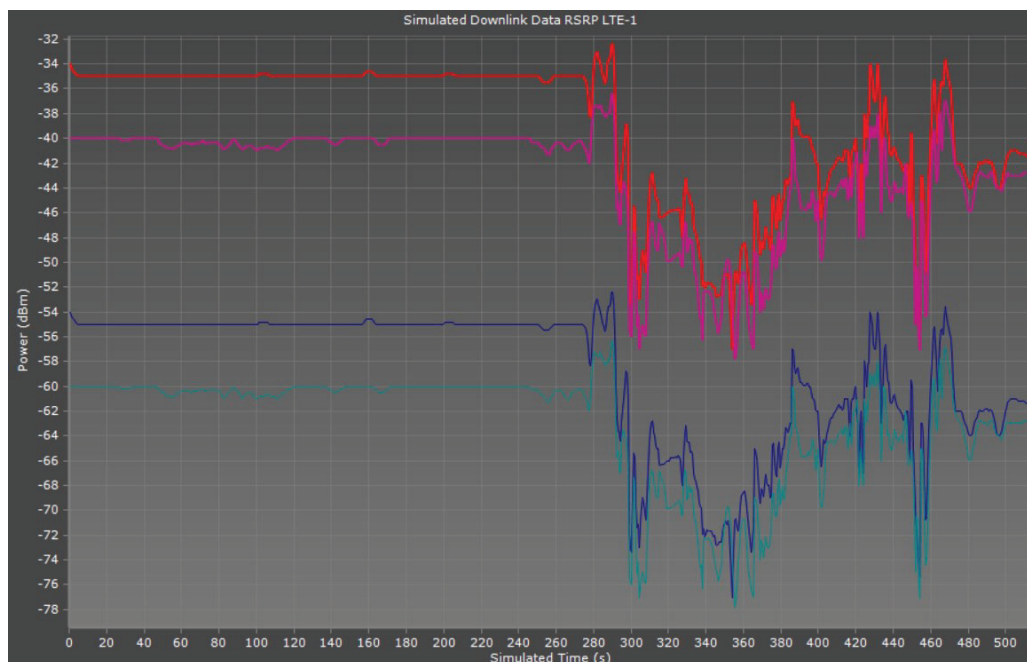
Figure 5.2.2-13. Simulated cells derived from VDT conversion.

The MAC layer data throughput is used as the KPI to evaluate the performance. The RB allocation and MCS order were stable during this field test. According to the field logs, the bandwidth, RB number and MCS is set to be 10 MHz, 50, 64 QAM respectively at BS. The frequency band is set to be 2630 MHz.

These are the findings from this test:

1. When the interference signal is added in the replay channel model, the DUT has troubles to get connection with BS. After the interference signal is disabled, the DUT could connect with the BS. One possible reason might be that the interference signal is also faded in CE, which may amplify the noise level on the signal. The investigation into this pending issue is required in future work.

2. As a result, the replay test was performed without noise. The comparison in data throughput between field test and lab test is summarized in Figure 5.2.2-14. This figure shows that the replay test has a pretty bad reproducibility, especially during the time period marked by green circle. It implies that the settings chosen in VDT conversion do not reproduce the same condition as field test. And the main source of this deviation should be the fading profile and MIMO correlation replay, because this information is missing in the field test and the replay of it becomes blind guess.
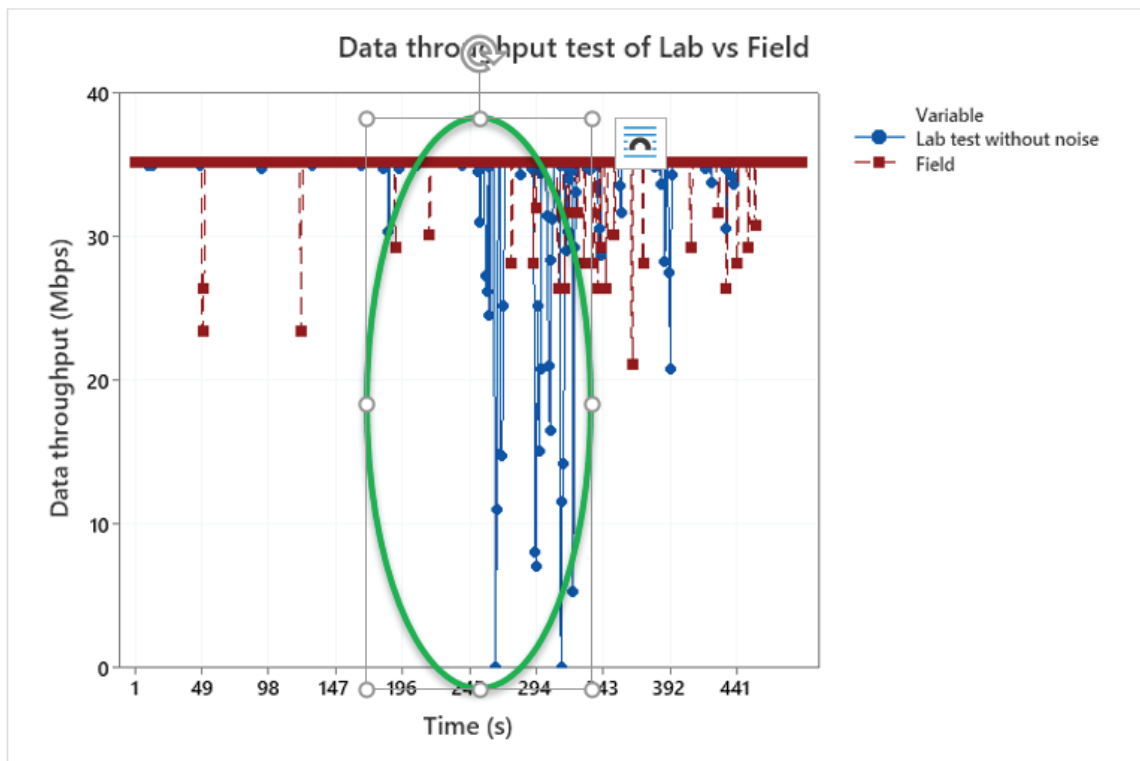
Figure 5.2.2-14. Field test vs Lab test without noise.

3. We also tried the replay test without noise and fading channel, the corresponding result is shown in Figure 5.2.2-15. With these new settings, the reproducibility of replay test has a big improvement. The data throughput in lab test is getting closer to the one in field test. However, the absolute level of throughput still differs a lot between each other. The main reason may be because of the difference in MIMO correlations, which affects a lot on the channel capacity.
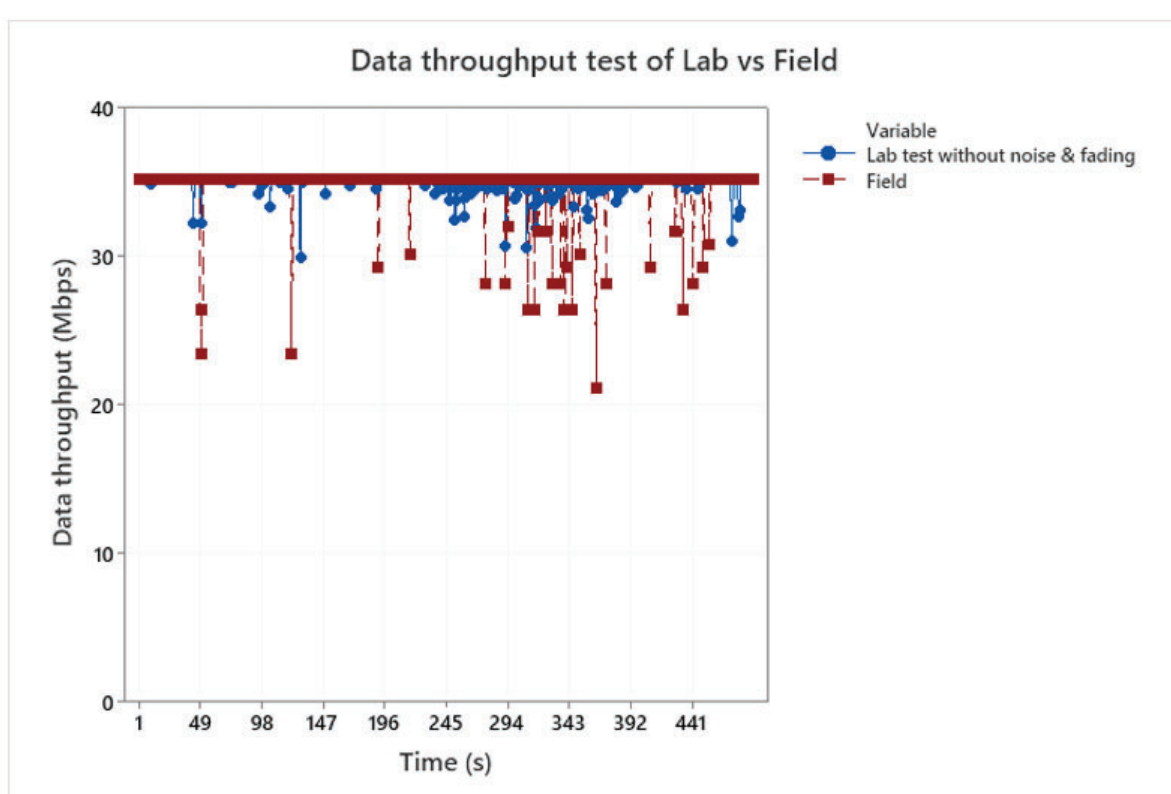
Figure 5.2.2-15. Field test vs Lab test without noise & fading.

5.2.2.2.6 Conclusions regarding VDT setup

A VDT setup is complex and requires interaction between different equipment. There are many factors on both network side and RF channel that should be controlled during the measurement to ensure good results. The limited study in this project has shown some simple VDT setup, however, more work is needed to gain repeatable results and thus replace field tests using this approach.

5.2.2.3 References

[WP2-1] Szini, B. Yanakiev and G. F. Pedersen, "MIMO Reference Antennas Performance in Anisotropic Channel Environments," in IEEE Transactions on Antennas and Propagation, vol. 62, no. 6, pp. 3270-3280, June 2014, doi: 10.1109/TAP.2014.2311468.

5.2.3 Work Package 3: System verification

5.2.3.1 WP3A: Multiprobe ring

This section will summarize the work regarding the implementation of the multiprobe ring test system for cars and trucks. The multiprobe ring, sometimes also called MPAC (Multi Probe Anechoic Chamber) or MPS (Multi Probe Simulator), is a test system for OTA tests of wireless devices originally developed for small-scale systems such as mobile phones [WP3A-1]. In the previous FFI WCAE project a multiprobe ring test was developed (the MPS [WP3A-2]) and in SIVERT, that solution is both further developed by combining it with a commercial CE as well as its characteristics analyzed, and it is used for test of full-scale vehicles.

The approach was to develop a less costly version of a fully equipped multiprobe ring as the available CE had only four output ports. Then, these four ports were then divided into a total of eight ports enabled by a modified version of the previously developed MPS. Commercial solutions of 16, 32, etc. ports exist but were not possible to invest prior to this project. Besides, one of the purposes of this project is to evaluate if such a large investment can be justified. As the Multiprobe ring setup only can be temporarily placed in the EMC chamber, up to 16 ports could be feasible (to cover horizontal and vertical polarization), but more will be limited due to practical reasons.

As already mentioned, this method was originally developed for smaller test objects such as mobile phones. A large test object such as a vehicle (car or a truck) destroys the quiet zone as it is defined in [WP3A-1] (in the sense of a phase-controlled plane wave). This raises requirements on a different test zone validation criterion.

5.2.3.1.1 Plane-waves synthesis

For the ability to generate phase-controlled plane waves emanating from an arbitrary horizontal direction, a rule of thumb for estimating the required number of multiprobe antenna elements is described in [WP3A-3]. Figure 5.2.3.1-1 below is based on that publication and describes the number of required multiprobe antennas needed for a DUT of a certain size and at a certain frequency. As can be seen from the figure, small DUT's or a low frequency is required for accurate plane wave synthesis when the system is limited to eight measurement antennas. For geometrically large DUT's in combination with high frequency, it is not unlikely that +100 MPS antennas are needed for plane-wave synthesis. This brings us to the conclusion that for a vehicle, tests in the multiprobe ring cannot be performed in a plane-wave sense. Rather a statistical approach must be used, where the superposition of DL signals has constant statistical distribution (a stationary process) in the test zone. Like a 2D RC.
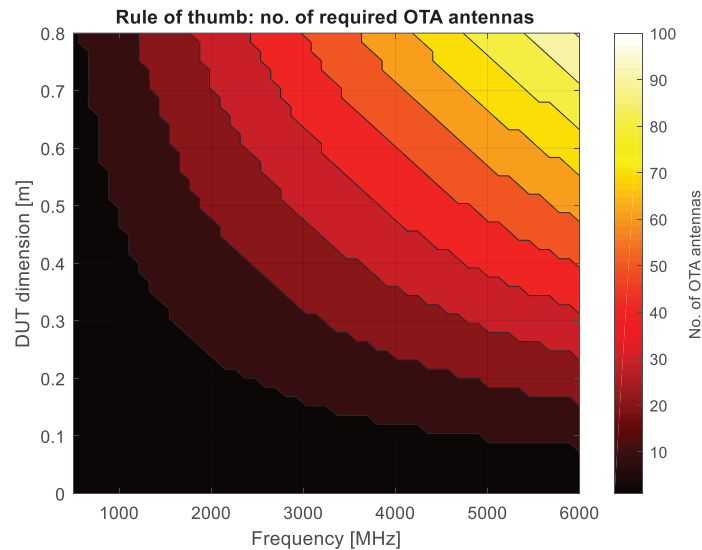
Figure 5.2.3.1-1. Number of vertically oriented antennas.

5.2.3.1.2 Semi-anechoic chamber setup

Generally, the multiprobe ring is set up in a large semi-AC capable of rotating a full-sized car. At RISE two facilities are capable of such tests: the Awitar chamber and the Faraday chamber. See Figure 5.2.3.1-2. The method requires suppression of ground reflection, which can be done by placing absorbers inside the multiprobe ring on the turntable. This is time-consuming work, but necessary for measurement accuracy as the ground reflection can cause large variations in received signal strength, see right of Figure 5.2.3.1-2. In its present implementation, the method requires the possibility to rotate the test object on a turntable and that the antennas on the test object are placed within a test zone of 2 m radius. As will be described later in this chapter we have examined two approaches for positioning the multiprobe antennas: with angle-of-arrival (AoA) according to 3GPP [WP3A-1], or in an omnidirectional manner. For the latter, it is fully possible to rotate the channel model electronically and not be limited to the capacity of the turntable.

In general, the method has the following advantages:
- Vehicle under test (VUT) internal EMI effects on the DUT radio receiver are tested correctly (for the systems activated).
- DUT radio internal EMI effects are tested correctly.
- Hidden or distributed antennas can be tested.
- Whole trucks/cars can be tested.
- No interference from the surroundings.

But it has also drawbacks:
- Long setup time.
- Complex setup.
- Test only performed in one horizontal cut around the vehicle. Since some measurements are performed in the near field region of the DUT the measurement uncertainty is affected.
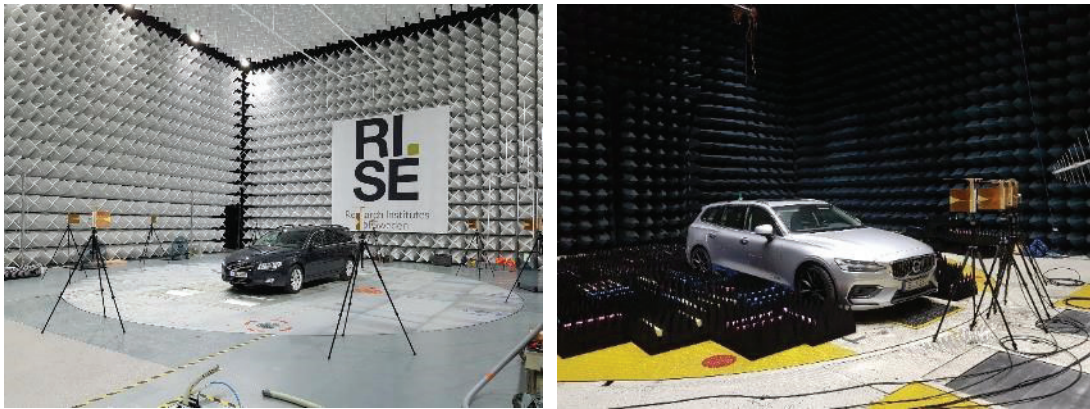
Figure 5.2.3.1-2. Awitar chamber (left) and Faraday (right).

5.2.3.1.3　Setup overview

The channel is emulated by combining the CE and the "MPS light". Distribution of channel properties:

- CE:
  - Doppler generation
  - Sub-path delays
  - Sub-path RF attenuation
  - Delay spread
  - Rayleigh fading on four output paths

- MPS (the MPS modifies signals on cluster level):
  - Expand from 4 to 8 paths. Four Rayleigh fading ports are available from the CE. Depending on channel model some Rayleigh fading ports are split into two paths through the MPS. This is a limitation to the method. These split paths share the same Rayleigh process but will have different attenuation and delays before reaching the UE.
  - Path delay (fixed delays by MPS fibre loops)
  - RF path attenuation
  - Test antennas (test antennas modify signals on cluster level)
    - Path AoA (by positioning test antennas)
    - Polarization and cross-polarization ratio (XPR) by orienting test antennas.

A graphic illustration of the measurement setup in the semi-AC can be viewed in the figure below. The BS generates two DL signals which are sent to the CE. The CE emulates the signals and sends four paths further to the "MPS light" which performs further emulation (attenuation and delay) and outputs eight paths to eight different DL antennas (Tx1 to Tx8).
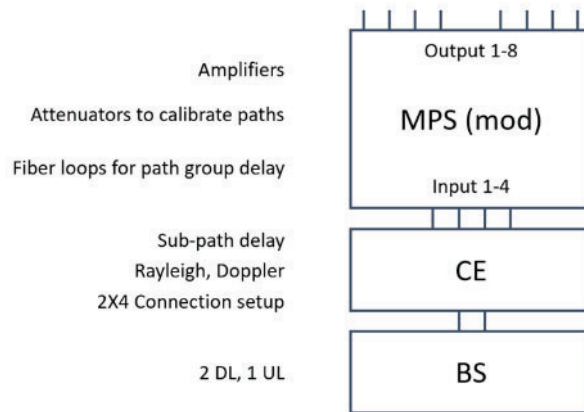
Figure 5.2.3.1-3. BS, CE and MPS setup.

Inside the multiprobe ring the signals are sent towards and registered by the DUT. The DUT returns parameters such as RSRP and block error rate (BLER) over the up-link (UL) channel to the BS. A separate UL antenna is used since the DL channels are unidirectional.

5.2.3.1.4　Channel emulation in CE

The channel emulation is performed within the CE in combination with a lightweight version of the MPS. During the test both the CE and the MPS are located inside of the semi-AC, this is due to the DL budget and does not affect the test. Three main channel models have been implemented and utilized to emulate the input signals: UMi and UMa as defined by 3GPP [WP3A-1], and an omni-directional model defined by the project.

5.2.3.1.5　MPS light software module

The "MPS light" software module is shown in Figure 5.2.3.1-4. This module should be used in a flow according to:
1. Calibration of the full system with omnidirectional antenna (like dipole).
2. Check system after calibration.
3. Load channel model (attenuation/path, AoA information).
4. Minimization of total attenuation (combine channel model information and system calibration to reduce DL attenuation as much as possible).

It is also possible to "manually" control the MPS/CE setup as well as save and load setups.

Figure 5.2.3.1-4. Print screen of MPS light software module.

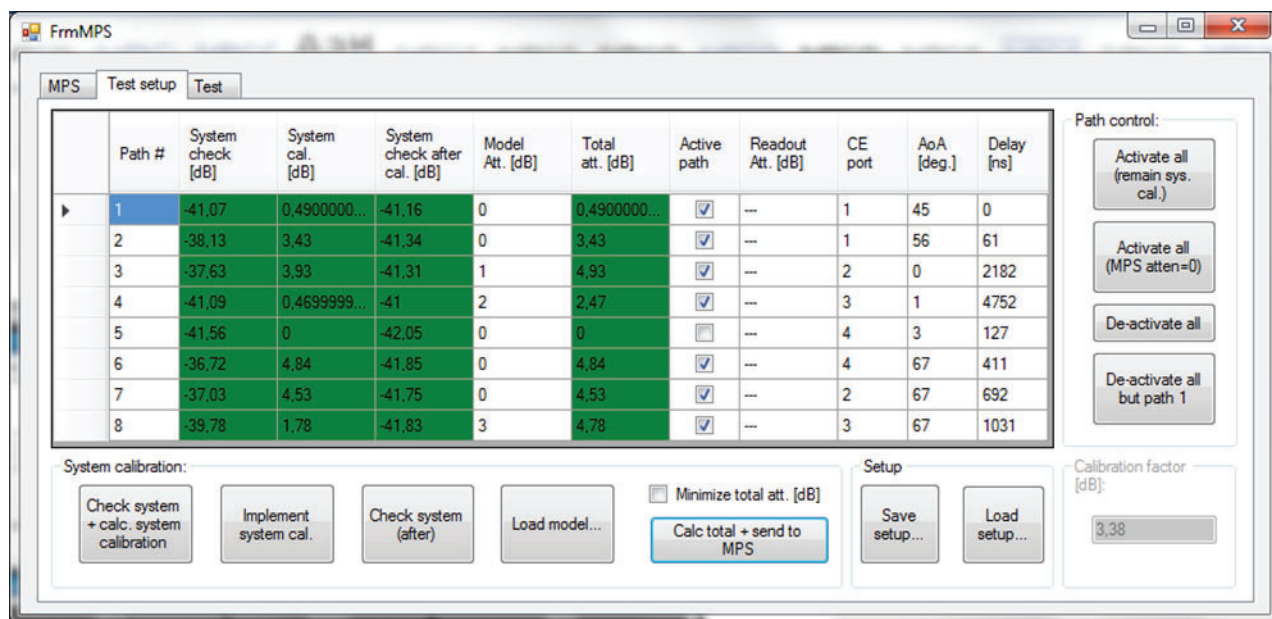| Path #	System check [dB]	System cal. [dB]	System check after cal. [dB]	Model Att. [dB]	Total att. [dB]	Active path	Readout Att. [dB]	CE port	AoA [deg.]	Delay [ns]
1	-41,07	0,4900000...	-41,16	0	0,4900000...	✓	---	1	45	0
2	-38,13	3,43	-41,34	0	3,43	✓	---	1	56	61
3	-37,63	3,93	-41,31	1	4,93	✓	---	2	0	2182
4	-41,09	0,4699999...	-41	2	2,47	✓	---	3	1	4752
5	-41,56	0	-42,05	0	0	☐	---	4	3	127
6	-36,72	4,84	-41,85	0	4,84	✓	---	4	67	411
7	-37,03	4,53	-41,75	0	4,53	✓	---	2	67	692
8	-39,78	1,78	-41,83	3	4,78	✓	---	3	67	1031

Path control: Activate all (remain sys. cal.) | Activate all (MPS atten=0) | De-activate all | De-activate all but path 1

System calibration: Check system + calc. system calibration | Implement system cal. | Check system (after) | Load model... | Minimize total att. [dB] | Calc total + send to MPS

Setup: Save setup... | Load setup...

Calibration factor [dB]: 3,38

5.2.3.1.6 Calibration

During calibration, the output power from the CE and MPS light is related to the power received by an omni-directional antenna placed in the center of the test zone (i.e., the center of the OTA ring). The calibration procedure also equalizes the power per branch (there are eight branches with different MPS characteristics, RF cable lengths, etc.) by adjusting steerable attenuators in the MPS.

5.2.3.1.7 Test method

Tests are performed automatically by the test SW. It starts, with a test channel playing, from a high enough CE output power to achieve 0% BLER, and then reduces output power stepwise (at CE output) while recording BLER. BLER measurements are in turn performed by the BS and are single-shot measurements of N samples. The software measures N samples times X repetitions:
- Use N = 10 000, X = 2 or,
- repeat the test in 30-degree steps around the vehicle by rotation of turntable (if twelve directions are tested samples can be reduced to N = 2 000 without repetition).

5.2.3.1.8 Channel modelling

Urban micro-cell (UMi), and urban macro-cell (UMa) channel models are implemented as defined in [WP3A-1]. Besides that, an omni-directional model has been defined in the project. This model is intended to emulate an omni-directional environment in the horizontal plane and can be thought of as an RC in 2D. For the omni-directional model all clusters are defined to have equal power, but it could also be possible to define power decay relative to the length of travel as indicated by the delays.

Table 5.2.3.1-1. Proposed omni-directional channel.

Cluster #	Delay [ns]			Power [dB]			AoA [°]
1	0	5	10	0	-2.2	-4	0
2	2182	2187	2192	0	-2.2	-4	45
3	61	66	71	0	-2.2	-4	90
4	4752	4757	4762	0	-2.2	-4	135
5	127	132	137	0	-2.2	-4	180
6	692	697	702	0	-2.2	-4	215
7	411	416	421	0	-2.2	-4	270
8	1031	1036	1041	0	-2.2	-4	315

5.2.3.1.9 Uncertainty estimate

As part of the project an uncertainty budget has been derived. As it was not possible to generate plane wave synthesis for a full-sized vehicle, the uncertainty budget focuses on the distribution of a 2D Rayleigh environment. For such environment the expanded uncertainty, with a 95% confidence interval, was evaluated to 1.7 dB excluding the most unpredictable, but sometimes significant, error contribution: the ground reflection. This part of the error is unpredictable due to that some DUTs might have antennas pointing into the ground, while some might have antennas, e.g., in the middle of the car roof which is less affected by the ground reflection in the test setup. The ground reflection can in both cases be reduced by adding RF absorbers on the floor between the DUT (or calibration antenna) and the test antennas. Our estimations result in approximately 3 dB 95% uncertainty including the ground reflection.

In the document 3GPP TR 37.977 [WP3A-1] an uncertainty budget for OTA-ring measurements is described. By comparing to that budget, it has been verified that the uncertainty budget derived in the SIVERT project covers all crucial contributions of that report.

5.2.3.1.10 Validations

In RISE semi-AC Faraday the multiprobe ring was set up for a full active UMi model test over twelve turntable directions. The VUT was a car with an antenna module in a fixed mount at the roof of the VUT (aka shark-fin antenna). The OTA test was repeated three times, with the VUT put in three different positions: with antenna module in the center of the ring setup (pos. 1), 1m back (pos. 2), and 2 m back (pos. 3), see Figure 5.2.3.1-5 for a sketch of two of those positions (pos. 1 and 2). Below the results from the validation can be seen, the maximum difference between the three positions was approximately 1 dB.
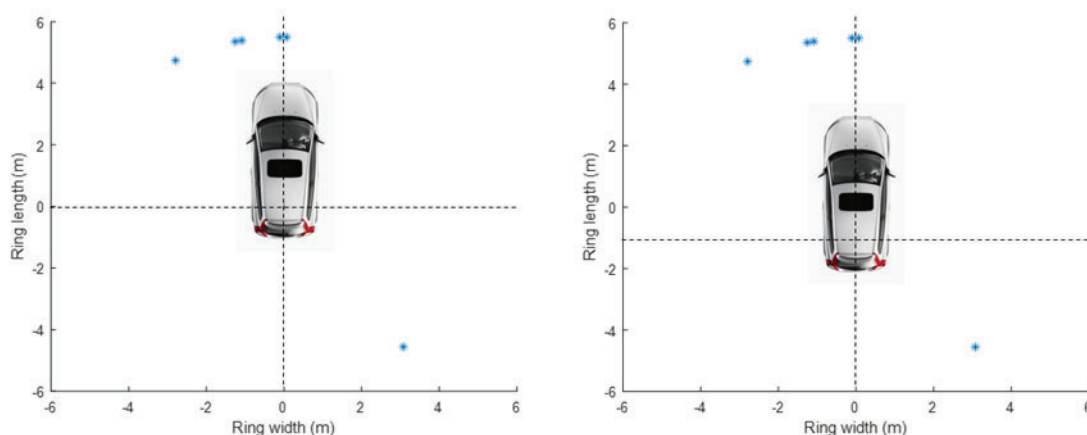
Figure 5.2.3.1-5. Test zone validation. Active test with fully sized vehicle in different positions.
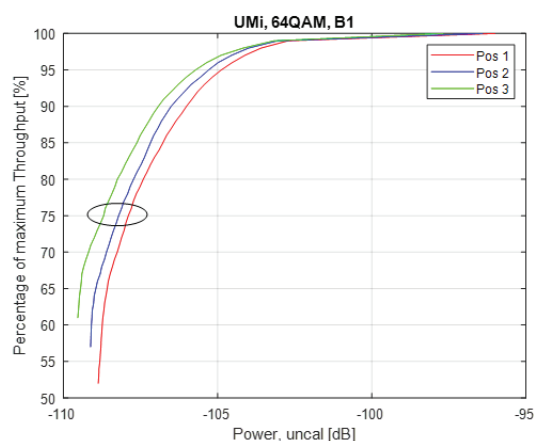
Figure 5.2.3.1-6. Test zone validation result. Maximum difference between the three positions is approximately 1 dB.

In RISE semi-AC Faraday, a radio unit (without a car) also was tested with two different models (UMi and the omni-directional model). As can be seen in the figures below the omni-directional model result in calmer test results and therefore converges faster to a stable average value. In the tests, the Umi model was tested in 12 directions, but for the omni-directional model it was enough to test in five directions. This indicates that the omni-directional model is a good candidate for tests, both regarding accuracy as well as test time.

Figure 5.2.3.1-7. Throughput at twelve directions and its average. DUT in center of turntable (left) and DUT 130 cm off center (right).
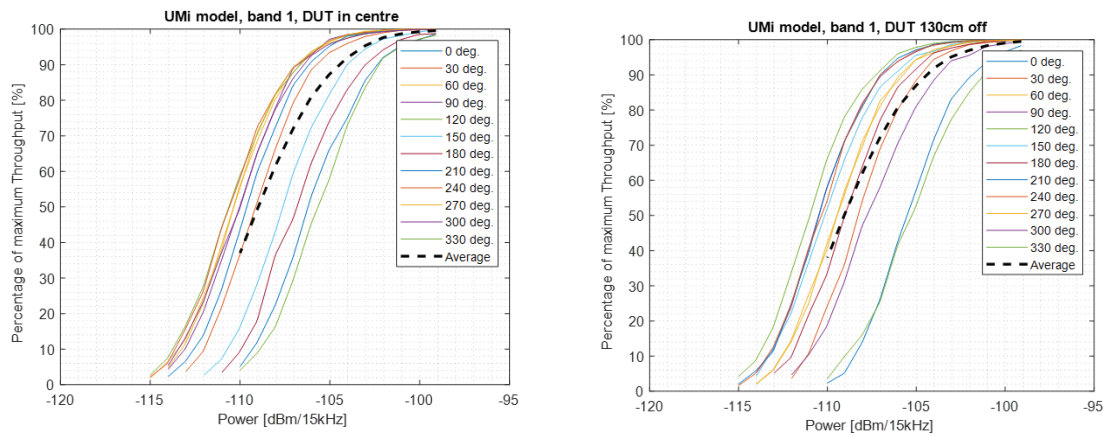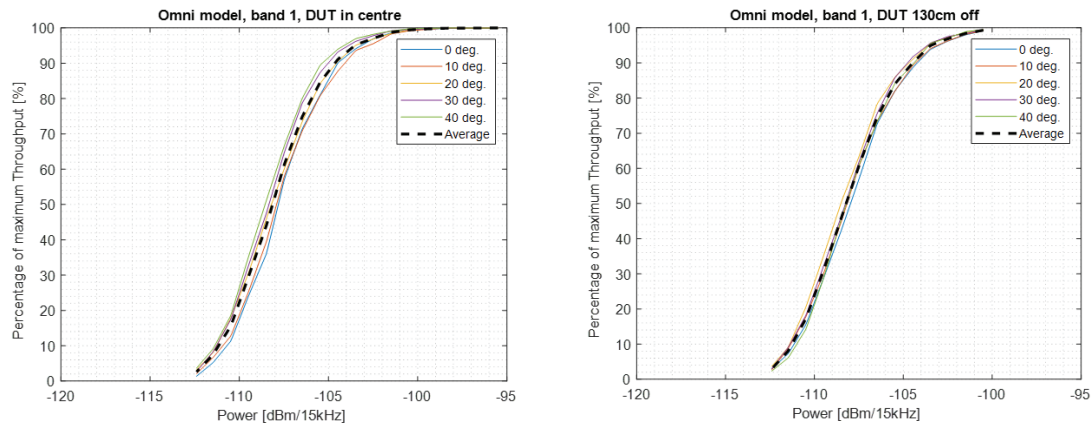

Figure 5.2.3.1-8. Throughput at five directions and its average. DUT in center of turntable (left) and DUT 130 cm off center (right).
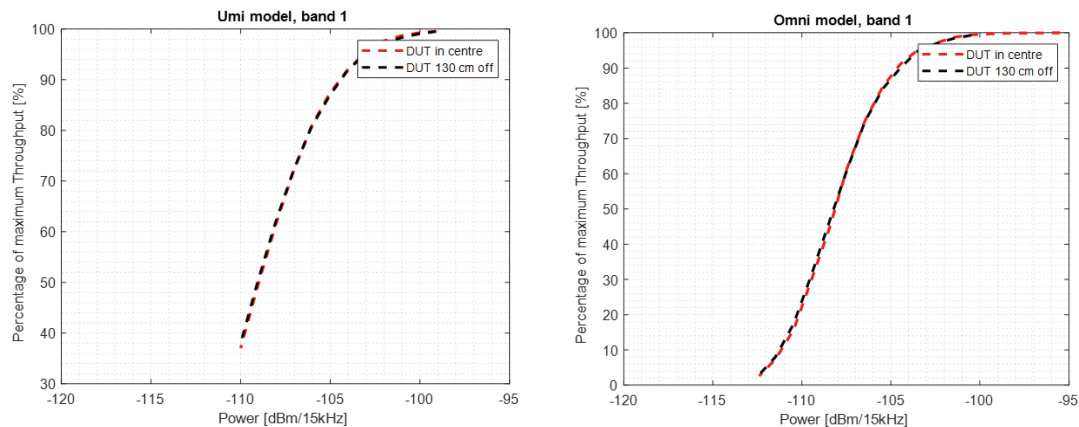

Figure 5.2.3.1-9. Comparison DUT in center of turntable and 130 cm off center. Almost identical result was achieved thus indicating good test zone for both the Umi model and the omni-model.

5.2.3.1.11 Conclusions

The results obtained in the project indicate that the method can, to some extent, provide the correct ranking of device performance.

Regarding test zone for large test objects, it has been concluded that using this implementation, it is not possible to generate phase-controlled plane waves to the DUT. Instead, the statistical distribution in the test zone is evaluated. Signals shall have the same Rayleigh distribution throughout the test zone. Like a 2D RC. See validation in chapter 5.2.3.1.10 where good repeatability has been found between tests performed at different positions within the test zone.

The omni-model was introduced showing promising results, both in terms of accuracy and in test time. It is however unclear what DUT performance aspects would be missed during evaluation using this simplified channel model.

5.2.3.1.12 References:

[WP3A-1] 3GPP TR 37.977, "Verification of radiated multi-antenna reception performance of User Equipment (UE)," Release 15, v15.0.0, September 2018.

[WP3A-2] M. G. Nilsson et al., "Measurement uncertainty, channel simulation, and disturbance characterization of an over-the-air multiprobe setup for cars at 5.9 GHz", IEEE Trans. Ind. Electron., vol. 62, no. 12, pp. 7859–7869, Dec. 2015.

[WP3A-3] T. Laitinen, P. Kyösti, and J. Nuutinen, "On the number of OTA antenna elements for plane-wave synthesis," in Proceedings of the 4th European Conference on Antennas and Propagation (EuCAP '10), Barcelona, Spain, April 2010.

5.2.3.2 WP3B: Wireless cable

This section will summarize the work regarding the implementation of the Wireless Cable (WC) test system for cars and trucks. Traditional MIMO OTA test solutions are based on emulating specific channel conditions inside a shielded chamber, in which the DUT is placed. The DUT antenna responses in these channel conditions are then directly included in the measured metric. The WC test method is instead based on convolving the channel model and the DUT antenna patterns inside the CE, thus reducing the complexity of the setup in the shielded chamber. The signal resulting from this combined channel model plus antenna response is then fed directly to the receiver of the DUT.

The relation to a more traditional conducted measurement setup and to the conducted two-stage method is shown in the table below. It can be emphasized that by feeding the signal wirelessly to the DUT self-interference is also included in the test results.

Table 5.2.3.2-1. Overview of test setups. From conducted to OTA test setup.

Conducted measurement	
Conducted two-stage method	
Wireless cable	
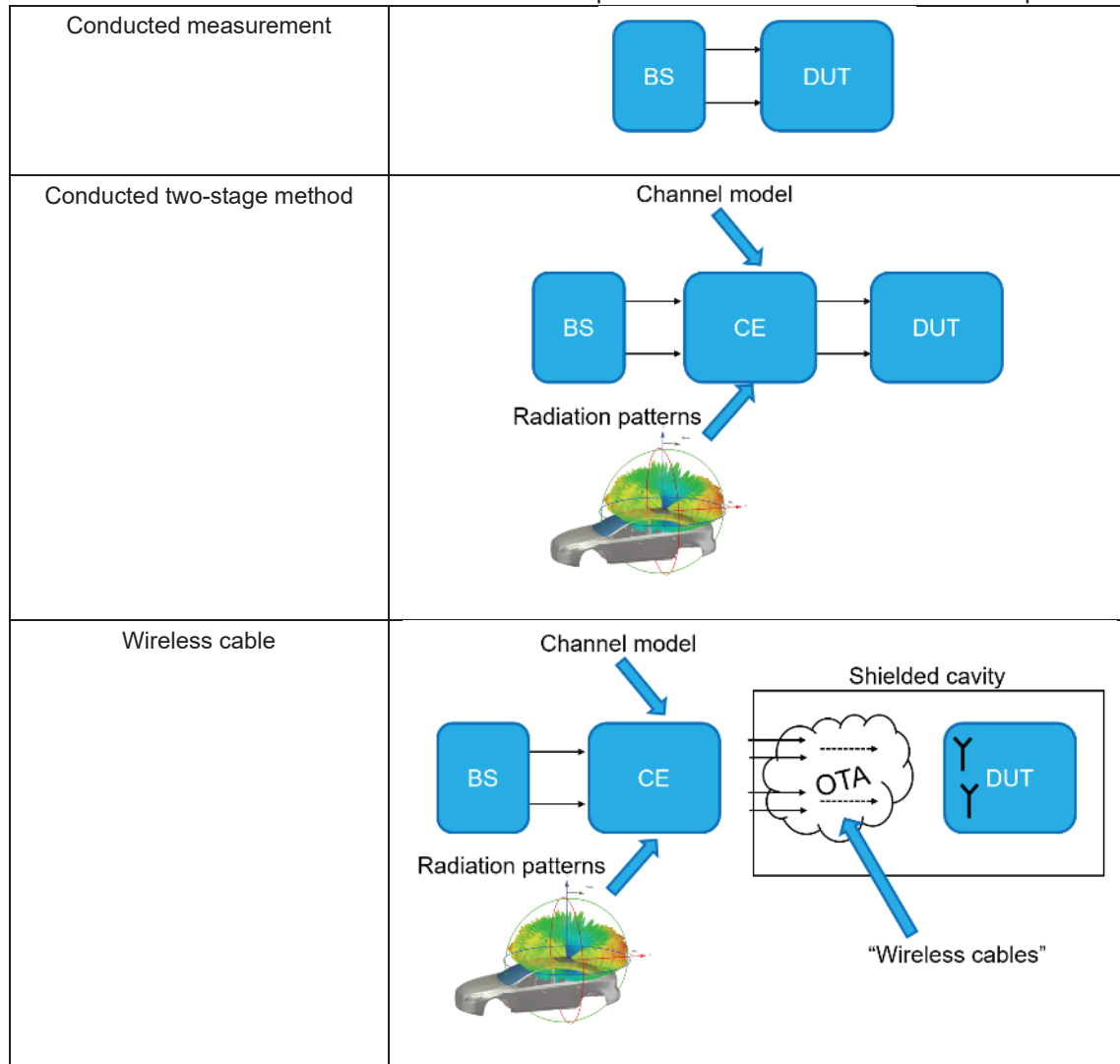
To create the "wireless cables" from CE to DUT, power readings per receiver branch are needed, i.e., RSRP per antenna (or similar). Although defined by 3GPP, RSRP per antenna cannot be read out by default. However, by means of additional software (e.g., ROMES4 [WP3B-1]) and a correct radio chip, this can be achieved. Nevertheless, the need for RSRP reading per antenna is the single most significant drawback of the method.

The method can be applied in a shielded box with absorbers or in a semi- AC. The method works similarly for both approaches.

The method starts with a search to find isolated paths through the cavity. After found isolation, branches are balanced, and then the loss through RF cables, connectors, cavity, antennas, etc. is calibrated. After that, the method is ready for testing a DUT.

5.2.3.2.1   Isolation search

Isolation search is crucial for the WC method as it is here where isolated paths, "wireless cables", are created from the CE to the DUT. During an isolation search, an algorithm is applied to find these isolated paths (referring to Figure 5.2.3.2-1):

- S1 to A1 via {B1 and B3} to Rx1
- S2 to A2 via {B2 and B4} to Rx2

To achieve this the amplitude of W1 and its phase is adjusted so that $max(Rx1/Rx2)$ is achieved for the first path, and accordingly for the second path. After isolation search, both branches are activated and adjusted so that they have equal attenuation through the cablings, connectors, cavity, antennas, etc. This is done by adjusting the output power pairwise on B1 and B3 (or B2 and B4).
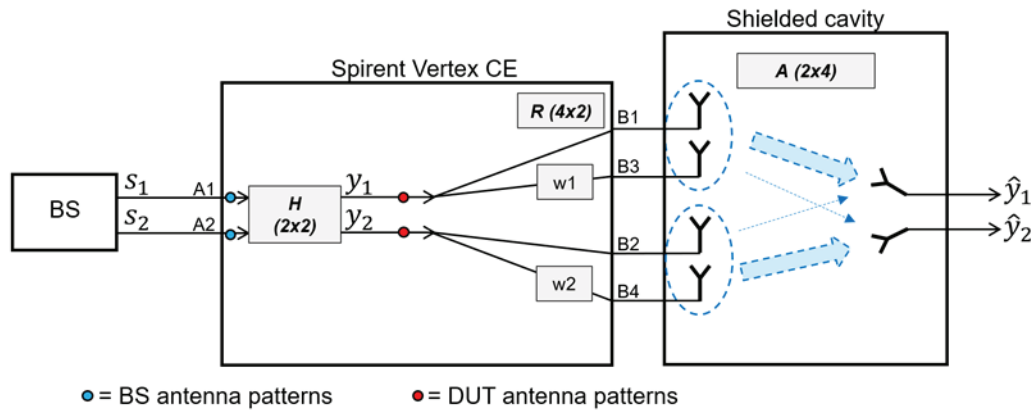
Figure 5.2.3.2-1. Test setup for isolation search, calibration, and test with DUT. Ai, Bj denotes Spirent vertex in- and output ports.

Based on [WP3A-1] we need a minimum of 15 dB isolation after isolation search for a successful WC test. However, tests performed in the SIVERT project on highly correlated MS antennas (correlation = 0.9) in UMa channel indicated that 12 dB was sufficient isolation.

The test setup used in that validation is shown in the figure below, where a 2x2 unidirectional setup is used in combination with splitters, attenuators, and combiners. The results are compiled for 75% throughput in Figure 5.2.3.2-3 where it can be seen that power at 75% throughput converges above 12 dB of isolation.

Figure 5.2.3.2-2. 2x2 Uni-directional setup in combination with splitters, attenuators, combiners to constitute an isolation test setup.

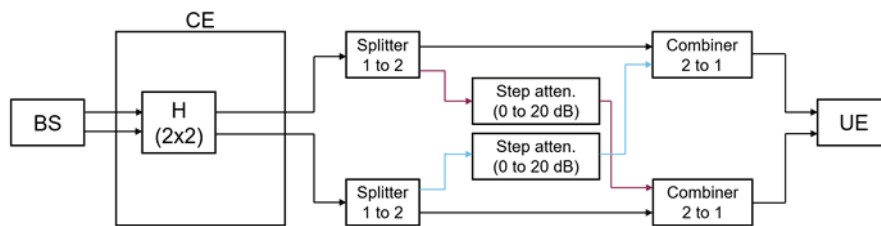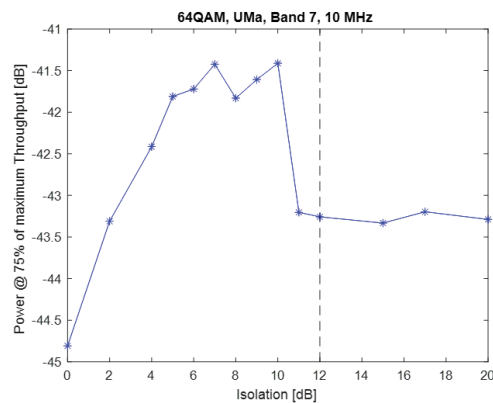Figure 5.2.3.2-3. Power at 75% throughput converges above 12 dB isolation.

Before test, the isolation search is performed automatically with control software (figure below). A meta description of the search procedure:

- Step phase shift in 30 deg. steps. Go to best phase shift.
- Step attenuation in 2 dB steps. Go to best attenuation.
- Step phase shift in 2 deg. steps. Go to best phase shift.
- Step attenuation in 0.2 dB steps. Go to best attenuation.

After the isolation search it is also important to balance the branches before test.

Figure 5.2.3.2-4. Control software for isolation search (left). Verification of isolation search: both paths – first path (blue) – second path (green) – both paths (right).

5.2.3.2.2   Chamber setup

Tests can be performed in three different ways: 1) in a shielded box, 2) in a rooftop shielded box, or 3) in a semi-AC.

Shielded box: If a sub-system is available tests can be performed in a shielded box. This test setup has a very small footprint and thus the advantage of being very flexible. It can be kept close to the test engineer and thus provide high availability.
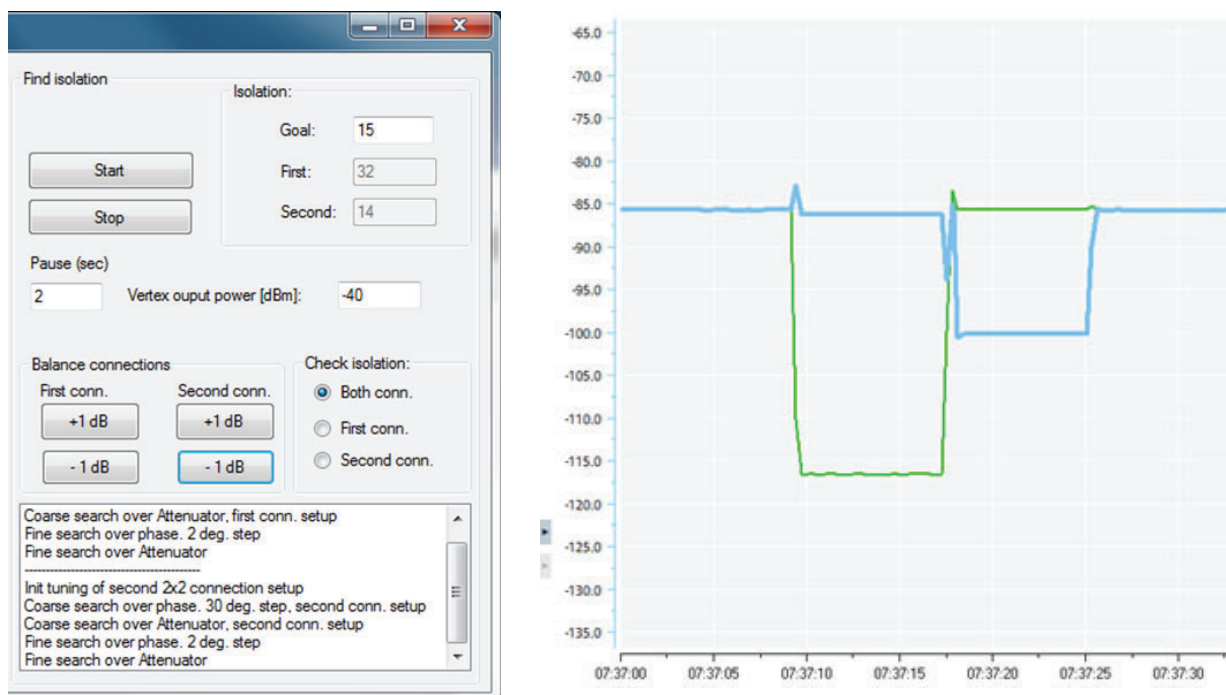
Rooftop shielded box: Due to the less stringent requirements on the shielded environment for the WC compared to other MIMO OTA test methods, the flexibility of where the measurements can be carried out is higher. A novel approach to implement the WC has been investigated, which is based on placing a shielded box on the vehicle roof, encapsulating the vehicular antenna module. Pictures of this setup can be found in the figure below.
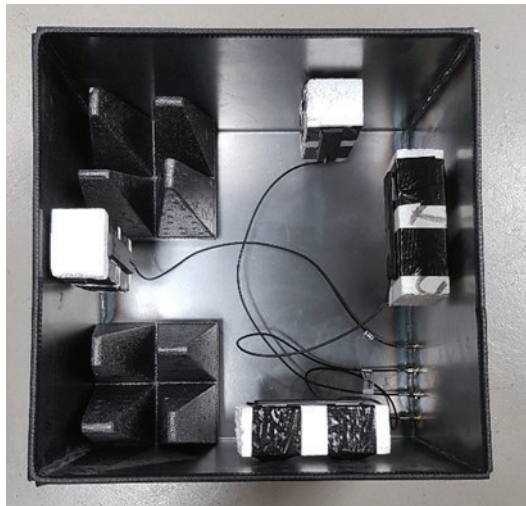

Figure 5.2.3.2-5. Rooftop shielded box (also named car box).

This test setup has a very small footprint and thus the advantage of being very flexible. It can be kept close to the test engineer and thus provide high availability. The approach could also potentially be used in a production line, where time is a critical parameter. The box could easily be placed on top of the car for a quick performance check. Also, often a vehicle is produced in a country different from the one in which the car will be used. This put some limitations on what frequencies that can be tested in a production line today, since frequencies could be country specific. With the rooftop box, this is not an issue since the box is shielding the environment around the vehicular antenna and can emulate all frequencies. The rooftop mounted box is promising in terms of flexibility, cost, and complexity. However, there are also some limitations that need to be further studied.

- The shielding of the rooftop box is presently not very high, which may cause interference from the surrounding environment leaking into the box and thus high measurement uncertainty.
- The rooftop box only provides a very local measurement in one position on the car. This means that distributed antennas (for example one in the front and one on top of the roof) cannot be measured.
- This approach requires the antenna module to be encapsulated by the box. If the antennas are hidden in lossy material (for example in the interior of the car) or the surface above the antenna is irregular, this is not possible.
- Performance degradation due to interference from other car electronics cannot be assessed since this interference is removed by the shielded box.

Semi-AC: Tests can also be performed in a semi-AC. Compared to the shielded box and the rooftop box this setup has several advantages:
- VUT internal EMI effects on the radio receiver are tested correctly (for the systems activated).
- DUT internal EMI effects are tested correctly.

- Hidden or distributed antennas can be tested.
- Whole trucks/cars can be tested.
- No interference from the surroundings (compared to rooftop box).

Figure 5.2.3.2-6. Example of test setup in AC with a VUT. Four downlinks and one uplink.

5.2.3.2.3   Setup overview

For either of the test setups shielded box, rooftop shielded box, or in a semi-AC, the general instrumentation setup is the same. Referring to Figure 5.2.3.2-1:
- Transmit with BS, S_1 and S_2 to CE.
- Use cables of same type and length between the BS and CE.
- RF cables from CE to shielded cavity does not have to be of same type or length.
- Signal received by DUT per port is reported to the test software via DUT specific software (e.g. ROMES [WP3B-1]).

5.2.3.2.4   Channel emulation

In order to mimic a certain environmental scenario, signals are emulated with a CE (RISE use Spirent Vertex). Embedded within the software of the CE are plenty of predefined channel models, but models defined by the user are easily implemented as well.

To understand the signal processing performed in the CE it is of help to look at the channel simulation model as defined by 3GPP in [WP3A-1, WP3B-3]. In the figure below the innermost term of the channel simulation is shown. It can be seen how channel model (H) is affected by radiation patterns, XPR, antenna positions and Doppler:
- P_n : Normalized power amplitude per cluster. Depending on how the channel is defined, some clusters/paths will have more power compared to other clusters.
- F_{rx} : Receiving antenna (DUT) radiation patterns. During a simulation AoAs are generated as simulation times proceed. This factor picks complex gain values for each given AoA. For a LOS channel with only one path this factor will not vary much. In a rich channel with large angular spread this factor will vary a lot.
- $\kappa_{n,m}$: XPR for each sub-ray m of each cluster n. High XPR will result in high $\kappa_{n,m}$, (and low $1/\sqrt{\kappa_{n,m}}$) which in turn will result in low cross polarisation in the channel.

- $\Phi(\theta, \Phi, n, m)$: Random initial phases for each ray m of each cluster n and for four different polarisation combinations ($\theta\theta$, $\theta\Phi$, $\Phi\theta$, $\Phi\Phi$). The distribution for initial phases is uniform within 0 to 360 degrees.
- F_{tx} : Transmitting antenna (BS) radiation patterns. During a simulation AoDs are generated as simulation times proceed. This factor picks complex gain values for each given AoD. For a LOS channel with only one path this factor will not vary much. In a rich channel with large angular spread this factor will vary a lot.
- $d_{rx,u}$: Vector describing positions (x,y,z) of receiving (e.g., DUT) antenna. This vector is projected on unit vectors aligned with each incoming ray generated by the channel simulation. If all antennas are in one single point, this factor will become static and equal to one.
- $d_{tx,s}$: Vector describing positions (x,y,z) of transmitting (e.g., BS) antenna. This vector is projected on unit vectors aligned with each transmitted ray generated by the channel simulation. If all antennas are in one single point, this factor will become static and equal to one.
- Phase variation due to Doppler. If velocity is zero, this factor will become static and equal to one.

Figure 5.2.3.2-7. Analogy with 3GPP TR 38.901 3D model.

5.2.3.2.5 Calibration

The system needs to be calibrated before the test. This is performed with the channel loaded into the CE, but with omnidirectional reference antennas. WC calibration relies in turn on calibrated RSRP readings from the DUT. Those can be calibrated by the supplier or, e.g., in the RC. The latter will include antenna efficiencies and antenna mutual coupling into the RSRP calibration. The bottom line is that, even though the DUT RSRP readings can be calibrated, it is important to know how, and under which assumptions.

WC calibration is performed on an active signaling system, therefore the distributions of the recorded RSRP's are not necessarily Rayleigh distributed. Reference [WP3B:2] defines RSRP as "the linear average over the power contributions (in [W]) of the resource elements that carry cell-specific reference signals within the considered measurement frequency bandwidth". This means that each RSRP reading is already an average over some samples in its distribution. In the figure below this effect is illustrated by comparing RSRP samples from a 1.4MHz with a 20 MHz bandwidth LTE connection.
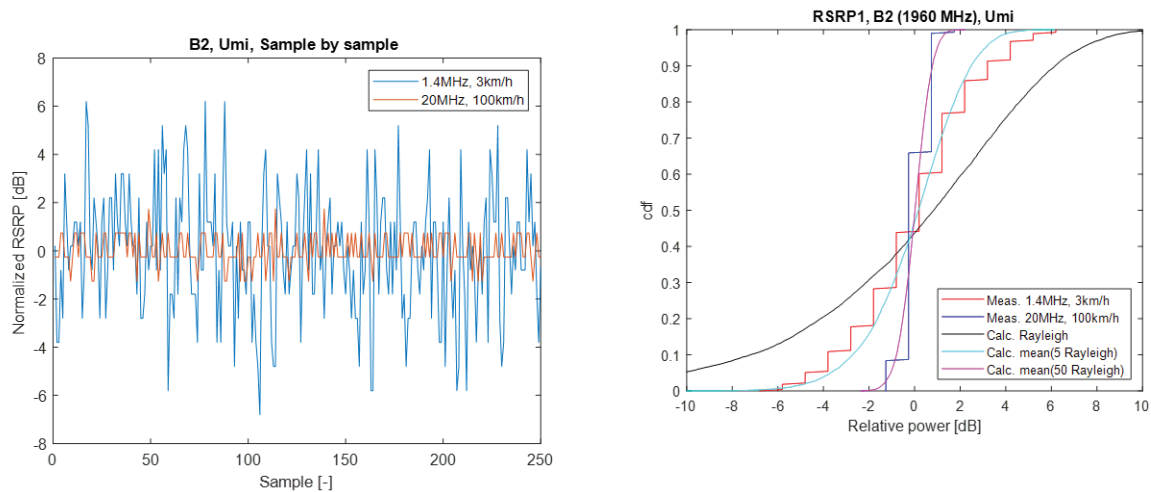
Figure 5.2.3.2-8. RSRP samples as function of time (left) and CDF of sampled RSRP values (right).

5.2.3.2.6   Test method

The test is performed similarly as in other MIMO OTA test methods: starting, with a test channel playing, from a high enough CE output power to achieve 0% BLER and then reduce output power stepwise (at CE output) while recording BLER. Before the test, it is important to load the DUT radiation patterns. BLER measurements are performed by the BS and are single-shot measurements of 10 000 samples repeated twice. After the test - adjust received power to absolute received power by the calibration factor. The test can be performed in two ways: 1) with the DUT traveling in a single fixed direction in the test channel, or 2) repeated twelve times (automatically by the software) where the test channel is rotated stepwise for each repetition (i.e., 30-degree steps).

Tests are performed automatically by the test SW.
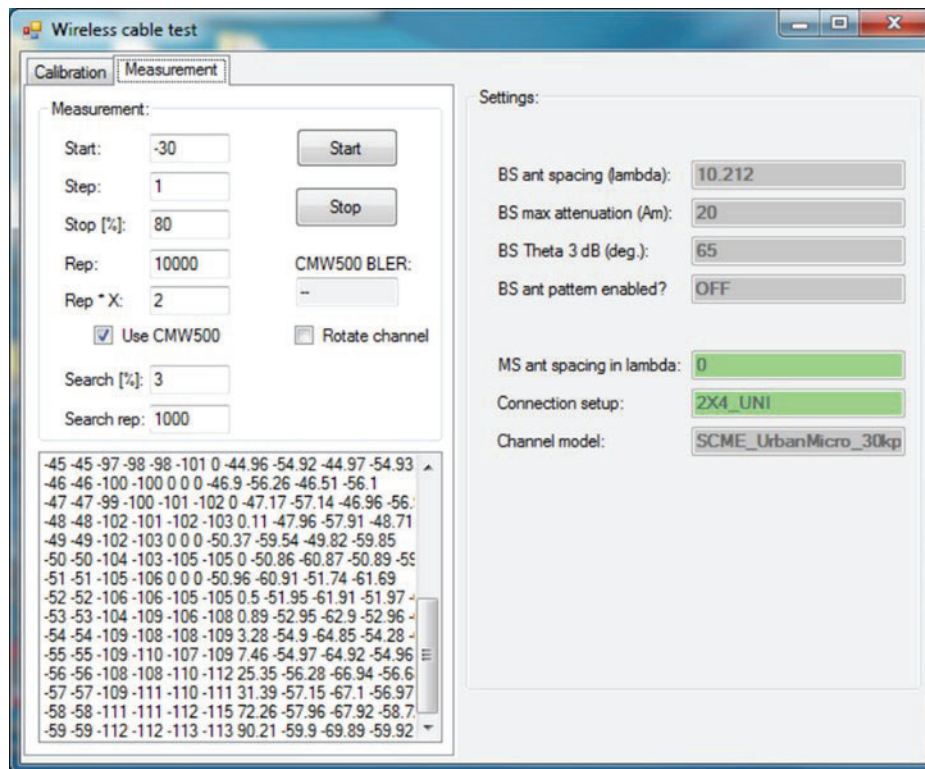
Figure 5.2.3.2-9. GUI for running BLER test. If "Rotate channel" is checked, twelve directions (30 deg. step) will be measured, and the test result will be an average over these directions/rotations.

5.2.3.2.7 Uncertainty estimate

As part of the project, an uncertainty budget has been derived. The expanded uncertainty, with 95% confidence interval, was evaluated to 2.4 dB. If an average over twelve directions is used the uncertainty is reduced to approximately 1.5 dB (depending on the accuracy of the DUT RSRP readings). In the document 3GPP TR 37.977 [WP3A-1] an uncertainty budget for WC measurements is described. By comparing to that budget, it has been verified that the uncertainty budget derived in the SIVERT project covers all crucial contributions of that document.

5.2.3.2.8 Validations

Here we show validations performed at LTE band 13, in an UMi channel with antennas from a CTIA measurement campaign for handset devices [WP3B-4]. The DUT is defined as the CTIA antenna module placed on a 1x1 m ground plane mimicking a vehicle roof, see figure below. The CTIA antennas come in three variants: a good, a nominal and a bad antenna pair. Radiation pattern measurements were performed in an AC for both vertical and horizontal polarization, with amplitude and phase and at a 5-degree elevation above the ground plane. In the data below we report an average gain in the specified 2D cut:

$$G_{avg} = 10log_{10}\left(mean\left(\sqrt{|G_V|^2 + |G_H|^2}\right)\right)$$

Average gain is not expected to be exactly mirrored in the throughput test results, but still some correlation between average gain of the antenna and throughput test result is expected.
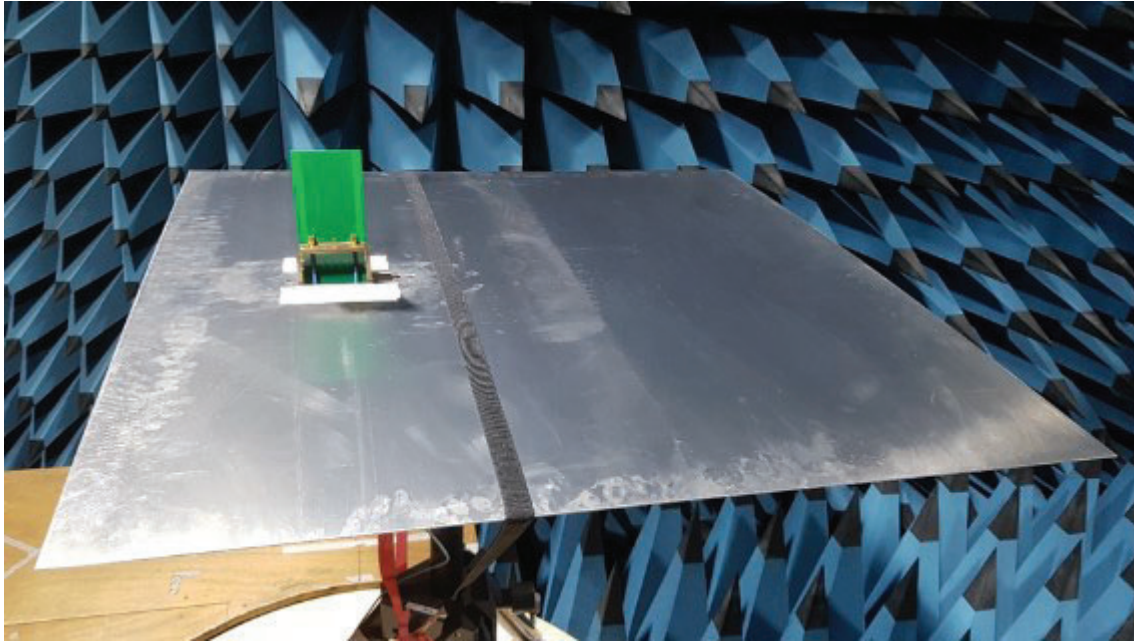
Figure 5.2.3.2-10. Radiation pattern measurement setup. CTIA reference antenna on 1x1 m ground plane.

In the validation average gain is compared to the test level needed for 50% throughput, where the 50% throughput value is derived from the average of twelve throughout tests (rotating of the test channel in 30 deg. steps between each test). As can be seen, the relative differences of average values are quite well reflected in the measured throughput data.

Table 5.2.3.2-2. Relative differences (in dB) good/nominal/bad for mean (2D cut) and WC throughput measurement.

Antenna	Mean (2D radiation patten)	WC throughput measurement @ 50%
Good	0	0
Nominal	-1.8	-1.1
Bad	2.4	-2.0
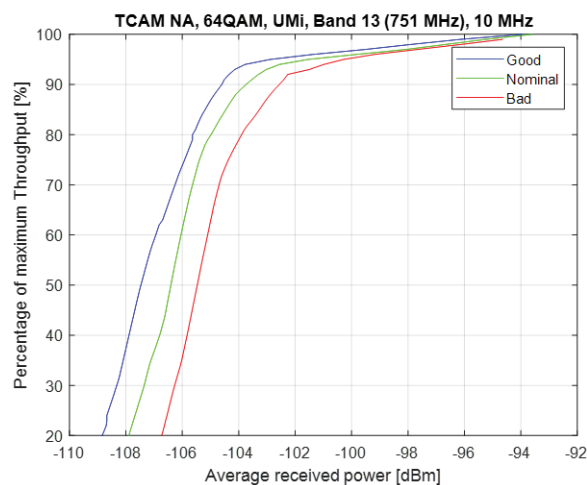
Figure 5.2.3.2-11. Throughput test. Average of twelve measurements with AoA rotated in 30 deg. steps.
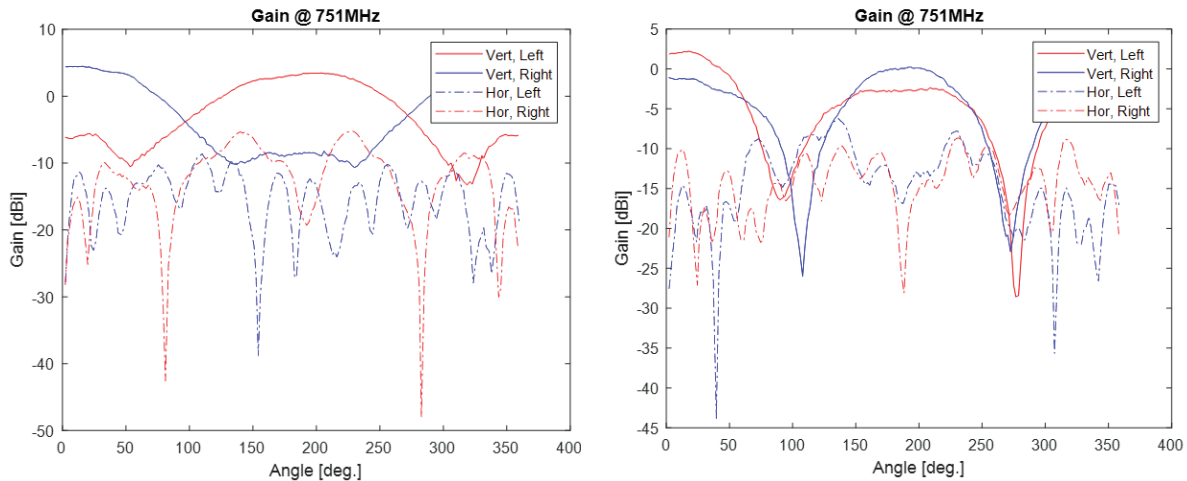
Figure 5.2.3.2-12. Reference antenna modules: Good (left), and bad (right).

5.2.3.2.9 Validations – WC intra Round Robin

Four ways of implementing the WC method have been evaluated within the project: Conducted-Two-Stage (CTS), WC with radio unit in a shielded box, WC with a novel rooftop shielded box (this is the first time this method is investigated), and WC in a semi-AC. The four implementations were evaluated with one radio, but two sets of antenna diagrams: antenna module radiation properties when placed in a roof position, and antenna module radiation properties when placed in a parcel shelf position. The installation effects of the different positions are illustrated in Figure 5.2.3.2-13 when measured in semi-AC Awitar. Here it is also illustrated how the effect of internal EMI on radio performance is revealed by the method when the engine is on. In Figure 5.2.3.2-14 results from the four WC implementations are compared, the agreement is good, especially at band 7, but also at band 13.
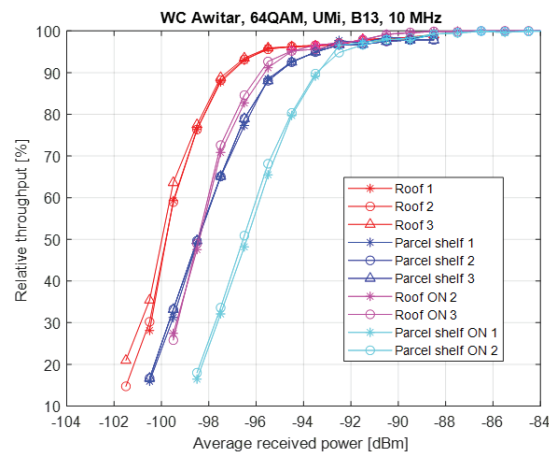
Figure 5.2.3.2-13. WC OTA test of radio with Roof positioned antenna module and Parcel positioned antenna module. Measured in semi-AC Awitar, including effects of engine on/off.
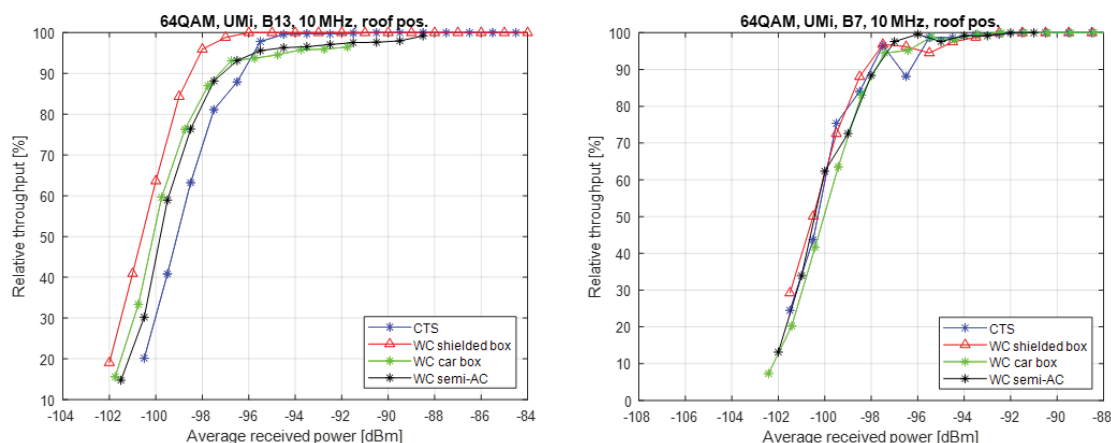
Figure 5.2.3.2-14. WC OTA intra-Round-Robin test results at band 13 and band 7.

5.2.3.2.10 Conclusions

A method and tools for WC OTA tests have been developed. The method can be applied in a rooftop shielded box, a regular shielded box, or in an AC. Each of these approaches has specific pros and cons. In general, tests with the wireless cable setup can distinguish good antennas from nominal and bad, order them in the correct order, with reasonable (based on the radiation patterns) relative differences. Also, the test time is reasonable, about 30 min for 1000 repetitions and twelve AoAs.

5.2.3.2.11 References:

[WP3B-1] https://www.rohde-schwarz.com/th/product/romes-productstartpage_63493-8650.html

[WP3B-2] 3GPP TS 36.214, "Physical layer; Measurements," V16.0.0, December 2019.

[WP3B-3] 3GPP TR 38.901, "Study on channel model for frequencies from 0.5 to 100 GHz," Release 16, v16.0.0, October 2019.

[WP3B-4]: I. Szini, B. Yanakiev and G. F. Pedersen, "MIMO Reference Antennas Performance in Anisotropic Channel Environments," in IEEE Transactions on Antennas and Propagation, vol. 62, no. 6, pp. 3270-3280, June 2014, doi: 10.1109/TAP.2014.2311468.

5.2.3.3 WP3C: Random line-of-sight

The Random-LOS environment is an environment which can be represented by one dominant wave, i.e., a line-of-sight (LOS) contribution [WP3C-1]. The LOS contribution is arriving at a random angle-of-arrival, because of the randomly oriented user device, e.g., a vehicle. The RanLOS measurement system, that realizes the Random-LOS environment, is basically a dual-polarized passive antenna that generates a plane wave at a short distance from the antenna. In this respect, the RanLOS system simulates the signal from, e.g., a base station at a large distance from the vehicle or device-under-test (DUT). The random angle-of-arrival is realized by a turntable where the DUT is placed.

The system can be configured for two different types of measurements, passive and active. For passive measurement, radiation pattern for an antenna mounted on a vehicle is obtained using a network analyzer. For active measurements, such as data throughput of a complete wireless system, typically a communication tester is used. A CE could also be added, e.g., to simulate Doppler, however this has not been tested in the project.

The passive antenna used in the RanLOS measurement system consists of a large reflector which is fed by a linear array of antennas, as shown in Figure 5.2.3.3-1. The array is dual-polarized and through a distribution network it is fed through two RF-connectors, one for each polarization. The reflector system in Figure 5.2.3.3-1 is designed for frequencies below 6 GHz and is therefore called the RanLOS Sub-6 GHz measurement system. The frequency range spanning from 750 MHz-6 GHz, requires three different antenna arrays. The measurements in the SIVERT project were all performed using the antenna array covering 1.5 GHz-3 GHz. Ideally should the RanLOS measurement system be placed inside a shielded semi-AC so that the measurements are not affected by disturbing signals from other sources, and reflections from the surrounding. However, in the SIVERT project we have used the RanLOS system at the SMP test site at Volvo Cars. This is an outdoor site, so we do have problems with disturbing signals from, e.g., base stations in the vicinity. This can most clearly be observed when performing active measurements, i.e., during throughput measurements. To perform the measurements, the RanLOS measurement system is used together with the RanLOS measurement software.
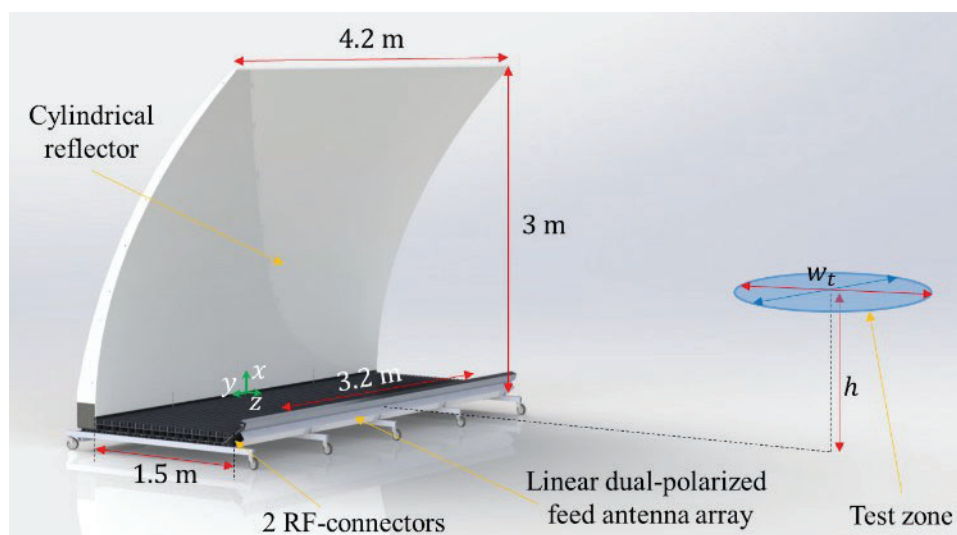

Figure5.2.3.3-1. The RanLOS Sub-6 GHz reflector antenna with the test zone in front.

5.2.3.3.1 Measurement and calibration description

As mentioned before, the RanLOS measurement system can be used to perform two types of measurements, passive and active measurements. In addition, a calibration measurement is also needed to get correct power levels in the measurements.

For the calibration, a reference antenna, with known gain, is placed at the center of the turntable, see Figure 5.2.3.3-2. The calibration routine then executes a frequency sweep on the network analyzer and the measured values are saved in a file. Depending on the need, the calibration is done for both horizontal and vertical polarizations, or for only one of them. Since the calibration is done for only one position of the reference antenna, the calibration procedure is very fast. The calibration must be repeated if something in the setup is changed, e.g., if the RanLOS reflector is moved or a cable is exchanged. Even though nothing has been changed in the setup, it is a good practice to perform a calibration in the morning before doing the real measurements.
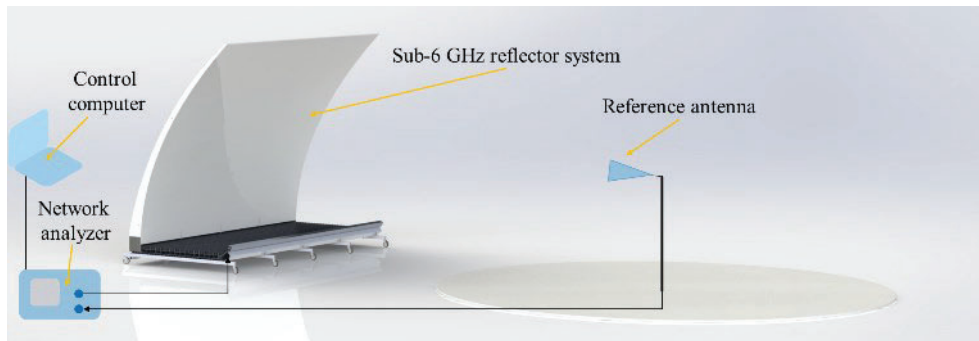
Figure 5.2.3.3-2. Calibration setup for the RanLOS Sub-6 GHz measurement system, as published in [WP3C-2].

To measure the radiation pattern for an antenna under test (AUT), e.g., an antenna mounted on a vehicle, the AUT is placed on the turntable as shown in Figure 5.2.3.3-3. Ideally, the vehicle should be positioned on the turntable so that the antenna under consideration is placed over the center of the turntable. One port of the network analyzer is connected to the antenna on the vehicle to be measured, and the second port is connected to one of the RF-connectors on the RanLOS antenna. Which RF-connector depends on which polarization that should be measured. The measurement is fully controlled by the software whereby the turntable is rotated and measurements for a full frequency sweep are taken in desired angular positions. By loading the calibration file created during the calibration procedure described above, the absolute antenna gain can directly be plotted after a completed measurement, see Figure 5.2.3.3-4. By using a multiport network analyzer, several antennas and/or polarizations can be measured at the same time.
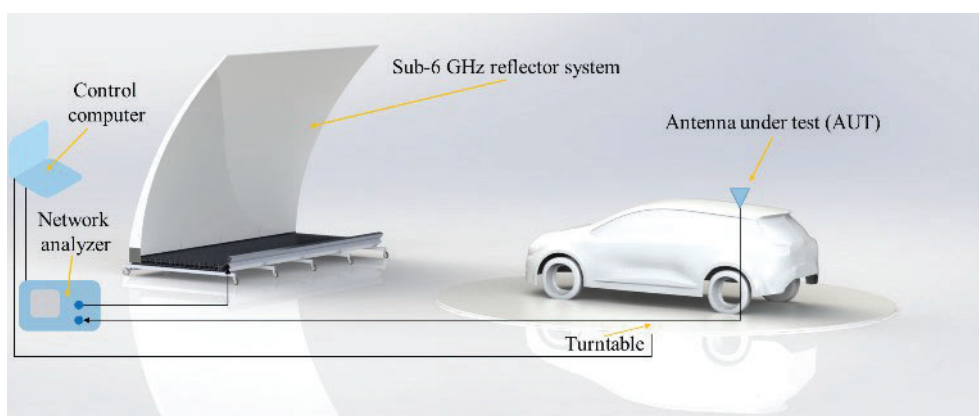
Figure 5.2.3.3-3. Passive measurement setup for the RanLOS Sub-6 GHz measurement system, as published in [WP3C-2].
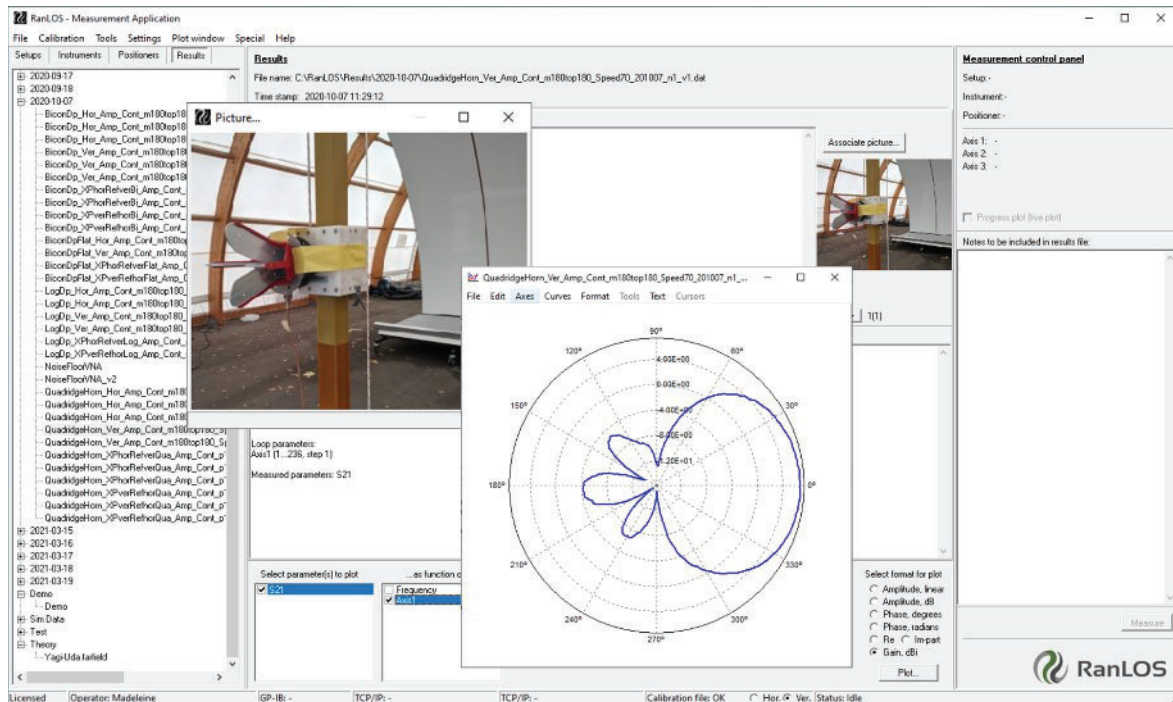
Figure 5.2.3.3-4. The RanLOS measurement software used for the passive measurements.

The basic setup for an active measurement, e.g., throughput measurement, is shown in Figure 5.2.3.3-5. The figure shows the setup for a 2-by-2 MIMO measurement. As shown in Figure 5.2.3.3-5, power amplifiers (PA) for the two DL streams and a low noise amplifier (LNA) for the UL might be needed. With the communication tester used in the project, both DL power amplifiers and an LNA for the UL were needed. A separate UL is commonly used in active measurement setups to keep the connection to the DUT during the measurements.
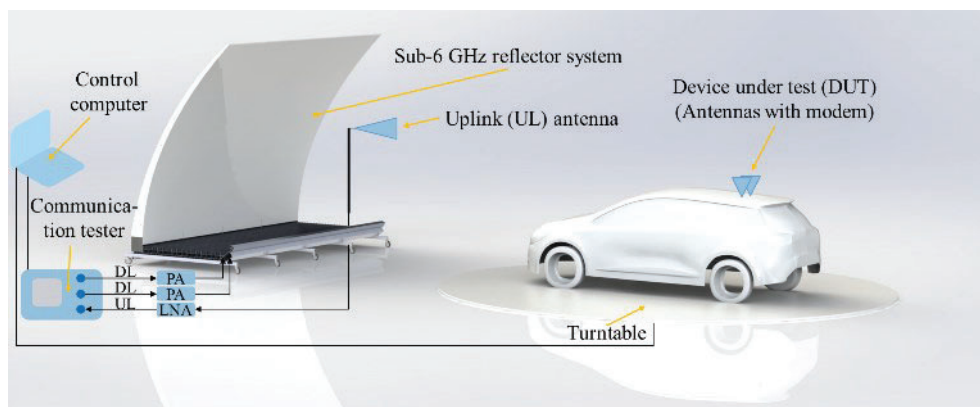
Figure 5.2.3.3-5. Active measurement setup, 2-by-2 MIMO, using the RanLOS
Sub-6 GHz measurement system, as published in [WP3C-2].

The calibration setup and procedure for the active measurement setup is in principle the same as for the passive setup. The differences are that the power amplifiers need to be included and that the measured calibration values, i.e., transmission losses for the two polarizations, are transferred to and stored in the communication tester. By doing it in this way the values read from the instrument will be corrected, and there is no need to do any post processing in the software.

Just as for the passive measurement, the vehicle is placed on the turntable, which for the measurement is rotated in steps. For each angular position, the DL power is swept from a high to a low value and at each power level the throughput (or any relevant parameter available from the communication tester) is recorded using the RanLOS measurement software, see Figure 5.2.3.3-6. The result is several throughput curves (as function of power), one for each angular position. By taking the average of all curves, the overall performance is obtained. For a 2x2 MIMO configuration, one DL stream is transmitted using the vertical port and the other stream using the horizontal port on the RanLOS system.

Figure 5.2.3.3-6. The RanLOS measurement software used for the active measurements.

5.2.3.3.2   Measurement results

Characterization of the test zone:
One of the tasks (T1) in the SIVERT project was to characterize the test zone in front of the reflector. This was done to see if the desired plane wave was generated in the test zone in front of the reflector. The field in front of the reflector was therefore measured, see Figure 5.2.3.3-7, and compared with numerical simulation results. The measured power density compares well to the numerical simulations, as the example result in Figure 5.2.3.3-8 shows. These results show that we get the desired field variations in front of the reflector system.

Figure 5.2.3.3-7. Measurement setup for measuring the field in front
of the reflector, placed at the SMP test site at Volvo Cars.
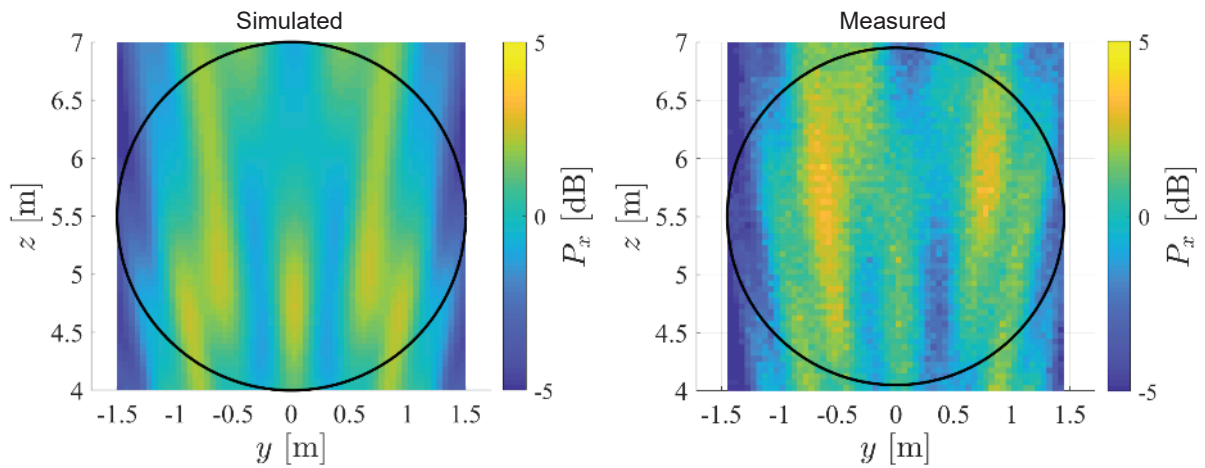
Figure 5.2.3.3-8. Simulated and measured power density for the vertical polarization, as published in
[WP3C-3]. The figure is shown for the height (h) 1.4 m above the base of the reflector and for 2
GHz. The origin of the of the coordinate system is at the center of the base of the reflector, as seen
in Figure 5.2.3.3-7.

The results from Figure 5.2.3.3-8 can be summarized in terms of standard deviation, σ, of the power, P, and phase, ϕ, within the test zone, i.e., the values within the black circles in Figure 5.2.3.3-8. The standard deviation results are shown in Figure 5.2.3.3-9 for the power and Figure 5.2.3.3-10 for the phase. The results show that we have good agreement between the measurements and the simulations.

Figure 5.2.3.3-9. Simulated and measured standard deviation of the power, $\sigma_{dB}(P)$, within the test zone, as a function of the test zone diameter w_t for 2 GHz, as published in [WP3C-3].
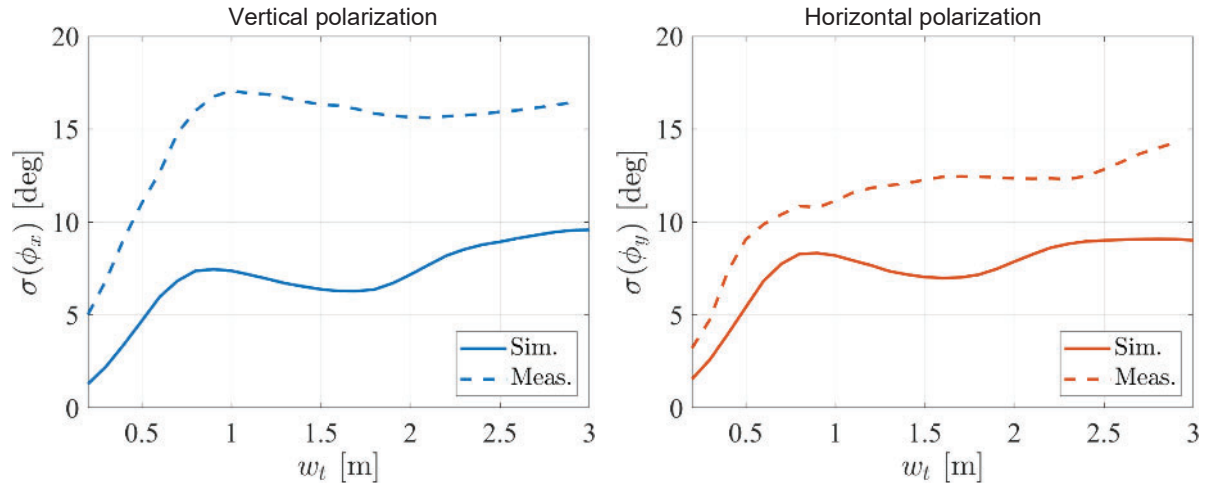
Figure 5.2.3.3-10. Simulated and measured standard deviation of the phase, $\sigma_{dB}(\phi)$, within the test zone, as a function of the test zone diameter w_t for 2 GHz, as published in [WP3C-3].

Radiation pattern measurements:

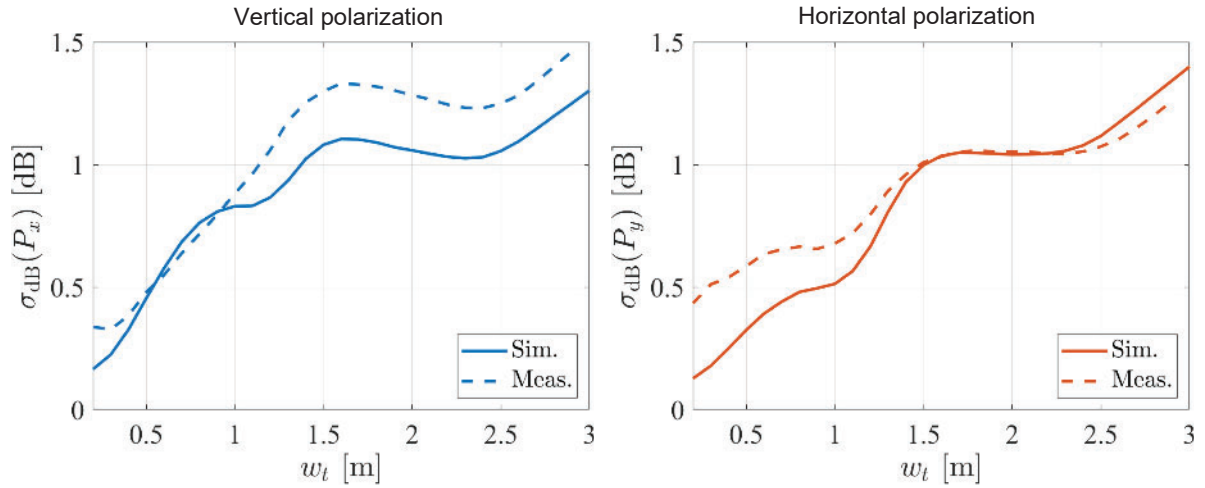As a part of Task 2 and Task 4 were radiation pattern, i.e., passive, measurements performed using the RanLOS measurement system. Radiation patterns have been measured for several stand-alone antennas, as well as vehicle mounted antennas. Here will two example results be shown, one corresponding to each task.

The presented radiation patterns have been performed using a setup like the one shown in Figure 5.2.3.3-3. However, for the stand-alone antenna measurements was the car exchanged with a stand-alone Quadridge horn antenna (ETS Lindgren, Open Boundary Quadridge Horn 3164-05), i.e., no vehicle was placed on the turntable. The measured radiation patterns are shown as absolute gain-values, which was acquired by doing a calibration measurement first, according to Figure 5.2.3.3-2. A biconical dipole antenna (Schwarzbeck Microwave Biconical Antenna SBA 9113), was used as the reference antenna in Figure 5.2.3.3-2.

The measured radiation pattern for the stand-alone Quadridge Horn antenna is shown in Figure 5.2.3.3-11. The measured radiation pattern using the RanLOS measurement system compares well to the

theoretical data from the data sheet of the Quadridge horn antenna. Both the absolute level and the shape of the curves agree.
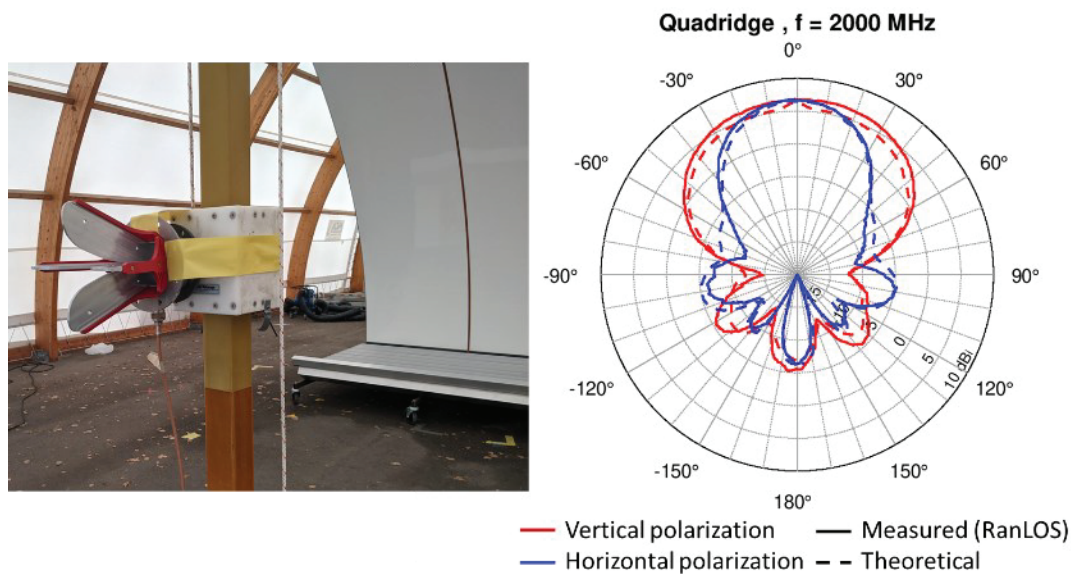
Figure 5.2.3.3-11. Measured radiation pattern of a Quadridge horn antenna. To the left is the measurement setup using the RanLOS measurement system. To the right is the comparison between the measured radiation pattern using the RanLOS system and theoretical data from the data sheet of the antenna. The example result is shown for the frequency 2 GHz.

Measured radiation pattern results are shown for a vehicle body with a roof-mounted antenna in Figure 5.2.3.3-12. The same vehicle body and antenna was measured both using the RanLOS measurement system and a near-field to far-field (NF/FF) lab in Denmark. The comparison between the two different measurement systems shows good agreement in the measurement results.
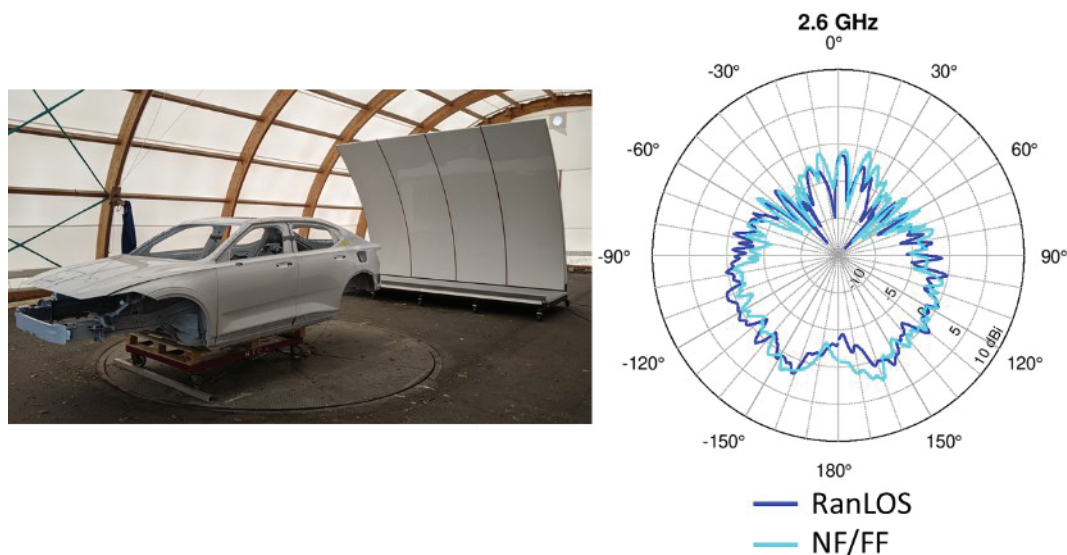
Figure 5.2.3.3-12. Measured radiation pattern of a vehicle body and roof-mounted antenna. To the left is the measurement setup using the RanLOS measurement system. To the right is the comparison between the measured radiation pattern using the RanLOS system and measurements using a NF/FF lab. The example result is shown for the frequency 2.6 GHz.

Throughput measurements:
Throughput measurements, i.e., active measurements, have been performed both for a stand-alone antenna as well as for a vehicle mounted antenna (Task 3 and 6). SISO, SIMO and MIMO throughput

measurements have been performed. However, only 2-by-2 MIMO measurements for the vehicle mounted antenna with a telematics connectivity unit (TCU) will be presented in this report. This is also the configuration that was compared for all the different measurement systems in the SIVERT project.

Throughput measurements were performed using four different measurement antennas, two for LTE Band 2 and two for LTE Band 7. The measurement antennas in each band are called nominal and good. The TCU that was used for the measurements did not support LTE Band 2, therefore was the LTE Band 2 reference antennas used for the nearby LTE Band 3 instead.

In the setup for the throughput measurements was the V60 placed on the turntable in front of the reflector, see Figure 5.2.3.3-13. The reference antenna was mounted on the vehicle roof and connected to the TCU through two RF-cables. The TCU was placed inside the car and connected to a power supply. The communication tester was connected to the two ports of the reflector system through two power amplifiers, see Figure 5.2.3.3-5. A separate UL had to be used to not lose the connection. The UL antenna was connected through an LNA to the communication tester. To get correct power levels was a calibration measurement, see Figure 5.2.3.3-2, performed for each of the communication links and compensated for accordingly in the communication tester.
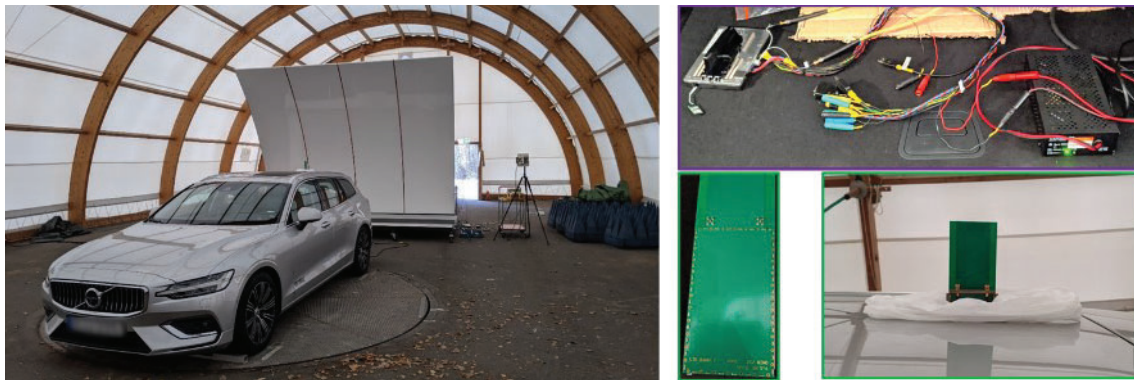
Figure 5.2.3.3-13. To the left- V60 used for the throughput measurements placed on the turntable at the Volvo SMP test site. To the top right (purple border)- TCU with power supply, and to the bottom right (green border)- Reference antenna mounted on the roof of the V60.

For the RanLOS measurements the vehicle was placed on the turntable which was rotated in steps of 5 degrees. At every step, the output power from the communication tester was swept from a high to a low value, and the throughput was measured at every power level. The result is a number of throughput curves, one for each rotation angle, as function of power. The overall performance is obtained by taking the average of all curves. The RanLOS throughput measurement results for LTE Band 3 (channel 1575) and Band 7 (channel 3100) are shown in Figure 5.2.3.3-14.
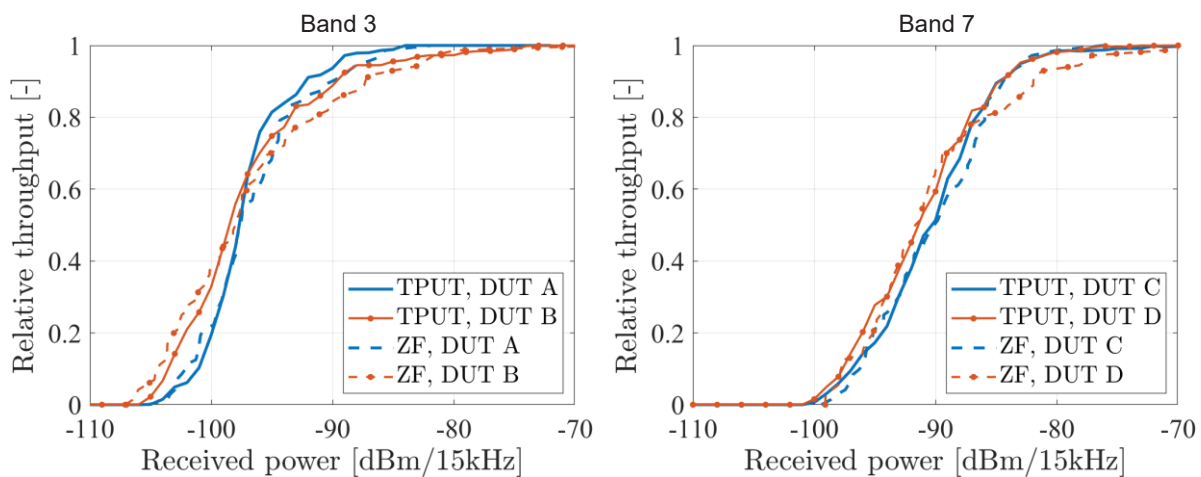
Figure 5.2.3.3-14. Throughput measurement results for the V60 with the roof-mounted reference antennas, for LTE Band 3 (channel 1575) and Band 7 (channel 3100), as published in [WP3C-3].

Also computed curves are shown in Figure 5.2.3.3-14. These curves assume the receiver to use a zero-forcing algorithm and the calculations are based on measured radiation patterns of the antennas mounted on the car, see [WP3C-3]. The radiation pattern measurements were done as described in Figure 5.2.3.3-3. We do not know if the receiver actually is using zero-forcing (ZF) but we can see that the ZF-curves are very similar to the measured throughput curves. More importantly we can conclude that we can hardly distinguish the good from the nominal antennas using either method, i.e., direct throughput measurements respectively calculations based on radiation patterns.

Repeatability measurements:
A measurement system analysis (MSA) has been performed during the SIVERT project. The repeatability has been measured for radiation pattern measurements on a vehicle. A Volvo S90 was used for the MSA measurements and a TCU was mounted in three different positions in the vehicle to simulate three different antennas. The three positions were roof, rear window shelf and dashboard. Three different operators were performing the MSA measurements.

A randomized order between the operators and the three antenna positions was used. In total was 27 measurements performed, 9 measurements for each antenna position, and 9 measurements for each operator. The measurements were performed over two consecutive days. In between each of the measurements was the car repositioned on the turntable, the cables were disconnected from the TCU and the TCU was moved to a new position according to the predefined schedule.

A sample result from the MSA measurements can be seen in Figure 5.2.3.3-15. The "Back", "Roof" and "Front" contain each nine measurements that are plotted in the same figure. We can easily distinguish the different radiation patterns from each other for the three different antenna positions, and the different operators do not significantly change the shape of the pattern.
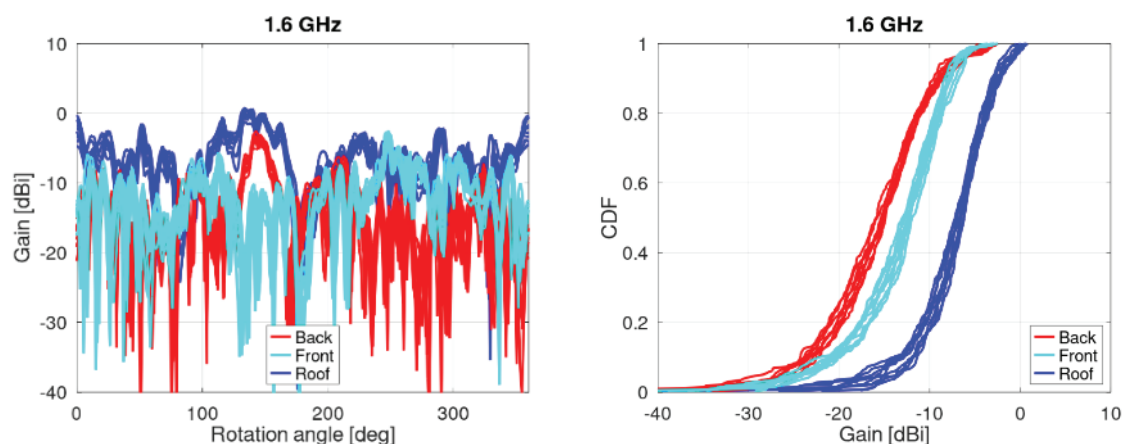
Figure 5.2.3.3-15. Radiation pattern and CDF of the radiation pattern from the MSA measurements at 1.6 GHz.

One MSA was evaluated on the CDF of the radiation pattern, at the 0.4 and 0.8 level. A summary of these results for two different frequencies are shown in Table 5.2.3.3-1. The MSA gives very good results with several cases of ideal or close to ideal performance.

Table 5.2.3.3-1. MSA results for the CDF of the radiation pattern.

Antenna position	1.6 GHz				2.7 GHz			
	CDF =0.4		CDF =0.8		CDF =0.4		CDF = 0.8	
	Mean [dB]	STD [dB]	Mean [dB]	STD [dB]	Mean [dB]	STD [dB]	Mean [dB]	STD [dB]
1 = Roof	-7.71	0.46	-3.88	0.33	-16.42	0.26	-12.24	0.19
2 = Back	-16.77	0.48	-11.17	0.20	-24.10	0.41	-17.13	0.59
3 = Front	-13.51	0.49	-9.09	0.34	-21.09	0.38	-16.01	0.32
MSA, Total Gage R&R	1.08% Close to Ideal		0.67% Ideal		0.89% Ideal		2.60% Okay	

Additional MSA analyses were made to conclude how the system performed when looking at the maximum gain in the radiation pattern. We wanted to know how large differences in gain that can be detected with the RanLOS Sub-6 GHz system. To look at this, the MSA should ideally have been done with the same antenna where the performance is reduced by adding attenuators to it. So the different units should therefore have been the same antenna but with attenuators of different values, e.g. 1 dB, 2 dB, 3 dB etc., added to it. Instead the attenuation was added in the post processing, which means that the same set of data, but shifted, was used as input for the different units in the MSA, see Figure 5.2.3.3-16.
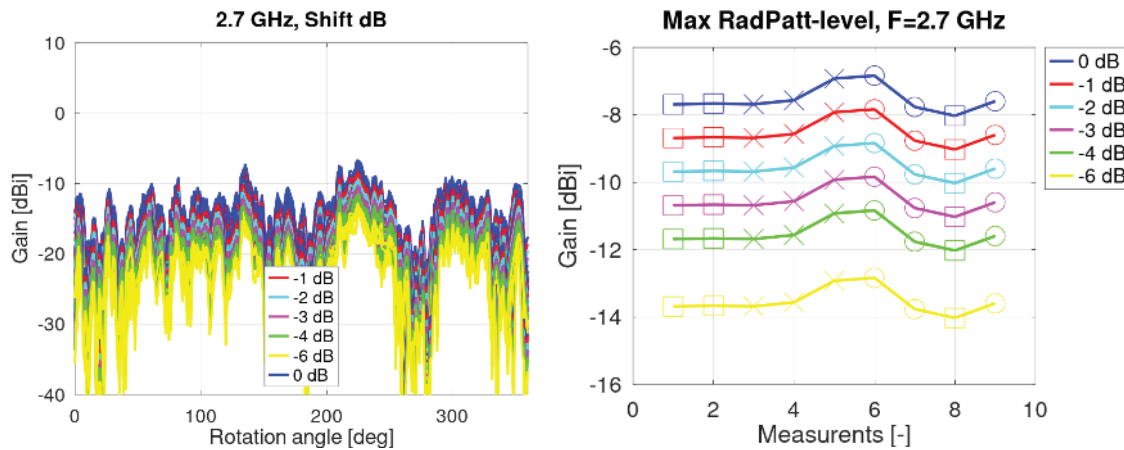
Figure 5.2.3.3-16. Left, radiation pattern for the roof position with added attenuation in the post-processing. Right, gain value at the angle 266 degrees for the different measurements with attenuation.

The MSA performance for the radiation pattern is summarized in Table 5.2.3.3-2. The system is usable when there is a difference of more than 2 dB in the maximum gain of the measured units. For 1.6 GHz the results are similar, but a difference of closer to 3 dB is needed to distinguish between the different units.

Table 5.2.3.3-2. MSA results for the radiation pattern when looking at the maximum gain angle, in this case 226 degrees.

Antenna shift	Gain @ 226 degree -1 dB shifts		Gain @ 226 degree -2 dB shifts		Gain @ 226 degree -3 dB shifts	
	Mean [dB]	STD [dB]	Mean [dB]	STD [dB]	Mean [dB]	STD [dB]
0 dB shift	-7.53	0.39	-7.53	0.39	-7.53	0.39
X dB shift	-8.53	0.39	-9.53	0.39	-10.53	0.39
2X dB shift	-9.53	0.39	-11.53	0.39	-13.53	0.39
MSA, Total Gage R&R	14.38% Not usable		3.98% Usable		1.8% Almost ideal	

The MSA results show that the RanLOS Sub-6 GHz system can be used to evaluate the performance the radiation pattern of different antennas mounted on vehicles. The evaluation can both be done in terms of CDF comparisons as well as looking at the maximum gain.

5.2.3.3.3   References

[WP3C-1] P.-S. Kildal and J. Carlsson, "New approach to OTA testing: RIMP and pure-LOS reference environments and a hypothesis," in 2013 7th European Conference on Antennas and Propagation (EuCAP), Apr. 2013, pp. 315–318.

[WP3C-2] M. S. Kildal, "The random line-of-sight over-the-air measurement system," PhD thesis, Chalmers University of Technology, Gothenburg, Sweden, 2020.

[WP3C-3] M. S. Kildal, S. M. Moghaddam, A. Razavi, J. Carlsson, J. Yang, and A. A. Glazunov, "Verification of the Random Line-of-Sight Measurement Setup at 1.5-3 GHz Including MIMO Throughput Measurements of a Complete Vehicle," *IEEE Transactions on Vehicular Technology*, vol. 69, no. 11, pp. 13165–13179, Nov. 2020.

5.2.3.4 WP3D: Reverberation chamber

In this section, it is described how to perform RC tests OTA, including a CE between the BS and the DUT. By applying different channel models, real-life events in an outdoor environment can be emulated. Historically, RCs are since long time used for both EMC tests as well as communication tests [WP3D-1]. The method in this document describes communication tests of both smaller devices such as radio units as well as radio equipment installed on larger objects such as cars or trucks; it only depends on the size of the RC (typically, a test object can occupy 1/8th of the total RC volume). In general, a small RC would have a higher starting point in terms of frequency compared to a larger RC. On the other hand, the average signal power loss will be higher in a larger RC, resulting in lower received signal levels that eventually hit the end of the dynamic range of the instrumentation for higher frequencies. However, for OTA tests below 6 GHz this is not an issue but, e.g., for the higher 5G bands (FR2) it must be considered.

Tests in an RC generally produces reliable, repeatable, and accurate results for measures such as:
- Efficiency (and total radiation efficiency)
- Coupling
- Diversity
- Throughput
- Sensitivity, etc.

It should be noted that the results are the isotropic response of the DUT and, e.g., a horn antenna pointing directly into the sky could have an equally good figure of merit as compared to, e.g., a dipole of equal efficiency – this is the major weakness of the method when it comes to evaluation of vehicles or other units that are not typically arbitrarily oriented during use.

For the OTA tests in the RC, channel models contain a set of rays/paths with separate Doppler and delays as described in, e.g., 3GPP, but the angle of arrival (AoA) is not modeled due to the RCs statistically isotropic characteristics (converges to isotropic angular distribution). In this project, the isotropic versions of the channel models UMi and UMa are used to simulate different aspects of urban environments, but of course other isotropic channel models can be defined and emulated as well.

5.2.3.4.1 Nested Rayleigh environments and the keyhole effect

One important decision when it comes to RC communication tests in combination with the CE is the number of RF connections between the CE and the RC. The reason for this being important is the keyhole effect which can arise when a CE is connected to an RC (or with two nested RCs), see Figure below.

In real life, the keyhole effect occurs in situations when scattering around the transmitter and receiver results in low correlation of the signals, while other propagation effects, like diffraction or waveguiding, lead to a reduction of the rank of the transfer function matrix [WP3D-2]. In a CE + RC constellation, we have the rich environment with low correlation in the RC, and similarly a reduction in channel rank due to the limited number of connections between the CE and the RC: a keyhole effect.

Moreover, as stated in [WP3D-2], for a single keyhole the channel matrix is rank one and the elements are distributed according to an i.i.d. double complex Gaussian distribution. Also known as double-Rayleigh. The keyhole effect can be reduced by having several RF connections from the CE (or first RC) to the (second) RC. Investigation of the Keyhole effect has been conducted with both simulations as well as measurements. For the simulations, we can express the channel matrix as:

$$H^{Keyhole} = H_{Rx} \cdot H_{Tx}$$

Where H_{Tx} is sized $N_{Keyholes} \times N_{Tx}$ and H_{Rx} is sized $N_{Rx} \times N_{Keyholes}$ and resulting capacity can be expressed as:

$$C^{Keyhole}(i) = log_2\left(\det\left(I_{N_R} + \frac{\rho}{N_T N_{Keyholes}} H^{Keyhole}(H^{Keyhole})'\right)\right)$$

For the measurements, a setup consisting of two RCs with four antennas on the transmitting side (located in RC 1) and three antennas on the receive side (in RC 2), see figure below, has been used. The dimension of RC 1 was 1.50 x 3.70 x 2.57 m³ and RC 2 was 4.54 x 3.70 x 2.57 m³. The two RCs were co-located with one joint wall where the keyholes were created. This wall was made of a 3 mm thick metal plate and to create the keyholes, holes were drilled and punctuated by putting short equal length electric conductors (with insulation) through each hole, see figures below. To avoid correlation between the keyholes, a minimum inter-distance between any of the holes was designed to be at least one wavelength. This nested chamber setup can be assumed to provide a similar keyhole effect as the RC and CE setup, where RC 1 represents the CE.

For the measurements, a 4-port Vector Network Analyzer (VNA) was used together with the two nested RCs. During the test a signal was sent by the VNA port 1 to a 4-port switch, then, depending on switch state, to one of four antennas in the transmit antenna configuration in RC 1, then through the keyholes, and finally received by the three receiving ports of the VNA. The frequency was chosen to match the resonance frequency (~ 1700 MHz) of the conducting wires, used as keyholes. To correctly sample the H-matrix stepwise stirring was used, and for each stirrer state twelve measurements were done (four transmit antennas manifested by the RF-switch and three receive antennas by the VNA traces).

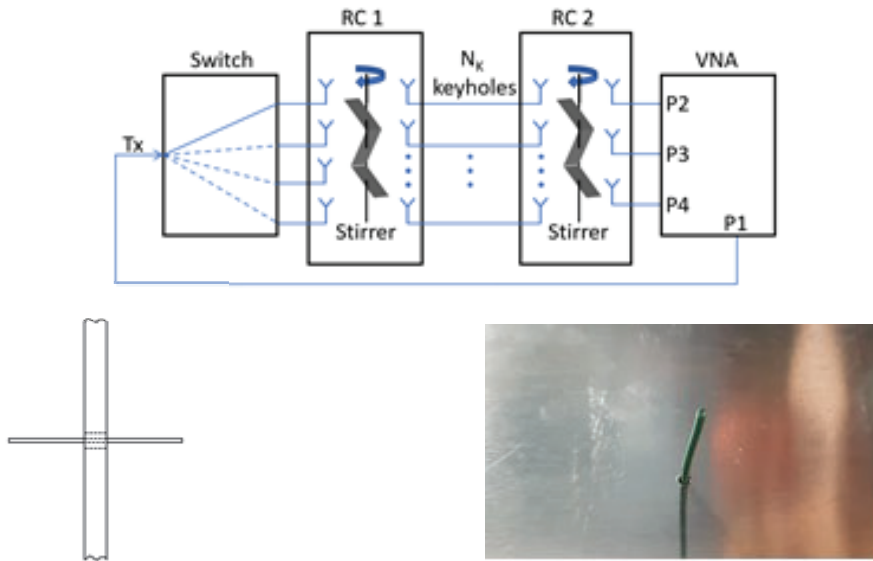Figure 5.2.3.4-1. Nested RC setup for characterization of keyhole effect (upper), realization of keyholes in common wall between RCs (lower).

The capacity of a Rayleigh distributed signal is shown together with capacity influenced by the keyhole effect, as a function of number of RF connections, for two examples of different MIMO system constellations without channel state information, in figures below.
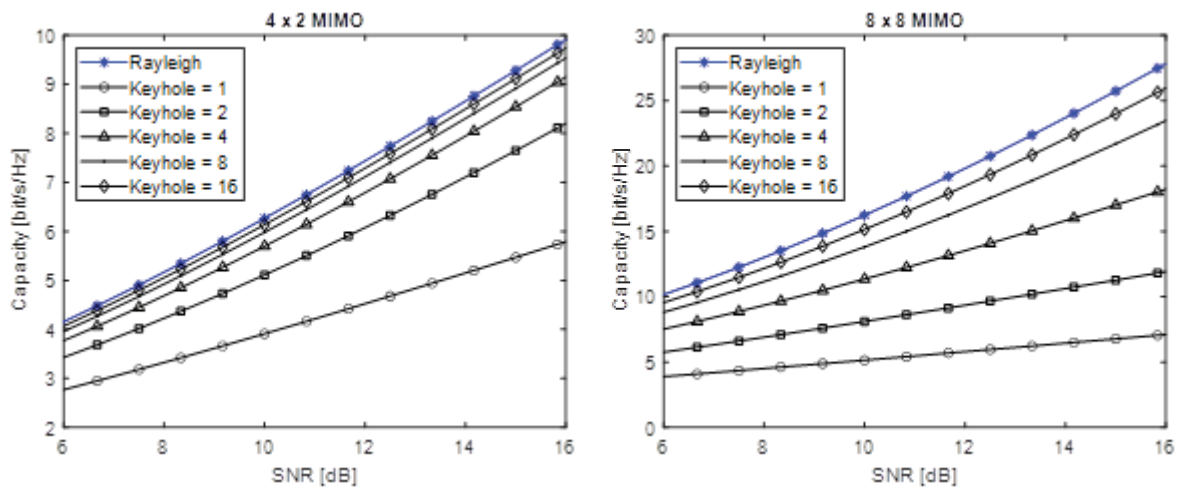
Figure 5.2.3.4-2. Capacity of an 4x2 and an 8x8 MIMO system for Rayleigh distributed signals as well as signals with keyhole effect.

In Figure 5.2.3.4-2 it can be seen that the capacity due to the keyhole effect is always underestimated compared to the expected capacity in a Rayleigh distributed environment. It has also been found that this effect can be corrected for and in the tables below the calculated correction factors for each investigated MIMO order, for an SNR around 10 dB, are shown. From the tables it can be seen that the keyhole effect is reasonably limited if the number of keyholes is two times the transmit order of the MIMO constellation under test. E.g., for 2x2 MIMO a correction of 1.2 dB should be applied if four keyholes are used, and for 4x4 MIMO a correction of 0.8 dB should be applied if eight keyholes are used.

Table 5.2.3.4-1. Keyhole Effect. 2 x N MIMO systems.

#RF Connections	MIMO constellation and correction [dB]		
	2x2 MIMO	2x4 MIMO	2x8 MIMO
2	2.4	3.0	2.9
4	1.2	1.3	1.3
8	0.8	0.8	0.7
16	0.3	0.3	0.4

Table 5.2.3.4-2. Keyhole Effect. 4 x N, 8 x 8 and 16 x 16 MIMO systems.

#RF Connections	MIMO constellation and correction [dB]				
	4x2	4x3	4x4	8x8	16x16
2	2.2	3.7	4.8	8.6	9.9
4	1.0	1.8	2.0	3.8	7.2
8	0.3	0.7	0.8	1.6	2.8
16	0.2	0.2	0.4	0.7	1.4

Furthermore, very good agreement between simulated and experimental results is achieved overall, except for one or two keyholes where the effect is underestimated in the measurement results compared to simulations (see Figure below). This underestimate can be explained by two effects: firstly, the average received power is lower for a low number of keyholes compared to a high number of keyholes. This results in the decreased dynamic range for a low number of keyholes, which in turn will increase the capacity estimate. Secondly, any measurement uncertainties, such as noise, will increase variation in the received signal and hence reduce the keyhole effect when estimated by a VNA. For real tests, however, signaling will not benefit from the noise, rather the opposite, and hence the keyhole underestimate is only present for one or two keyholes, and when characterized with the VNA.
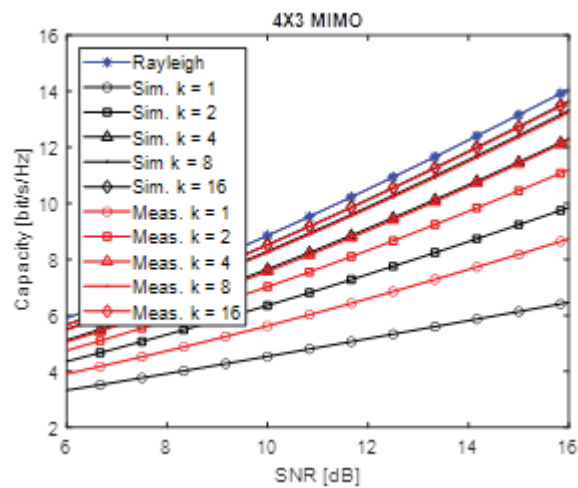
Figure 5.2.3.4-3. Capacity of a 4x3 MIMO system for Rayleigh distributed signals as well as signals with keyhole effect. Both simulated and measured.

The progress and results produced in the SIVERT project were published at the EuCAP conference in 2021.

5.2.3.4.2 RC facilities and the RC tent

RISE has three RCs of different sizes suitable for component test in frequencies from approximately 300 MHz to 18 GHz. To facilitate the test of cars and trucks an RC tent was invested by and put together at RISE during the project. This work has been done in collaboration with other personnel internally at RISE. The size of the RC tent is 16 x 8 x 6 m, and it works from approximately 100 MHz. For the RC tent, and some details of the work, see figures below.

Figure 5.2.3.4-4. Picture of RC tent from inside with a DUT truck.

Figure 5.2.3.4-5. Sand filled water hose to secure tent-to-ground connection (left), and a movable shielding wall (right) for reduction of the direct coupling.

Figure 5.2.3.4-6. Two pictures of a continuous mode stirrer. The movement of the motor creates waves in the textile walls (and roof to some extent). Two motors are built, and they are placed on opposing long sides of the RC tent before test.

To conform to radio spectrum emission regulations (and to get interference free measurement results) it was first believed that the RC tent needed to be placed inside a shielded room, and it was therefore placed in the Awitar semi-AC. But, by purchasing a conductive textile floor, and sealing the joints according to the figure below, it turned out that the shielding of the tent was sufficient for OTA test when placed in, e.g., a storage facility, or other building with enough space to host the tent.
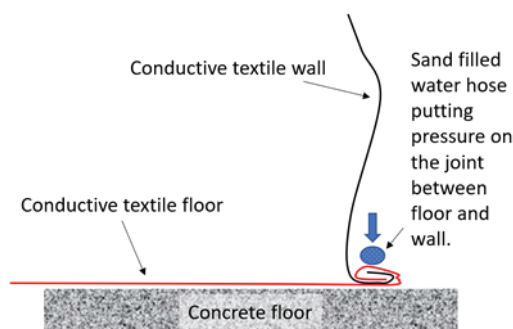
Figure 5.2.3.4-7. Method to RF seal joints between floor and walls.

Two types of tests were performed to estimate the shielding performance of the tent: measurement of ambient signals with a spectrum analyzer and direct measurement of the shielding effectiveness of the tent with a VNA. The measurement of ambient signals was performed with the spectrum analyzer connected via an RF cable to a wideband PICA antenna. Here the measurements were performed outside as well as inside the tent with doors closed. Results are shown in the figure below and it can be seen, except for a spike at 1722 MHz, that detected signal levels were sufficiently low. The signal at 1722 MHz was later identified as the LTE UL at band 3 from a mobile phone belonging to one of the

engineers present at the test site. **This teaches us that mobiles or other auxiliary equipment with wireless connections should be in flight mode during tests of, e.g., sensitivity**.
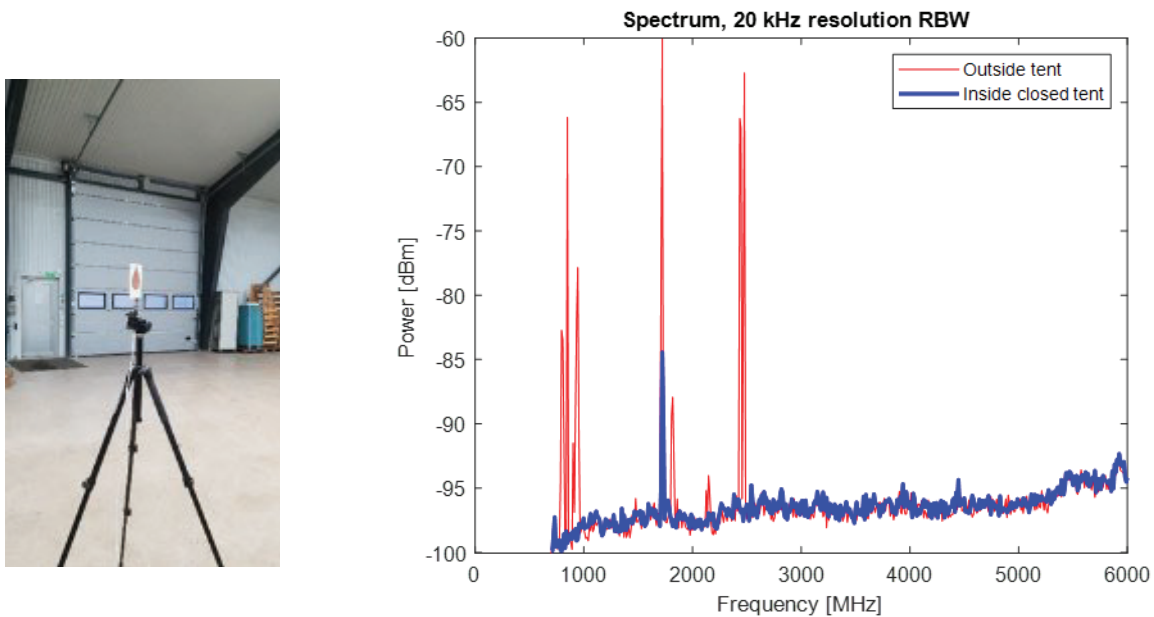
Figure 5.2.3.4-8. Rx antenna during measurement of ambient signals (left) and detected signals outside as well as inside the tent (right).

The results from the second measurement, using the VNA, resulted in approximately 40 dB of shielding.

5.2.3.4.3 Setup overview

A graphic illustration of the measurement setup in the RC can be viewed in the figure below. For a 2x2 MIMO test, the BS generates two DL signals that are emulated via the CE and distributed to four different transmit antennas (Tx1 to Tx4).

Inside the RC the signals are reflected towards the metallic floor, walls, and roof as well as stirrers and other objects - which ideally generate an isotropic and Rayleigh distributed environment within the chamber (after collecting enough statistics). The signal is finally registered by the DUT. The DUT maintains its connection to the BS via a separate UL channel to the BS. The BS will report measured DL BLER to the measurement software.

Figure 5.2.3.4-9. Graphic illustration of RC-measurement setup.
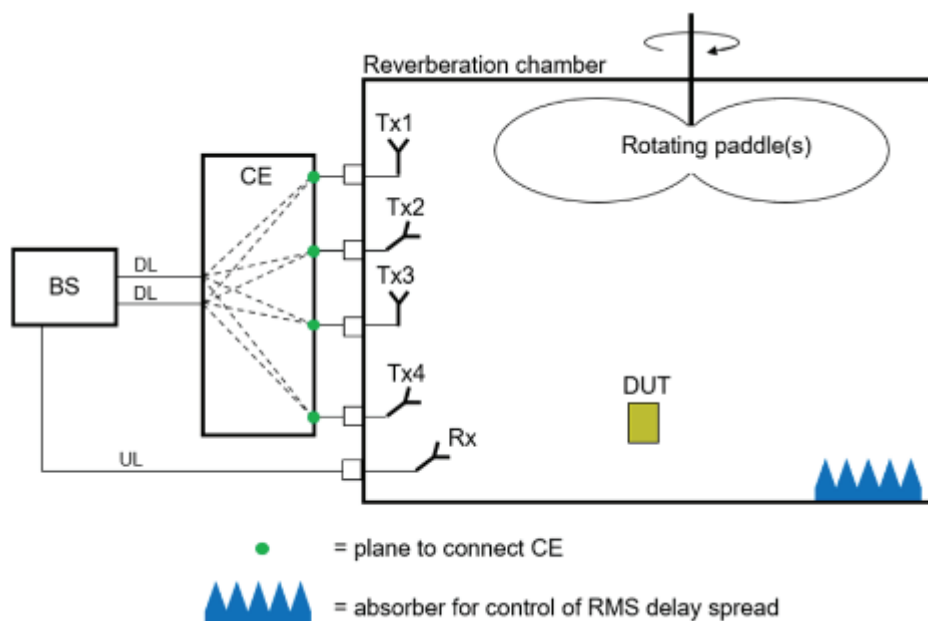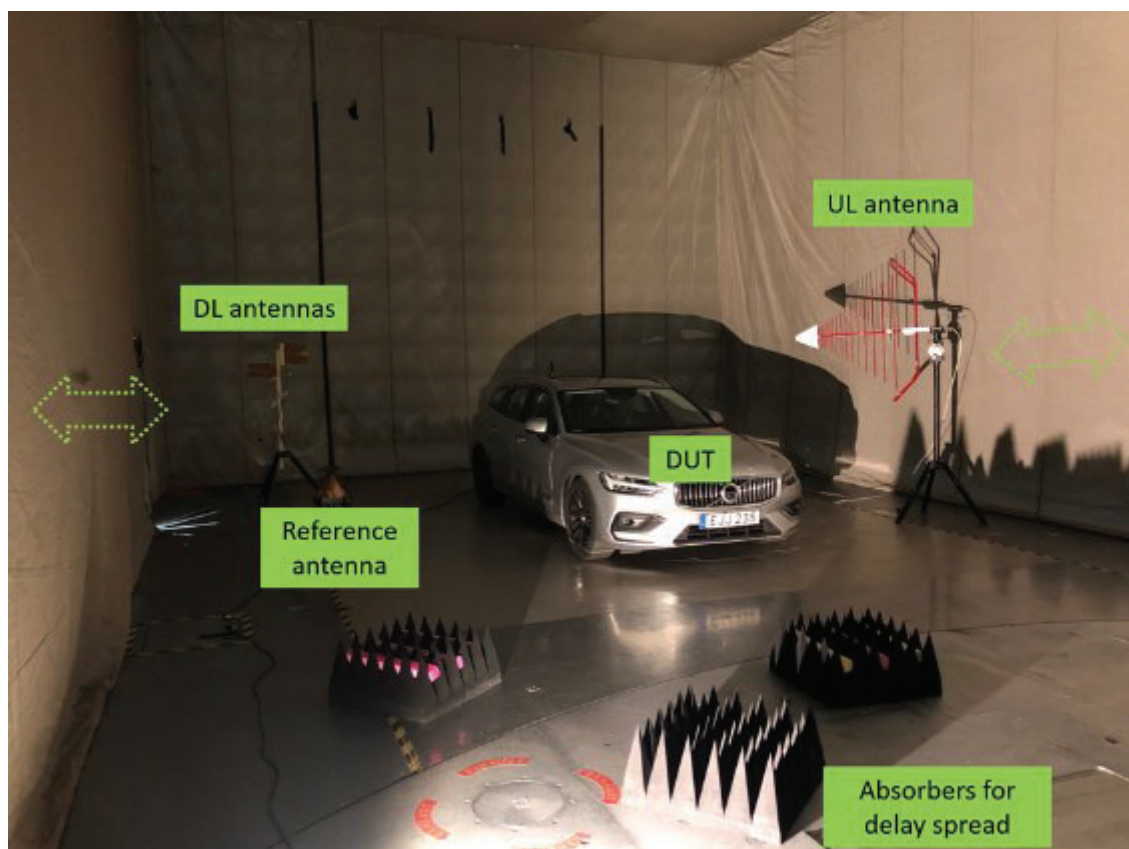

Figure 5.2.3.4-10. Picture of interior of RC tent with a DUT (Volvo V60), UL antenna, DL antennas, reference antenna, absorbers for controlling delay spread, and dashed arrows indicating slowly oscillating textile walls.

5.2.3.4.4 RMS delay spread

The CE is used to, e.g., mimic the delay properties of a real multipath environment, but in the RC OTA test setup there is also an inherent delay spread from the RC itself that needs to be considered. This inherent delay spread becomes larger, and hence more important to characterize, as the volume of the RC becomes larger (the RC tent measures 16 x 8 x 6 m and can be considered a large RC). RMS delay spread, σ_τ, is related to the coherence bandwidth, which in turn is dependent on the Power Delay Profile (PDP), $P(\tau_n)$, of the RC according to:

$$\sigma_\tau = \sqrt{\frac{\sum_n P(\tau_n)\tau_n^2}{\sum_n P(\tau_n)} - \left(\frac{\sum_n P(\tau_n)\tau_n}{\sum_n P(\tau_n)}\right)^2}$$

The control software has an inbuilt function to measure (with VNA) and thereafter calculate RMS delay spread, see Figure below. There PDP is calculated by an inverse chirp Z-transform. The chirp Z-transform is chosen as it enables control of the time axis after transformation which is useful when VNA bandwidth must be limited during evaluation, e.g., when the signal passes through the CE (presently limited to 40 MHz of bandwidth). The time span before the RMS delay spread calculation needs to be truncated at some point. In the figure below it can be seen how the power reaches the noise floor of the instrument after approximately 2500 ns and here somewhere the signal should be truncated before calculating the RMS delay spread.
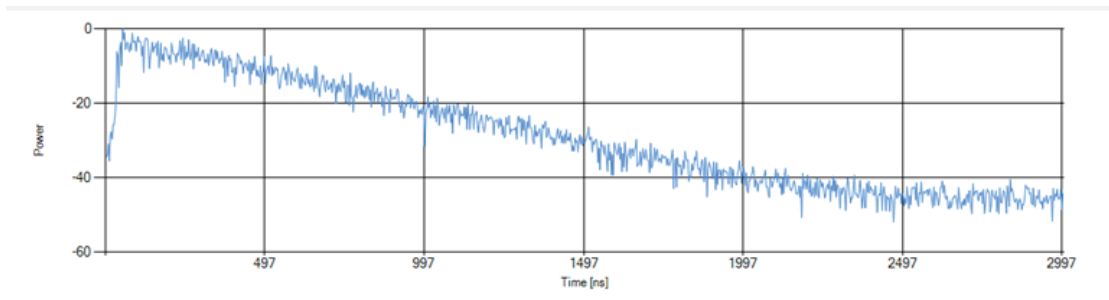
Figure 5.2.3.4-11. Part of software window for estimation of the RMS delay spread using the inverse chirp Z-transform.

Target values: 3GPP proposes 55 ns, or slightly above, in [WP3A-1]. This has shown hard to reach, especially for the large RC tent. Tests have been performed to investigate how sensitive a radio is to RMS delay spread, see figure below. As can be seen, level and shape are not significantly affected if the RMS delay spread is around 200 ns or less.
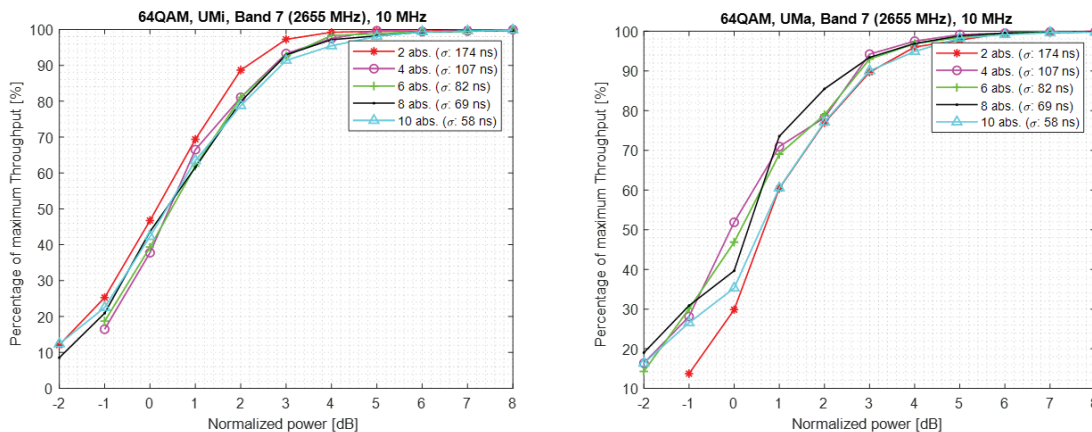
Figure 5.2.3.4-12. OTA test with several different RMS delay spreads.

To investigate the RMS delay spread of the RC tent in detail, the RMS delay spread as a function of one car plus a variable number of RF absorbers was characterized. This dependence is shown in the figure below. The model which extrapolates data indicates how many absorbers are expected to be needed to reach the 55 ns as proposed by [WP2A:2]. That many absorbers (~200) would load the chamber significantly and create unwanted LOS contributions to the measured data (Rician distribution).

Figure 5.2.3.4-13. RMS delay spread as function of number of RF absorbers.

5.2.3.4.5 Channel emulation

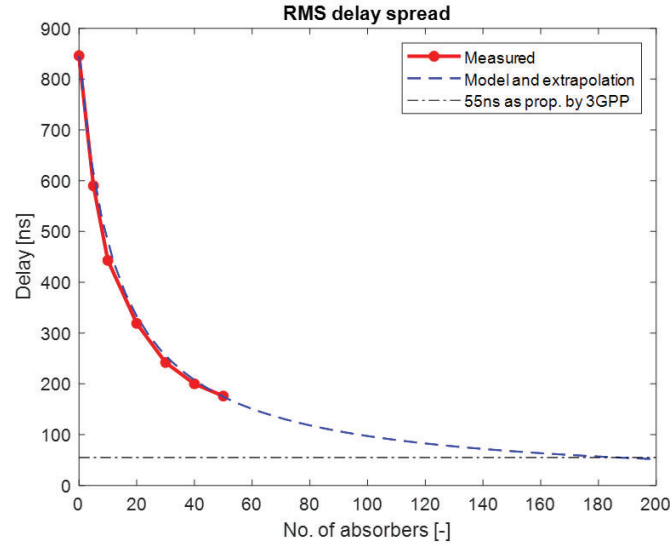All emulations are performed within a Spirent Vertex CE located outside of the RC, and every signal has therefore already gone through channel emulation before they reach the multipath environment within the RC.

Two main channel models have been implemented and utilized to emulate the input signals: UMi and UMa (isotropic versions) as defined by 3GPP [WP3A-1].

Delays are modelled according to 3GPP, but the resonant structure of the RC adds an additional inherent spread to the signals. How to treat this in the RC is described in the 3GPP standard and we adapt to that by adding proper loading in the RC.

The following properties are not modelled in the classical fading mode used in the RC:
- AoA and AoD
- Cluster AS AoD / AS AoA
- Cluster PAS shape
- Total AS AoD / AS AoA
- XPR

Both the UMi and the UMa model consist of 18 different paths with a Rayleigh fading, Doppler frequency (dependent on signal frequency and relative velocity), relative path losses as well as time delays. Besides the difference in delays and relative path losses the UMa has a BS correlation. To model that UMa is complemented with a correlation matrix which reflects both BS and MS antenna correlations. According to the Kronecker fading model for MIMO correlated channels, the BS and MS correlation matrices may be expressed as:

$$R_{BS} = \begin{bmatrix} 1 & \rho_{BS} \\ \rho_{BS}^* & 1 \end{bmatrix} \text{ and } R_{MS} = \begin{bmatrix} 1 & \rho_{MS} \\ \rho_{MS}^* & 1 \end{bmatrix}$$

The asterisk symbol represents complex conjugates of each correlation parameter. The total channel correlation matrix may then be constructed as $R_{chan} = R_{BS} \otimes R_{MS}$, where the explicit expression can be written in the following manner:

$$R_{chan} = \begin{bmatrix} 1 & \rho_{MS} & \rho_{BS} & \rho_{BS}\rho_{MS} \\ \rho_{MS}^* & 1 & \rho_{BS}\rho_{MS}^* & \rho_{BS} \\ \rho_{BS}^* & \rho_{BS}^*\rho_{MS} & 1 & \rho_{MS} \\ \rho_{BS}^*\rho_{MS}^* & \rho_{BS}^* & \rho_{MS}^* & 1 \end{bmatrix}$$

5.2.3.4.6 Calibration

The RC shall be calibrated with DUT inside the RC. By doing so the loss from the DUT will always be considered in a proper way prior to a test. Neither is the calibration very time consuming, and especially for the RC tent this is good practice as the tent size and therefore average chamber loss can vary between two independent tent mounts. For calibration, a low loss disc-cone antenna is used as a reference antenna. Besides very low loss, average chamber transfer function is corrected with the impedance (miss-) match of the reference antenna. Two ways of calibrating the RC have been defined: With CW source + CE, or with VNA:

- The advantage of the CW source + CE method is that almost no cables are changed when going from calibration to test. The disadvantage is that calibrations are performed per LTE band. However, those calibrations are fast (within minutes).
- The advantage of the VNA method is that a wide frequency band can be calibrated at one time, but the disadvantage is that several cables must be reconnected while changing from calibration to OTA test, which is a possible source of error.

The calibration with a CW source + CE, and a Spectrum Analyzer (SA) as a receiver, is mostly used in this project. For this setup, the calibration factor is defined as the power ratio marked by the red dots in the figure below. As normal for RC measurements, the results are average values, and for the calibration the result is an average of, e.g., 300 independent, uncorrelated power samples.
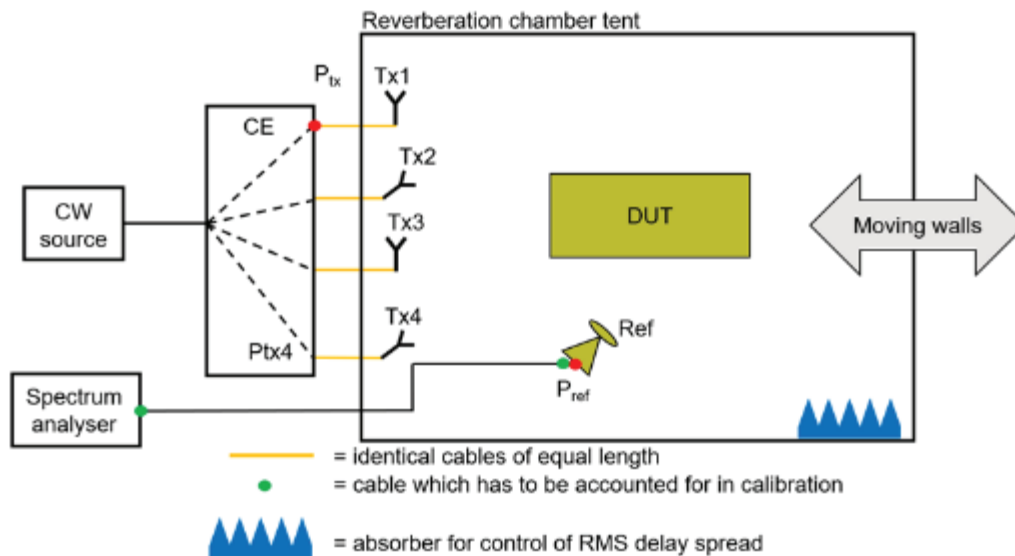
Figure 5.2.3.4-14. Calibration setup using a CW source and CE.

5.2.3.4.7 Test method

The test is performed similarly as in other MIMO OTA test methods: starting, with a test channel playing, from a high enough CE output power to achieve 0% BLER and then reduce output power stepwise (at CE output) while recording BLER. BLER measurements are performed by the BS and are single shot measurements of 10 000 samples repeated twice.

5.2.3.4.8   Uncertainty estimate

As a part of the project an uncertainty budget for OTA tests in the RC in combination with CE has been derived. The details of this uncertainty budget can be found in the test method report of WP3D, here only the final result is given, as well as specific details of the most significant contribution to the uncertainty budget: the standard deviation due to field uniformity. To find this standard deviation the RC transfer function between a transmitting and a receiving antenna is sampled (with VNA S21-parameter measurements) inside the RC while modes are continuously stirred. This uncertainty is then found by repeating the measurement while repositioning the receiving antenna inside the RC to new positions and polarisations around the DUT. In the project, field uniformity characterisations have been performed for OTA tests of both cars and trucks.

In the latter case loading of the RC is larger and the spatial distances between the receiving antenna positions are also larger due to the physical size of the truck. Also, in the measurement results, a small effect of a large-scale fading was observed in terms of a minor shadowing behind the truck (this was not observed in the case of the car). In Figure 5.2.3.4-15 RC transfer function measurements of 16 positions around the truck are shown, indicating quite equal power levels but with a small shift as a function of shadowing. In Figure 5.2.3.4-16 the standard deviation of those measurements is shown. Finally, in Figure 5.2.3.4-17, the standard deviation of the field uniformity for the OTA test of cars is shown. This standard deviation is smaller as the car is a physically smaller test object.

The expanded uncertainty of the complete OTA test method, with 95% confidence interval, was evaluated to 2.1 to 2.4 dB depending on whether the measurement object is a component, car, or a truck (the difference is due to the field uniformity). In the document 3GPP TR 37.977 [WP3A-1] an uncertainty budget for RC measurements is described. By comparing to that budget, it has been verified that the uncertainty budget derived in the SIVERT project covers all crucial contributions of that document.
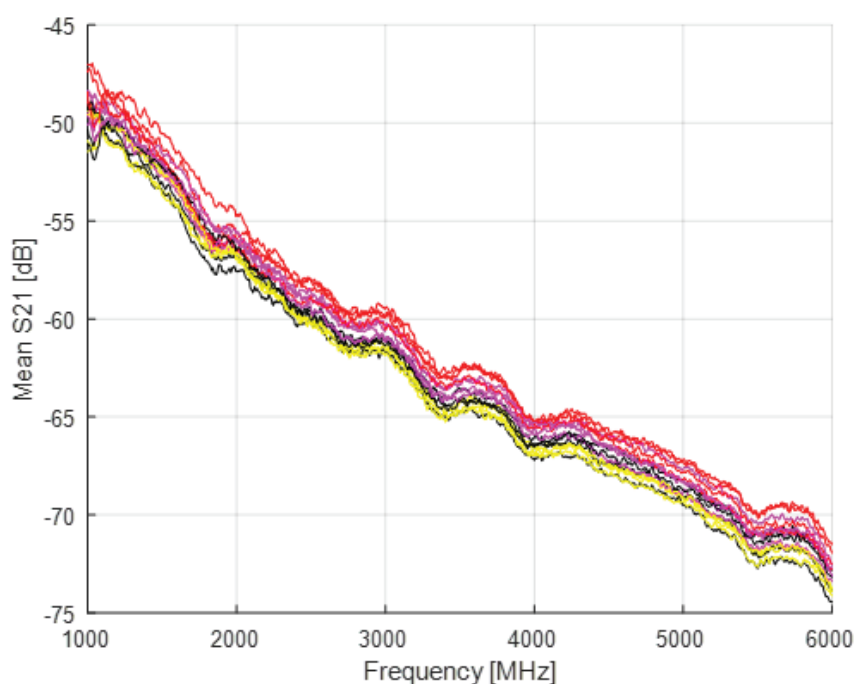
Figure 5.2.3.4-15. RC chamber transfer function during field uniformity evaluation of RC tent with a truck as DUT.
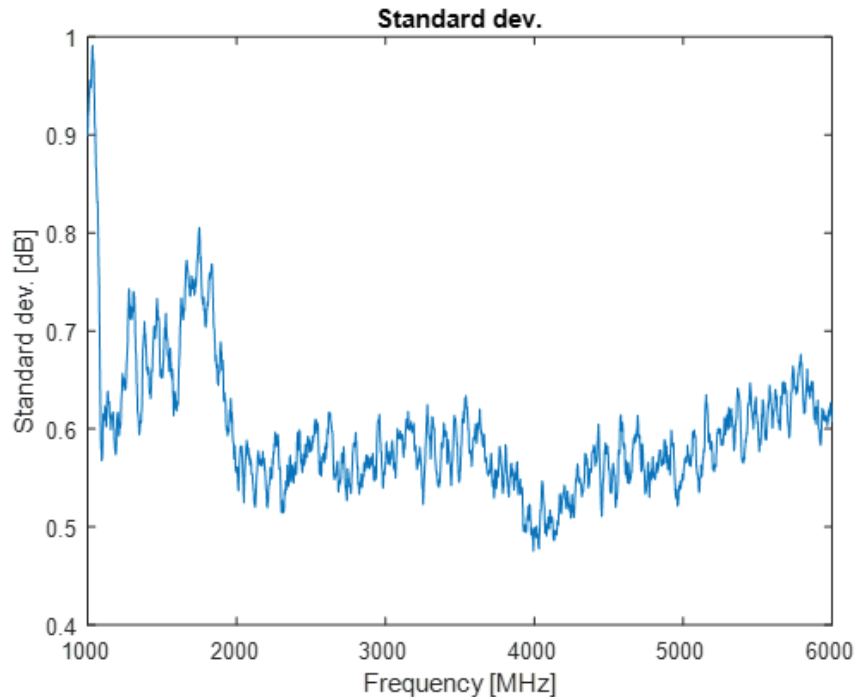
Figure 5.2.3.4-16. Standard deviation of field uniformity in RC tent with a truck as DUT.
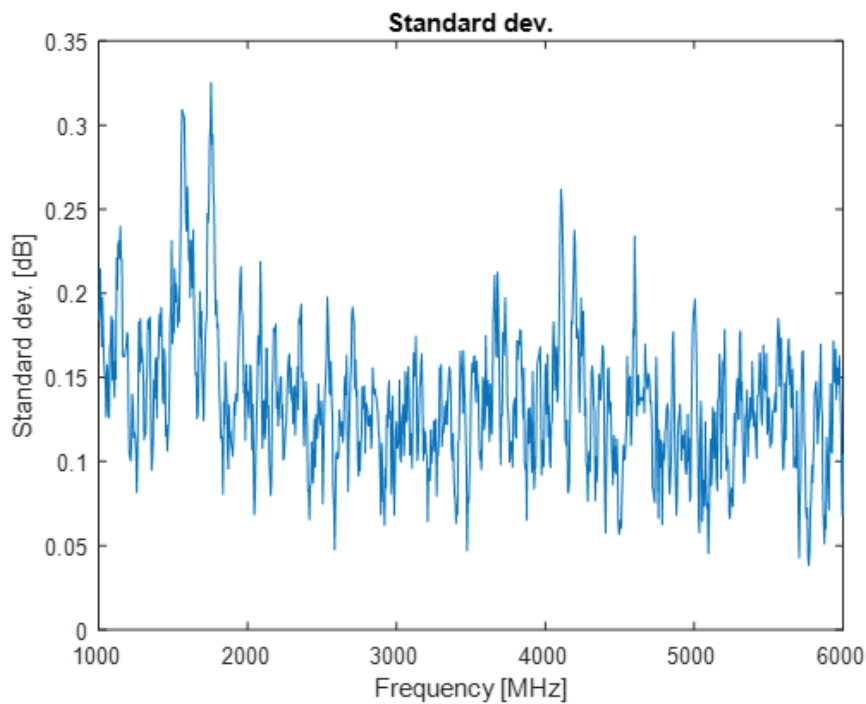
Figure 5.2.3.4-17. Standard deviation of field uniformity in RC tent with a car as DUT.

5.2.3.4.9 Validations

To evaluate the repeatability of the method a Measurement System Analysis (MSA) was performed where OTA throughput for a certain radio was tested when iterated between three different positions inside a vehicle: on the dashboard, on the armrest in the middle of rear seats, and on the parcel shelf. The tests were performed with the radio placed in these different positions according to a specific schedule defined by the MSA. Results showed that the method can find differences in OTA performance with high precision and good repeatability.
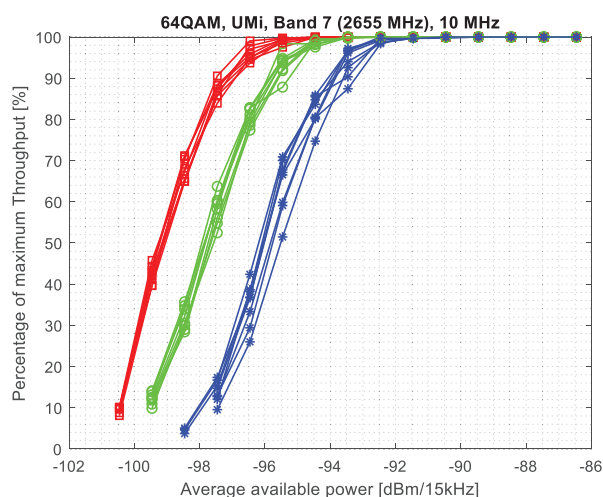
Figure 5.2.3.4-18. MSA measurement results. Throughput as function of received power.

5.2.3.4.10 PoC 4X4 MIMO

During the project, a new BS simulator was invested enabling tests of up to 4X4 MIMO systems. Such test (4X4) was conducted without CE in a so called NIST channel (only the RC). The test was performed on both a COTS mobile as well as on a vehicle graded radio, and the test was performed with varying settings. In Figure 5.2.3.4-19 test results of the vehicle graded radio are shown for different settings of the MCS index.
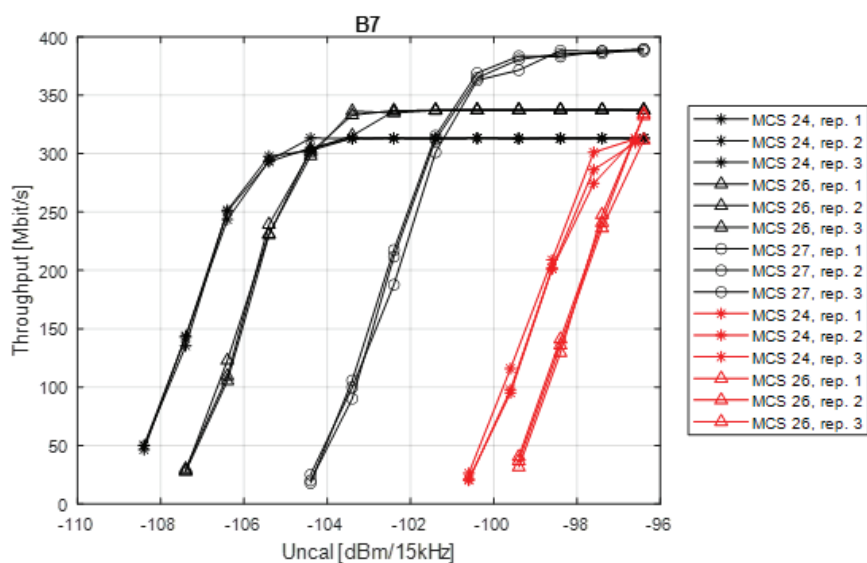
Figure 5.2.3.4-19. LTE throughput for different MCS index and 4X4 MIMO. COST mobile (red) and vehicle graded radio (black).

5.2.3.4.11 PoC Truck installation

The installation effects of radio including antennas on a truck were investigated by an OTA test in the RC tent. Two antenna configurations were tested and compared: 1) one external antenna in combination with an antenna in the overhead compartment inside the cabin, 2) two external antennas on top of the cabin. The antenna positions are illustrated in Figure 5.2.3.4-20 and Figure 5.2.3.4-21, and results are presented in Figure 5.2.3.4-22.

Figure 5.2.3.4-20. Antenna position combinations from outside. Dashed red + red circle: external antenna in combination of antenna in overhead compartment inside cabin. Yellow circles: two externally mounted antennas on top of cabin.

Figure 5.2.3.4-21. Antenna position combinations repeated. On top of cabin (left), in overhead compartment (right).
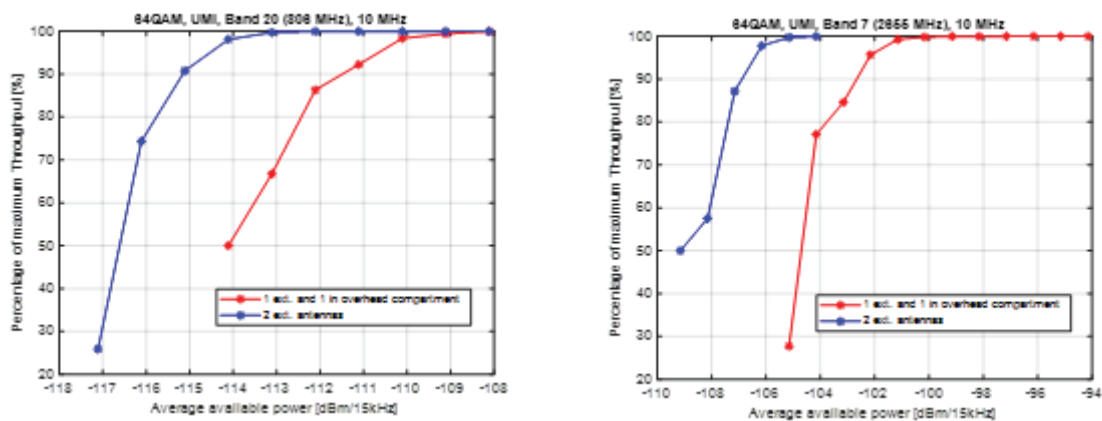
Figure 5.2.3.4-22. Test results. Averaged over the tested bands: configuration 2) is roughly 3 dB better than configuration 1).

5.2.3.4.12 Conclusions

During the SIVERT project, we have developed throughput test methods for components, as well as entire systems on, e.g., car or even full truck. We have shown that measurements now can be performed in the component test RC "Fourier" on sub-systems, or in the RC tent on full vehicular systems.

The method has two major advantages: tests are quick, and the accuracy of the test results is good. The major drawback of the method is that it takes only isotropic propagation aspects into account.

5.2.3.4.13 References

[WP3D-1] X. Chen et al., "Reverberation Chambers for Over-the-Air Tests: An Overview of Two Decades of Research," in IEEE Access, vol. 6, pp. 49129-49143, 2018.

[WP3D-2] P. Almers, F. Tufvesson and A. F. Molisch, "Measurement of keyhole effect in a wireless multiple-input multiple-output (MIMO) channel," in IEEE Communications Letters, vol. 7, no. 8, pp. 373-375, Aug. 2003.

[WP3D-3] C. Orlenius, M. Andersson, "Connected Reverberation Chambers with Variable Channel Rank for Measurement of MIMO Antenna System Performance", IEEE AP-S International Symposium on Antennas and Propagation, Charleston, USA, June 1-5, 2009.

5.2.3.5 WP3E: Evaluation and prototype

This section aims to compare the four MIMO OTA test methods described in the previous sections, in order to understand the applicability of each of them for full-vehicle OTA tests. The focus will be on comparing results from Round Robin measurements performed within the scope of the project.

The results presented here are extracted from the internal comparison report with more complete results and discussion [WP3E-1].

5.2.3.5.1 Methods Evaluation Approach

The overall goal with an OTA test method for vehicles is to provide performance assessment representative to what the user will experience in real world. The key aspect is that a good device in the field is also recognized as good in the lab testing and vice versa for a worse performing device. In other words, the lab testing needs to provide the same ranking of units as is experienced in the field. If this is the case, the lab testing will be able to identify issues related to a bad or erroneous antenna, chipset and or RF front end design.

For the methods developed within the FFI SIVERT project it is important that this aspect of the test method is confirmed. In order to do so, a Round Robin measurement campaign was carried out utilizing antennas with known performance. The RF properties of the antennas had been designed so to provide good, nominal and bad performance in a multipath environment. These antennas were then measured using the different methods.

In addition to lab tests, field tests have been performed utilizing the same antennas. In this way the performance assessment based on lab testing can be directly compared to what is seen in real-world operation.

In addition to making sure that the methods provide representative real-world performance assessment, other aspects of an OTA test method for vehicles are also of importance. For example, the repeatability and full uncertainty need to be understood. Other aspects, like the complexity, flexibility and extension possibilities to future technologies are also important when selecting a test method for vehicles. Such Key Performance Indicators (KPIs) have also been defined and analyzed for each of the methods within the scope of this project.

Round Robin Measurement Campaign

The Round Robin measurement campaign utilized well-defined testing scenarios and devices, in order to make the test results as comparable as possible. The goal with the test methods is to provide a testing environment for arbitrary vehicular wireless technologies utilizing multiple antennas. However, due to time and practical constraints the measurement campaign focused on LTE 2x2 MIMO technology. Base station simulator settings were aligned for all methods, as well as the basic channel model (if used by the method) and the devices to be used. The metric used in the measurements was MAC layer throughput as a function of cell power level. This is a common metric utilized in the industry and the standards (see for example [WP3E-2]).

Devices

The Round Robin measurement campaign utilized a copy of the 2x2 MIMO reference antennas developed for a CTIA measurement campaign for handset devices [WP3E-3]. These antennas can be seen in Figure 5.2.3.5-1. They consist of two antenna elements connected to an RF enclosure (in which the RF connectors are placed), which was intended to be used for easy placement of a handset during the original campaign.
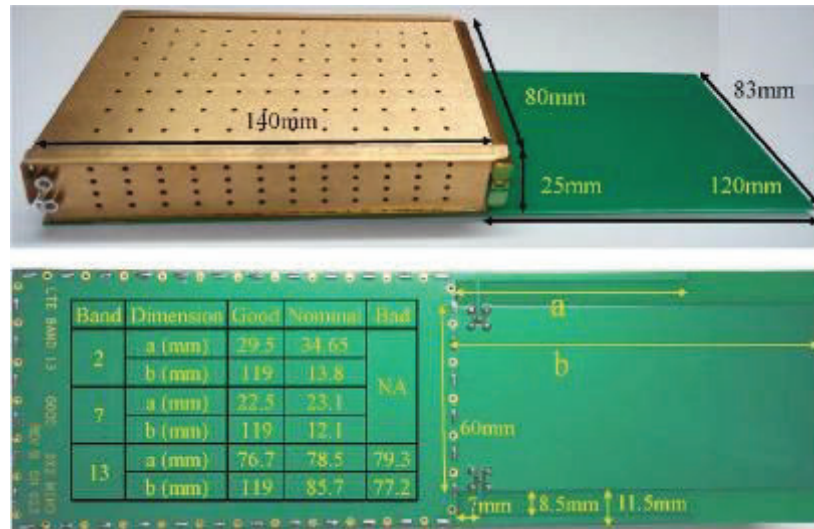
Figure 5.2.3.5-1. Details of the reference antennas utilized in the measurement campaign. This picture is reproduced from [WP3E-3].

In total there are 7 reference antennas for three different LTE frequency bands (band 2,7 and 13). The RF properties of the antennas (efficiency and correlation) are designed to provide Good, Nominal and Bad performance for each frequency band. The efficiency and the 3D isotropic correlation for the band 7 and band 13 antennas are shown in Figure 5.2.3.5-2 and Table 5.2.3.5-1 (when antennas are mounted on top of a big ground plane). As can be seen, the Good antenna has higher gain and lower correlation compared to the Bad antenna. For band 2 and 7 only good and nominal antennas have been designed, since it is difficult to obtain highly correlated antennas for these bands.
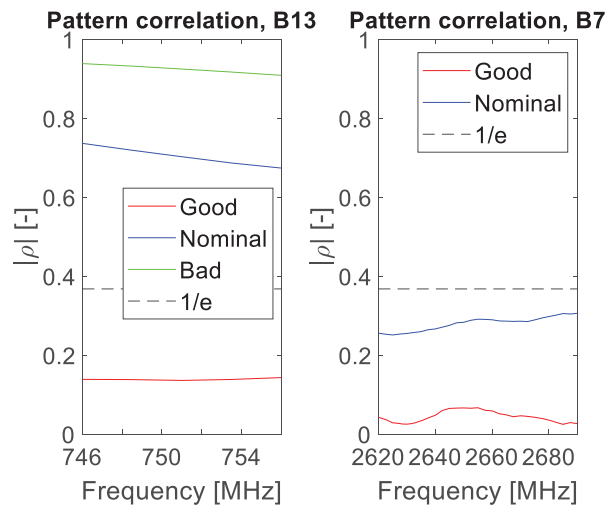
Figure 5.2.3.5-2. Free space 3D isotropic antenna gain correlation measured for the reference antennas placed on top of a big ground plane for band 13 (left) and band 7 (right).

Table 5.2.3.5-1 Average gain of reference antennas when mounted on a 1x1 meter metallic ground plane.

Antenna	Average Gain Vertical [dBi]
Good, B13	-0.25
Nominal, B13	-2.10
Bad, B13	-2.7
Good, B7	-3.06
Nominal, B7	-3.30

The reference antennas were connected via external connectors to a VCM, which acted as the receiver. In this way, the signals received by the antennas were fed to the respective MIMO ports of the VCM chipset (Figure 5.2.3.5-3). The supplier of the VCM ensured that the internal antennas were disconnected when using these external cables so that no additional energy could leak via the built-in antennas in the module. A couple of different VCM were used during the tests, which ideally should have the same performance but in practice contributes to some additional uncertainty in the measurement results due to unit variation. The same VCM was used for each methods results, so the relative comparison between antennas should be correct even if the performance is slightly different. Furthermore, due to the limited bands supported by the VCM version utilized for a specific measurement, some measurements were carried out on a different but adjacent band compared to what the antennas were designed for.
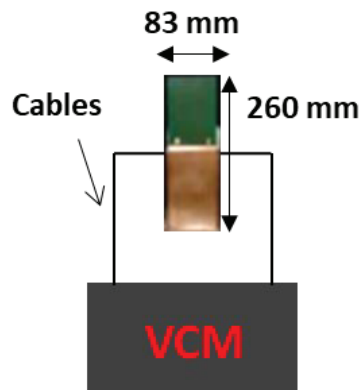
Figure 5.2.3.5-3. Reference antenna connected to the VCM.

Method Setup
Each method was setup in line with what is described in previous sections. The base station simulator settings defined in [2] were used by all methods. As a basic channel model, the SCME UMi was used, as defined in [WP3E:2]. Each method implements this channel model differently and thus the exact channel conditions as seen by the DUT will vary between the methods. The exception is the RLOS method, which does not use the SCME UMi channel model, but instead provides a Line-Of-Sight scenario.

5.2.3.5.2   Round Robin Results

Test Method Comparison
Figure 5.2.3.5-4 shows the throughput results for each of the methods for LTE band 7 and LTE band 18. For both bands, the methods provide expected ranking of the units. The relative difference between the antennas vary between 0.5 to 1.5 dB at the 70% throughput level for band 7. This is a quite small

difference but in the same range as the measured average gain values from Section 5.2.3.5.1 (given the low correlation values for the band 7 antennas this is not expected to have any significant impact). For band 18, the good to nominal and nominal to bad difference is about 3 dB and 3,5 dB, respectively. Comparing against the correlation values from Section 5.2.3.5.1, these results seem reasonable. The difference is about 1.8 dB and 0.8 dB in efficiency for good to nominal and nominal to bad, respectively. In addition, there is significant correlation for the nominal and bad antenna, which could account for the rest of the difference in throughput between the antennas.

For OTA Ring, issues with the unit were encountered during the measurements. Due to the complexity of the test setup and equipment and chamber availability, it was not possible to collect further data. Due to this, no data is presented here for this method.
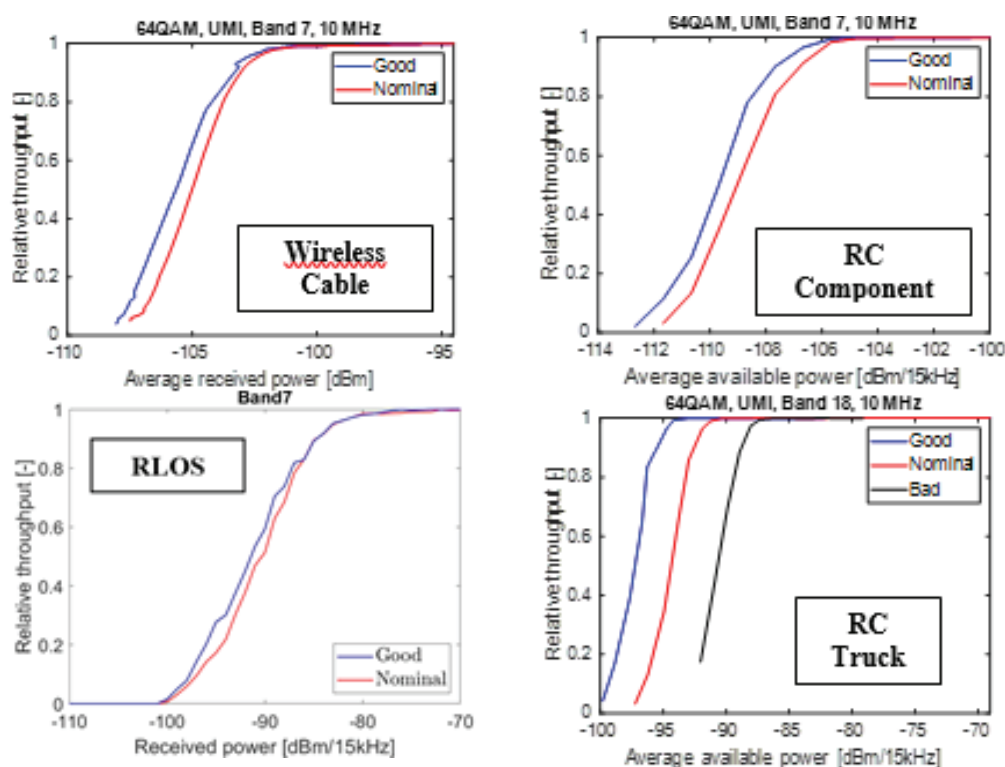
Figure 5.2.3.5-4. Throughput as a function of average cell power for the different methods. From the top: Wireless Cable, RLOS, RC component, RC truck.

Comparison to Field Tests

The mounting of the reference antennas for the field tests and the results can be found in Figure 5.2.3.5-5. From this data it is confirmed that the good antenna outperforms the nominal antenna also in field tests. It can further be concluded that the relative difference between the good and the nominal antennas align fairly well between lab and field tests, given the relatively high uncertainties in the field and the lab test comparison. The field and lab tests yield a difference between the antennas of about 3 dB and 1 dB, respectively.
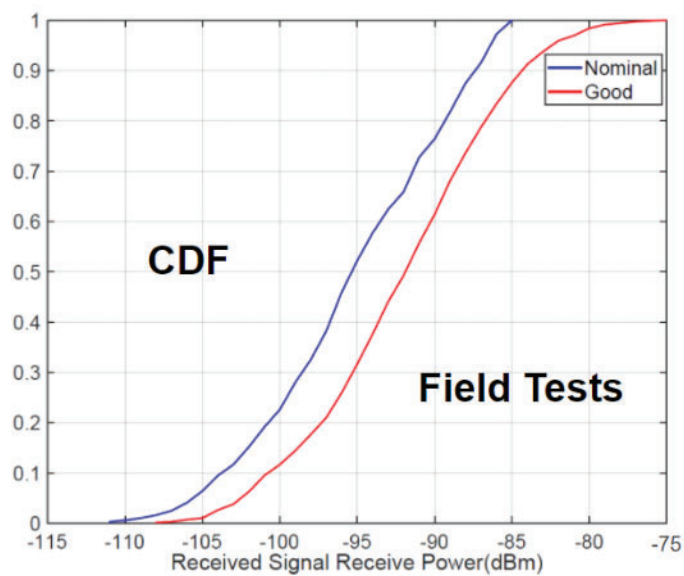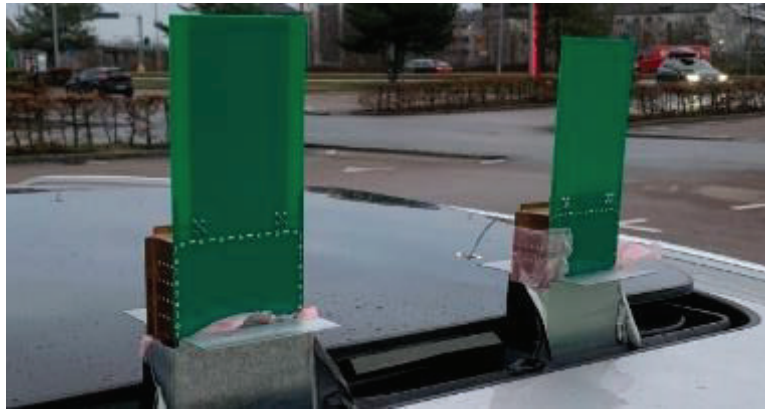
Figure 5.2.3.5-5. The reference antenna mounting during drive tests (top) and the CDF of RSRP for the band 7 good and nominal reference (bottom).

5.2.3.5.3 Comparison of Key Performance Indicators

This section has so far been focused on comparing test results from the different methods, to understand if these can represent the performance in real-world operation. This is of course a very important aspect of a test method, but there are also other aspects that need to be considered. For this reason, Key Performance Indicators have been defined and evaluated for each method within the course of the project. A similar table as developed within 3GPP for handset devices (captured in [WP3E-2]) has been developed. Some aspects of the table below are based on this 3GPP table, however, it has been modified for vehicular applications and the test setups used in this project. The table is included in [WP3E-1], however, too big to be included in this report. In summary, this study concluded that there are significant differences between the test methods in terms of complexity and flexibility of the test setups, the environmental conditions emulated and practicalities of executing the tests. Also, there are significant differences regarding other wireless tests that can be performed and the future extension possibilities for testing other wireless technologies. Also the measurement uncertainty varies between the methods.

5.2.3.5.4 Conclusions

From the Round Robin results, despite a limited set of data and some findings that need further study, it can be concluded that all methods rank the devices in an expected way. The relative difference between devices also seems to be in the expected range when comparing towards efficiency, gain and correlation values, as well as towards field tests.

For the OTA ring test method, issues with the reference receiver were experienced and due to the complexity of the test setup only limited Round Robin tests were thus possible. This implementation needs further work to understand if it can represent real-world conditions.

Regarding the Key Performance Indicators, there are significant differences between the test methods, which all have their unique pros and cons. In general, it can be concluded that the more specific and flexible channel modelling that is desired, the more complex the test setup. Some methods may be better suited for early verification at the beginning of a vehicular project development phase, whereas others may be more suited for verification in later phases or for R&D. The table developed within the project comparing KPIs is meant to provide guidance in the decision of what is an appropriate test method for a specific testing need. A combination of methods that fulfills the desired uncertainty levels is seen as the best approach to ensure a comprehensive, flexible, efficient and future-proven OTA test base for vehicles.

5.2.3.5.5 References

[WP3E-1] C. Lötbäck, "Comparison of Over-The-Air Test Methods for Vehicles", October 2020, FFI SIVERT Internal report.

[WP3E-2] 3GPP TR 37.977, *Universal Terrestrial Radio Access (UTRA) and Evolved Universal Terrestrial Radio Access (E-UTRA); Verification of radiated multi-antenna reception performance of User Equipment (UE)*, v16.0.0, July 2020

[WP3E-3] *MIMO Reference Antennas Performance in Anisotropic Channel Environments,* I. Szini, et al., IEEE Transactions on Antennas and Propagation, Vol. 67, No. 6, June 2014

6 Dissemination and publications

The finding from the SIVERT project have been shared via numerous publications and disseminations throughout the project. A final demo has been organized to share the most important outcomes from the project to a broad audience. The simulation framework developed within WP1 has also been made publicly available. This section summarizes all disseminations and publications within the scope of the project.

6.1 Knowledge and results dissemination

The table below shows a summary of how the results from the project has been or is planned to be used or disseminated.

How has/will the project results be used and disseminated?	Defined [8]	Actual (at project conclusion)	Comments
Increase knowledge within the area	X	X	A final demo of the findings in all work packages has been held with a wide audience (see below). Also other disseminations and publications have been delivered. The SIVERT simulation tool will be made publicly available.
Carried over to other advanced technical research projects		X	A follow-up project based on the findings from SIVERT is currently being defined.
Carried over to product development projects	X	X	Volvo Cars is using the developed simulation framework, field test cases and test methods within the scope of the test strategy for next generation vehicular connectivity module. Volvo Technology has implemented wireless technology testing in their vehicle development projects. RISE has commercialized full vehicle test methods developed in the project for use by vehicle OEMs. RanLOS has commercialized the RLOS test system developed and verified in the project.
Market introduction			
Be used in investigations/regulations/political decisions			

6.1.1 Final demo

The project held a final demo in October 2021, to showcase the main deliverables in the project to a broad audience. The demo was originally intended as a physical, onsite meeting at RISE in Borås, where a number of demos of the simulation tool and the verification methods were planned. Unfortunately, due to the Corona virus and the resulting restrictions, the demo was moved to the virtual domain. At the same time, this allowed for inviting more representatives from the industry. In total, approximately 60 persons joined the demo (including project participants).

6.1.1.1 Agenda

The final demo intended to mix short presentations of each work package with demos and videos, to give the audience the best possible experience. The audience also had the opportunity to ask questions via a chat window, which was monitored and moderated by a dedicated resource. The detailed agenda can be found below.

6.1.1.2 Invitation

The invitation to the event was sent out via email by the project leader to a broad audience within the wireless industry. This was done well in advance of the event. The list of invited companies was based on input from all project partners and representatives from for example network providers, testing companies, Universities, competitors, VINNOVA and partner internal were invited. The focus was on Swedish representatives, but also a few international representatives were invited. A registration web page was set up but was later discarded when the demo was moved to the virtual event, to facilitate participation. Also, there was no upper limit on the number of participants and the recipients of the invitation email were encouraged to forward the invitation to colleagues.

6.1.1.3 Demo Execution

The SIVERT virtual final demo was live streamed from the Awitar chamber at RISE in Borås. All speakers from the project were participating onsite and they showcased the deliverables from each work package by a mix of live presentations, live demos and recorded videos. Also, a few participants from the project partners were joining onsite. The Microsoft tool Teams Live was used and two producers assisted with the live streaming of the event.

Below is a picture from the event.

6.1.2 Other disseminations

- WP1 simulation framework internal demo at the Volvo Cars Computer-aided engineering event October 2019
- WP1 poster presentation at ELLIIT workshop in Karlskrona October 2019
- WP1 IEEE WWVC 2019 presentation
- Madeleine Schilliger Kildal's doctoral defense June 2020
- WP1 presentation at IEEE VTS Workshop on Wireless Vehicular Communications 2020
- Fredrik Tufvesson Keynote speaker at EuCAP2021
- RISE Connectivity Day February 2021
- WP1 presentation at Asilomar 2021 special session on Joint "Dependable vehicle-to-everything connectivity". Title: Implementation of spatially consistent channel models for real-time full stack C-ITS V2X simulations.
- Volvo Cars internal demo of simulation and test framework March 2021
- Internal meetings: Monthly conference calls and F2F meetings four times per year (some of the F2F meetings had to be replaced by virtual meetings due to the Corona pandemic).

Additional disseminations were planned but had to be cancelled due to the Corona pandemic.

6.2 Publications

6.2.1 Journal papers

M. S. Kildal, J. Carlsson, and A. A. Glazunov, "Measurements and simulations for validation of the random-LOS measurement accuracy for vehicular OTA applications," *IEEE Transactions on Antennas and Propagation*, vol. 66, no. 11, pp. 6291–6299, Nov. 2018.

M. S. Kildal, S. M. Moghaddam, A. Razavi, J. Carlsson, J. Yang, and A. A. Glazunov, "Verification of the Random Line-of-Sight Measurement Setup at 1.5-3 GHz Including MIMO Throughput Measurements of a Complete Vehicle," *IEEE Transactions on Vehicular Technology*, vol. 69, no. 11, pp. 13165–13179, Nov. 2020.

To Be Submitted: N. Lyamin, A. Fedorov, C. Nelson and F. Tufvesson, "SIVERT system level V2X simulation framework", *IEEE Vehicular Technology Magazine*

6.2.2 Conference papers

M. S. Kildal, A. Razavi, J. Carlsson, and A. A. Glazunov, "Test Zone Verification Procedures in a Random-LOS Measurement Setup," in 2019 13th European Conference on Antennas and Propagation (EUCAP), Krakow, Poland, Apr. 2019.

M. S. Kildal, A. A. Glazunov, and J. Carlsson, "A Numerical Analysis of the Random-LOS Measurement Accuracy for Vehicle Applications," in 2018 12th European Conference on Antennas and Propagation (EUCAP), London, U.K., Apr. 2018.

C. S. P. Lötbäck, K. Karlsson, M. S. Kildal, A. Haliti, M. Nilsson, R. Iustin, "Evaluation of Complete Vehicle Over-The-Air Verification Methods for Multiple-Input Multiple-Output Communication Systems", 15th European Conference on Antennas and Propagation (EUCAP), March 2021.

K. Karlsson, M. Wersäll, F. Harrysson, C. S. P. Lötbäck, " On the Keyhole Effect in Over-The-Air Testing of Higher Order MIMO Systems", 15th European Conference on Antennas and Propagation (EUCAP), March 2021.

A. Fedorov, C. Nelson, G. Sidorenko, F. Tufvesson, A. Vinel, "Derivations of Doppler Shifts from Higher Order Reflections for 3D Vehicle-to-Everything Channel Modeling", Globecom, May 2021.

6.2.3 Internal technical reports

A number of internal technical reports have been provided during the project:

J. Carlsson, "Pre- & Post RanLOS Measurements at Volvo Cars SMP Test Range", SIVERT internal report, June 2019.

K. Karlsson, M. Wersäll, "Multiprobe ring", SIVERT internal report, September 2019.

R. Iustin, "Sirius Signal Emulation / Benchmark and setup instructions", SIVERT internal report, December 2019.

T. Huang, "Virtual Drive Test Report", SIVERT internal report, January 2020.

A. Haliti, "ROMES4 Cellular Drive Test Tool Report", SIVERT internal report, February 2020.

C. Lötbäck, "Comparison of Over-The-Air Test Methods for Vehicles", SIVERT internal report, October 2020.

M. Nilsson, K. Karlsson, "Measurement system analysis on reverberation chamber using conductive textile as cavity material (RC tent) when the test object is a car", SIVERT internal report, March 2021

M. Nilsson, M. S. Kildal, "Measurement system analysis on the random line-of-sight (RLOS) test setup for radiation pattern measurements at Störmätplatsen (VCC) when the test object is a car", SIVERT internal report, July 2021.

J. Carlsson, M. S. Kildal, L. Granbom, "RanLOS - Sub-6 GHz measurement system - Work done in SIVERT, WP3C", SIVERT internal report, July 2021.

K. Karlsson, M. Wersäll, C. Lötbäck, "Reverberation chamber OTA testing", SIVERT internal report, November 2021.

K. Karlsson, M. Wersäll, "Wireless cable OTA testing", SIVERT internal report, November 2021.

N. Lyamin, "Base framework selection and literature review; Licensing investigation; Full framework architecture description; PoC study of C-ITS scenario.", SIVERT internal report, October 2021.

6.2.4 Theses

M. S. Kildal, "The random line-of-sight over-the-air measurement system," PhD thesis, Chalmers University of Technology, Gothenburg, Sweden, 2020.

6.2.5 Other

M. S. Kildal, L. Granbom, J. Carlsson, "Measuring wireless performance of vehicles", Article in Electronic Environment, Published 2019-09-30.

"Enkelkrökt yta förenklar antennmätningarna", Article in Elektroniktidningen August 2020, No. 7-8, page 10-11.

6.3 Patents

C. Lötbäck, F. Tufvesson, M. Nilsson, "Wireless Cable automotive telematics verification using shielding cover", patent application, ref. no. I5691SE00US01, June 2021.

6.4 Publication of simulation framework

SIVERT simulation framework will be publicly distributed. Public git repository will be shared with the research community and mentioned in the research paper (see Journal papers above), describing the developed tool.

7 Conclusions and future research

The SIVERT project has addressed verification of vehicle connectivity modules in a comprehensive manner, from simulations in early phases of a vehicular project to final verification of implemented systems in complete vehicles.

In WP1, the main deliverable has been the complete simulation framework and scenarios for V2V communication, including channel model, communication stack, antenna patterns and mobility. Both LTE-V2X and ITS-G5 technologies are included. Further studies in this work package include the development of additional simulation scenarios, e.g., for V2I, V2P and V2N.

In WP2 the focus has been on defining test scenarios for field tests in commercial 4G cellular networks and how this can be realized with a field logging tool. Also, a feasibility study of VDT test setups have been provided, however, with limited outcome. Further work in this area includes more comprehensive studies of the VDT setup and how these fit into the overall verification strategy for vehicles.

In WP3, three prototype OTA test setups for complete vehicle testing have been provided, both for passive antenna pattern measurements and for active MIMO throughput tests. These prototype setups has been extensively investigated in terms of key performance indicators and uncertainty (using standardized Six Sigma evaluation approaches). Further work includes how these test methods can be extended to cover even more complex features of radio access technologies.

Comparing the outcome form the project with the originally defined scope of the work, most of the targets have been met. The only exception is the VDT prototype test setup, where only a feasibility study was managed within the scope of the project. The findings from the project have laid the foundation for the overall Volvo Cars verification strategy for cellular connectivity, facilitated implementation of wireless technology testing in vehicle development projects for Volvo Technology, provided prototype test setups and scenarios for complete vehicles that have been commercialized by RISE and RanLOS and provided a complete simulation framework for V2X communication. At the same time, additional work has been identified in the different work packages, which can be used as input to a follow-up project. The results from the project have also been widely shared within the industry, partly by conference and journal papers, but also by various disseminations. Also, the SIVERT simulation framework has been shared with the public, which is believed to be useful for many players in the wireless industry.

8 Participating parties and contact persons

The following organizations were part of this project (listed below in alphabetical order with main contact persons):

- Lund University: Fredrik Tufvesson, Aleksei Fedorov, Christian Nelson
- RanLOS: Jan Carlsson, Madeleine Schilliger Kildal, Lars Granbom
- RISE: Kristian Karlsson, Martin Wersäll, Fredrik Harryson
- Volvo Car Corporation: Christian Patané Lötbäck, Mikael Nilsson, Nikita Lyamin, Argjent Haliti, Tai Huang, Anton Skårbratt, Mujeeb Ur Rehman
- Volvo Technology: Roman Iustin

9   Annex

9.1   References

[1] M. G. Nilsson et al., "Measurement uncertainty, channel simulation, and disturbance characterization of an over-the-air multiprobe setup for cars at 5.9 GHz", IEEE Trans. Ind. Electron., vol. 62, no. 12, pp. 7859–7869, Dec. 2015.

[2] 3GPP TR 37.976, Measurement of radiated performance for Multiple Input Multiple Output (MIMO) and multi-antenna reception for High Speed Packet Access (HSPA) and LTE terminals (Release 11), v11.0.0, March 2012.

[3] CTIA Test Plan for 2x2 Downlink MIMO and Transmit Diversity Over-the-Air Performance, v.1.1.1, September 2017

[4] CTIA Test Plan for Wireless Large-Form-Factor Device Over-the-Air Performance, v1.1, July 2017

[5] Wei Fan et al., "MIMO Terminal Performance Evaluation With a Novel Wireless Cable Method", IEEE Transactions on Antennas and Propagation, Volume: 65, Issue: 9, Sept. 2017

[6] P.-S. Kildal, A. A. Glazunov, J. Carlsson, and A. Majidzadeh, "Cost-effective measurement setups for testing wireless communication to vehicles in reverberation chambers and anechoic chambers," in 2014 Conference on Antenna Measurements Applications (CAMA), Nov. 2014, pp. 1–4.

[7] M. S. Kildal, A. A. Glazunov, J. Carlsson, J. Kvarnstrand, A. Majidzadeh, and P. S. Kildal, "Measured probabilities of detection for 1- and 2 bitstreams of 2-port car-roof antenna in RIMP and Random-LOS," in 2016 10th European Conference on Antennas and Propagation (EuCAP), Apr. 2016, pp. 1–5.

[8] FFI application to Elektronik, mjukvara och kommunikation för fordonsindustrin, Simulation and verification of wireless technologies (SIVERT), Anton Skårbratt VCC, 2018-03-05.

Note: Further references can be found in Section 5.2 for each work package.

9.2 Abbreviations

3G	3rd Generation mobile networks
4G	4th Generation mobile networks
5G	5th Generation mobile networks
AC	Anechoic Chamber
AoA	Angle-of-Arrival
API	Application Programming Interface
BLE	Bluetooth Low Energy
BLER	Block Error Rate
BSM	Basic Safety Message
C-ITS	Cooperative Intelligent Transport Systems
DL	Downlink
DUT	Device Under Test
EEBL	Emergency Electronic Brake Light
FFI	Fordonsstrategisk Forskning & Innovation
IEEE	Institute of Electrical and Electronics Engineers
IP	Internet Protocol
KPI	Key Performance Indicator
LOS	Line of Sight
LTE	Long Term Evolution
LU	Lund University
MAC	Media Access Control
MCS	Modulation Coding Scheme
MIMO	Multiple Input Multiple Output
MPAC	Multiprobe Anechoic Chamber
MPS	Multi-Probe ring Setup
MSA	Measurement System Analysis
OEM	Original Equipment Manufacturer (here automaker)
OLOS	Obstructed Line-Of-Sight
OTA	Over The Air
PHY	Physical layer
RC	Reverberation Chamber
RF	Radio Frequency
RISE	Research Institutes of Sweden
RLOS	Random Line-Of-Sight
RSRP	Reference Signal Received Power
RSRQ	Reference Signal Received Quality
RTS	Radiated Two Stage
RX	Receiver
SIMO	Single Input Multiple Output
SISO	Single Input Single Output
SIVERT	Simulation and verification of wireless technologies
SNR	Signal to Noise Ratio
TCP	Transmission Control Protocol
TCU	Telematics Connectivity Unit
TX	Transmitter
UE	User Equipment
UL	Uplink
UMa	Urban Macro
UMi	Urban Micro
VCC	Volvo Car Corporation
V2I	Vehicle-to-Infrastructure
V2N	Vehicle-to-Network
V2P	Vehicle-to-Pedestrian
V2V	Vehicle-to-Vehicle
V2X	Vehicle-to-everything (vehicle to other vehicles, infrastructure, etc.)
VCC	Volvo Car Corporation
VCM	Vehicle Connectivity Module
VNA	Vector Network Analyser
VUT	Vehicle Under Test

WC	Wireless Cable
WCAE	Wireless Communication in Automotive Environment (former FFI project)
Wi-Fi	Wireless Fidelity
WP	Work Package
XPR	Cross Polarization Ratio

9.3   Report authors

Many people have provided input to this report and several authors have written different chapters and parts. Thus, the language can vary and we hope that the readers have patience with this. The list below shows the main author or authors of the different parts of the report.

Chapter/Section	Author/Authors
1 – 3, 4.2, 5.1, 5.2.2, 6 – 9	Christian Patané Lötbäck (VCC)
4.1 and 5.2.1	Fredrik Tufvesson, Aleksei Fedorov (LU) and Nikita Lyamin (VCC)
4.3	Kristian Karlsson (RISE), Madeleine Schilliger Kildal (RLOS) and Jan Carlsson (RanLOS/Provinn)
5.2.3	Kristian Karlsson (RISE), Jan Carlsson (RanLOS/Provinn), Madeleine Schilliger Kildal (RanLOS) and Christian Patané Lötbäck (VCC)

9.4   Acknowledgement

The project participants want to thank Bluetest for providing the reference antennas used for the Round Robin measurements described in section 5.2.3.5.

The project participants further want to thank Yilin Ji, who participated partly in the project as part of his PhD programme at Aalborg University. He provided expertise knowledge on the wireless cable test method described in section 5.2.3.2 and contributed to the development of this method within the project.